Manual for Code

VISCO-PLASTIC SELF-CONSISTENT (VPSC)

Version 7d

(last updated: May 30, 2012)

C.N. Tomé
(Los Alamos National Laboratory - USA) tome@lanl.gov

and

R.A. Lebensohn
(Los Alamos National Laboratory - USA) lebenso@lanl.gov

INDEX

SECTION 2: Description of VPSC code

SECTION 3: Examples and applications of VPSC code

SECTION 4: Appendices

Code Visco-Plastic Self-Consistent (VPSC)

Version 7d – May 2014

C.N. Tomé, Los Alamos National Laboratory, USA, tome@lanl.gov

R.A. Lebensohn, Los Alamos National Laboratory, USA, lebenso@lanl.gov

==========

==========

DISCLOSURE

We distribute this code free of charge on a personal basis and ask you not to make it available to other users. We would appreciate if you acknowledge its use when reporting your results.

These notes contain a description of the theory, the capabilities of the VPSC code, and several examples. The code itself is in a permanent state of change and new options, bug-fixes and changes are incorporated as required by new developments, new applications, or as suggested by interactions with the users. In addition, not every possible combination of running conditions is tested when the code is modified. As a consequence use it at your own risk and let us know if you find bugs or run into trouble while using it. We appreciate comments and suggestions that may improve the interface with the users. We strongly recommend running the benchmark cases included in the examples and make sure that you can reproduce the same results.

GENERAL DESCRIPTION

VPSC is a computer code written mostly in Fortran 77 which simulates the plastic deformation of polycrystalline aggregates. VPSC stands for Visco Plastic Self Consistent and refers to the particular mechanical regime addressed (VP) and to the approach used (SC). VPSC was developed for application to low-symmetry materials (hexagonal, trigonal, orthorhombic, monoclinic, triclinic), although it also performs well when simulating plasticity of cubic materials.

VPSC accounts for full anisotropy of properties and response of the single crystals and the aggregate. It simulates the plastic deformation of aggregates subjected to external strain, external stress, or a combination of both. VPSC is based on the physical shear mechanisms of slip and twinning, and accounts for grain interaction effects. In addition to providing the macroscopic stress-strain response, it accounts for hardening, reorientation and shape change of individual grains. As a consequence, it predicts the evolution of hardening and texture associated with plastic forming. The simulation procedure can be applied to deformation of metals, inter-metallics and geologic aggregates.

RECOMMENDATION

The VPSC7 manual includes a thorough description of the theoretical formulation. Most of Section 1 can be skipped if you are only interested in running the code. However, Subsections 1-6 and 1-7, dealing with hardening and twinning models, should be read. Most of Section 2, describing input and output files, should be read. The user is advised to become familiar with the examples in Section 3, because they highlight different capabilities of the code. Reproducing the numerical results of the examples is highly recommended both, to become familiar with the input/output files and procedures, and to make sure that the code was properly installed in the user's computer.

When compiling VPSC, **always** use the double precision option. When using G-FORTRAN compile with the following switches:

- gfortran –fdefault-real-8 –fdefault-double-8 vpsc7.for –o vpsc7

WHAT IS NEW IN VPSC7d?

By comparison with VPSC6, several features and improvements were added to VPSC7. In general: we have improved and accelerated some of the numerical algorithms, subroutines have been added/modified aiming for more flexibility and modulation in the code, and the structure of the main input file (VPSC7.IN) has changed a bit.

WHAT IS NEW IN VPSC7c?

* We have retained (from VPSC6) the full constraints, secant, tangent and n^{eff}=10 linearization procedures that control grain-matrix interaction.

* We have implemented a new 'affine' linearization procedure which not only represents a more realistic linearization, but allows the user to run simulations when different deformation modes have different rate sensitivities (parameter NRS).

* We have implemented a new 'second order' linearization procedure based on calculating and using intragranular stress fluctuations for describing the grain response. This procedure is onerous in computing time but is more appropriate for simulation of systems with large variations in stiffness between grains (either directional variations because of anisotropy, or grain-to-grain variations associated with multi-phase systems).

* We have retained (from VPSC6) the capability to impose mixed stress and strain-rate boundary conditions, and we have added the possibility of enforcing a stress component as test control variable. This feature allows for simulations of creep tests.

* A new type of 'process' was added. When ivgvar=4 the code rotates rigidly the crystallographic and morphologic texture of the aggregate without imposing deformation.

WHAT IS NEW IN VPSC7d?

* The reading of hardening parameters is done inside the specific routine that handles the hardening law being used. Before, hardening parameters were read simultaneously with the active crystallographic systems. Now, active systems and their hardening parameters are read separately.

* New hardening routines have been added, based on evolution of dislocation densities.

* A 5-dim calculation of the Polycrystal Yield Surface has been added, motivated by the possibility of using an Interpolation Table approach as the constitutive law in FE codes.

SECTION 1: THEORY AND MODELS

1-1 INTRODUCTION

During plastic forming the contribution to deformation from elasticity is negligibly small (typically 10^{-3}) by comparison to the plastic component (typically $>10^{-1}$). In addition, once the elasto-plastic transition is over, the evolution of stress in the grains is controlled by plastic relaxation (slip activity). This means that the size and evolution of the single crystal yield surface controls the stress in the grain. As a consequence, in our formulation we disregard elasticity and describe only plastic contribution to deformation.

1-2 KINEMATICS

In this Section we provide a brief overview of the equations used in kinematics. They apply to any continuum plastic body and, in particular, to crystallographic grains and to aggregates. The reader is referred to the book of Gurtin (1981) for a comprehensive treatise on kinematics. We define:

X : initial coordinates of a point in the undeformed crystal

x(**X**) : final coordinates of a point in the deformed crystal

u=**x**-**X** : displacement of the point

The deformation in the grain is characterized by the displacement gradient tensor $\mathbf{L}^c$ and the deformation gradient tensor $\mathbf{F}^c$, defined as:

$$L_{ij}^c = \frac{\partial \dot{u}_i^c}{\partial x_j} \tag{2-1}$$

$$F_{ij}^c = \frac{\partial x_i}{\partial X_j} \tag{2-2}$$

With the property:

$$x_i = F_{ij} X_j \tag{2-3}$$

Using the definitions of the different tensors it can be shown that:

$$\dot{F}^c = L^c : F^c \tag{2-4}$$

In addition, since plastic deformation is accommodated by shear, and since shear preserves the orientation of the crystal, it is useful to utilize what is called the 'polar decomposition' of the deformation gradient. Such procedure amounts to treat displacements as two sequential steps: a 'plastic stretch' F_o^c which distorts the crystal without reorienting it, followed by a rigid crystal rotation R^c that transforms from initial to final crystal axes:

$$F^c = R^c . F_o^c \tag{2-5}$$

In crystal axes the stretch obeys a relation like (2-4):

$$\dot{F}_o^c = L_o^c F_o^c \tag{2-6}$$

where

$$L^c_{o_{ij}} = \frac{\partial \dot{u}_i^c}{\partial X_j} \tag{2-7}$$

is the velocity gradient in the reference frame attached to the crystal axes, given by the linear superposition of shear rates on all active slip and twinning systems:

$$L^c_{o_{ij}} = \sum_s \dot{\gamma}^s b_i^s n_j^s \tag{2-8}$$

The vectors **n** and **b** remain invariant in crystal axes. Decomposing the dyadic $b^s \otimes n^s$ into the symmetric and skew symmetric components:

$$\begin{aligned} m_{ij}^s &= \tfrac{1}{2}\left(b_i^s n_j^s + b_j^s n_i^s\right) \\ q_{ij}^s &= \tfrac{1}{2}\left(b_i^s n_j^s - b_j^s n_i^s\right) \end{aligned} \tag{2-9}$$

allows us to decompose the velocity gradient into a strain rate and a rotation rate (spin):

$$L^c_{o_{ij}} = D^c_{o_{ij}} + W^c_{o_{ij}} \tag{2-10a}$$

where

$$D^c_{o_{ij}} = \sum_s \dot{\gamma}^s m_{ij}^s \tag{2-10b}$$

$$W^c_{o_{ij}} = \sum_s \dot{\gamma}^s q_{ij}^s \tag{2-10c}$$

Replacing (2-5) in (2-3) and using (2-6):

$$L^c = \dot{F}_0^c F^{c^{-1}} = \left(\dot{R}^c F_0^c + R^c \dot{F}_0^c\right)\left(F_0^{c^{-1}} R^{c^T}\right) = \dot{R}^c R^{c^T} + R^c L_0^c R^{c^T} \tag{2-11}$$

Which can be decomposed, using (2-10), into a strain rate and a rotation rate:

$$L_{ij}^c = D_{ij}^c + W_{ij}^c \tag{2-12}$$

where

$$\begin{cases} D^c = R^c D_o^c R^{c^T} = D_o^{c,R} \\ W^c = R^c W_o^c R^{c^T} + \dot{R}^c R^{c^T} = W_o^{c,R} + \dot{R}^c R^{c^T} \end{cases} \tag{2-13}$$

The distortion rate D^c is simply a transformation from crystal into 'current' frame, but the rotation rate W^c contains an extra contribution.

1-3 UPDATING CRYSTAL ORIENTATION AND GRAIN SHAPE

The kinematics expressions of the previous section are completely general, and applicable to any polycrystal model. Specifically, the polycrystal model will provide a value for the velocity gradient in each grain $L^c = D^c + W^c$. With it we do the following:

1) We use (2-13) to obtain the rate of change of the crystal orientation matrix

$$\dot{R}^c = (W^c - W_o^{c,R})R^c \tag{3-1}$$

which is in turn used to update incrementally the orientation of the crystal and, as a consequence, to follow the texture evolution. The matrix $\dot{R}^c$ is skew-symmetric and, as a consequence, $\dot{R}^c \Delta t$ does not represent a transformation and cannot be used to calculate an incremental rotation of the crystal. Instead, the Rodrigues formula has to be used. See Appendix D for explanation and SUBROUTINE RODRIGUES for algorithm. The calculation of $\dot{R}^c$ is done in SUBROUTINE UPDATE_ORIENTATION.

2) We use an incremental form of (2-4) for updating the deformation gradient of the grain:

$$F^{c^{new}} = (F^{c^{old}} + \dot{F}^c \Delta t) = (I + L^c \Delta t) F^{c^{old}} \tag{3-2}$$

(See SUBROUTINE UPDATE_FIJ).

3) We use the updated deformation gradient to update the shape of the grain as follows: assume a spherical locus of points X in the undeformed state, which obey the equation

$$X \cdot X^T = 1 \qquad (3\text{-}3)$$

The corresponding locus in the deformed state can be calculated using Eq (2-4) as:

$$(F \cdot F^T)^{-1}_{jk} x_j x_k = 1 \qquad (3\text{-}4)$$

which is the equation of a general ellipsoid. The eigenvectors and the (square root of the) eigenvalues of $(F \cdot F^T)$ define the direction and length of the axes of the ellipsoid which represents the grain.

(See SUBROUTINE UPDATE_SHAPE).

1-3-1 CRYSTALLOGRAPHIC & MORPHOLOGIC TEXTURE ROTATION

Section 1-3 above gives the kinematic expressions used to update crystal axes orientation and the grain's deformation gradient. These magnitudes are updated incrementally by VPSC during a deformation simulation. However, there are some situations when the ellipsoid and the 'attached' crystal axes need to be rotated rigidly with respect to a 'laboratory' reference system. VPSC allows the user to apply a 'process' (IVGVAR=4) which is a rigid rotation of the crystallographic and morphologic textures. This is done inside SUBROUTINE TEXTURE_ROTATION. The input in this case is the rotation matrix ROTMAT that operates on crystallograpic and morphologic texture as follows:

a- rigid rotation of the sample with respect to laboratory axes: ROTMAT rotates the sample from 'old' to 'new position. Columns of ROTMAT are the sample axes after rotation, expressed in the laboratory system. An example of this process is sequential passes during ECAE route: the sample leaving the exit channel of the die is rotated and reinserted into the entry channel. The texture and grain shape need to be referred to the axes attached to the die (lab system)

b - change of reference system : columns of ROTMAT are 'old' system axes expressed in 'new' system. ROTMAT transforms vectors and tensors expressed in 'old' set of axes, and expresses their components in 'new' set of axes:

vnew(i) =rotmat(i,j)*vold(j) and tnew(i,j)=rotmat(i,k)*rotmat(j,l)*told(k,l)

An example is a Lankford test, where tension is applied at an angle α with respect to the rolling direction. For numerical simplicity in applying load conditions it is easier to assume that the tensile direction is always 'axis 1', and that the rolling texture appears as rotated by α with respect to such system.

1-3-2 GRAIN CO-ROTATION

It is to be expect that the reorientation of a grain during deformation will be affected (to some extent) by the neighboring grains. Specifically, if neighboring grains exhibit different reorientation trends, it can be expected that they will 'drag' each other. An empirically simple way of accounting for such effect inside VPSC is to assign a neighbor at random to every grain, to calculate the spin of each grain 'c' (given by $(W^c - W_o^c)$), to average the spin of the two randomly paired grains, and to assign this average spin to each of them. As a result of this procedure grains with the same initial orientation will reorient differently during deformation because each of them will interact with a different neighbor (see Tomé, Lebensohn, Necker (2002) for details).

This procedure is controlled by the variable NNEIGH which is read from file VPCS6.IN. If NNEIGH=0 no neighbor is assigned, and if NNEIGH=1 one neighbor is assigned to each grain.
(see SUBROUTINE_NEIGHBOURS)

1-5 SELF-CONSISTENT POLYCRYSTAL FORMALISM

In what follows, we present the basic equations of the 1-site viscoplastic selfconsistent model, originally due to Molinari et al (1987) and extended to fully anisotropic behavior by Lebensohn and Tomé (1993). The present derivation is completely general, based on the fully incompressible formulation of Lebensohn et al. (1998a) and the generalized affine linearization scheme of Masson et al. (2000). Comprehensive derivations can be found in Lebensohn et al. (2004) and Tomé and Lebensohn (2004).

In brief, the polycrystal is represented by means of weighted orientations. The orientations represent grains and the weights represent volume fractions. The latter are chosen to reproduce the initial texture of the material. Each grain is treated as an ellipsoidal visco-plastic inclusion embedded in an effective visco-plastic medium. Both, inclusion and medium have fully anisotropic properties. The effective medium represents the 'average' environment 'seen' by each grain. Deformation is based on crystal plasticity mechanisms -slip and twinning systems- activated by a Resolved Shear Stress.

1-5-1 Local constitutive behavior and homogenization

Let us consider a polycrystalline aggregate. The viscoplastic constitutive behavior at local level (in a given grain) is described by means of the non-linear rate-sensitivity equation:

$$\varepsilon_{ij}(\bar{x}) = \sum_s m_{ij}^s \gamma^s(\bar{x}) = \gamma_o \sum_s m_{ij}^s \left(\frac{m_{kl}^s \sigma_{kl}(\bar{x})}{\tau_o^s} \right)^n \qquad (5\text{-}1)$$

In the above expression τ^s and $m_{ij}^s = \frac{1}{2}\left(n_i^s b_j^s + n_j^s b_i^s\right)$ are the threshold stress and the symmetric Schmid tensor associated with slip (or twinning) system (s), where $\bar{n}^s$ and $\bar{b}^s$ are the normal and Burgers vector of such slip (or twinning) system, $\varepsilon_{ij}(\bar{x})$ and $\sigma_{kl}(\bar{x})$ are the deviatoric strain-rate and stress, and $\gamma^s(\bar{x})$ is the local shear-rate on slip system (s), which can be obtained as:

$$\gamma^s(\bar{x}) = \gamma_o \left(\frac{m_{kl}^s \sigma_{kl}(\bar{x})}{\tau_o^s} \right)^n \qquad (5\text{-}2)$$

where γ_o is a normalization factor and n is the rate-sensitivity exponent. Linearizing Eq. (5-1) inside the domain of a grain (r) gives:

$$\varepsilon_{ij}(\bar{x}) = M_{ijkl}^{(r)} \sigma_{kl}(\bar{x}) + \varepsilon_{ij}^{o(r)} \qquad (5\text{-}3)$$

where $M_{ijkl}^{(r)}$ and $\varepsilon_{ij}^{o(r)}$ are the viscoplastic compliance and the back-extrapolated term of grain (r), respectively. Same relation holds for the average strain-rate and stress in grain (r):

$$\varepsilon_{ij}^{(r)} = M_{ijkl}^{(r)} \sigma_{kl}^{(r)} + \varepsilon_{ij}^{o(r)} \tag{5-4}$$

Depending on the linearization assumption, $M_{ijkl}^{(r)}$ and $\varepsilon_{ij}^{o(r)}$ can be chosen differently. Later in this section we discuss the possible choices for the local linearized behavior. Performing homogenization on this linearized heterogeneous medium consists in assuming a linear relation analogous to (5-3) at the effective medium (polycrystal) level:

$$E_{ij} = \overline{M}_{ijkl} \Sigma_{kl} + E_{ij}^{o} \tag{5-5}$$

where E_{ij} and Σ_{ij} are overall (macroscopic) magnitudes and $\overline{M}_{ijkl}$ and E_{ij}^{o} are the macroscopic viscoplastic compliance and back extrapolated term, respectively. The latter moduli are unknown *a priori* and need to be adjusted self-consistently. Invoking the concept of the equivalent inclusion (Mura 1987), the local constitutive behavior can be rewritten in terms of the homogeneous macroscopic moduli, so that the inhomogeneity is 'hidden' inside a fictitious eigen-strain-rate, as:

$$\varepsilon_{ij}(\bar{x}) = \overline{M}_{ijkl} \sigma_{kl}(\bar{x}) + E_{ij}^{o} + \varepsilon_{ij}^{*}(\bar{x}) \tag{5-6}$$

$\varepsilon_{ij}^{*}(\bar{x})$ is the eigen-strain-rate field, which follows from replacing the inhomogeneity by an equivalent inclusion. Rearranging and subtracting (5-5) from (5-6) gives:

$$\tilde{\sigma}_{ij}(\bar{x}) = \overline{L}_{ijkl} \left(\tilde{\varepsilon}_{kl}(\bar{x}) - \varepsilon_{kl}^{*}(\bar{x}) \right) \tag{5-7}$$

The symbol "~" denotes local deviations of the corresponding tensor from macroscopic values and $\overline{L}_{ijkl} = \overline{M}_{ijkl}^{-1}$. Combining (5-7) with the equilibrium condition:

$$\sigma_{ij,j}^{c}(\bar{x}) = \tilde{\sigma}_{ij,j}^{c}(\bar{x}) = \tilde{\sigma}_{ij,j}(\bar{x}) + \tilde{\sigma}_{,i}^{m}(\bar{x}) \tag{5-8}$$

where σ^c and σ^m are the Cauchy and mean stresses, respectively. Using the relation $\tilde{\varepsilon}_{ij}(\bar{x}) = \frac{1}{2}\left(\tilde{u}_{i,j}(\bar{x}) + \tilde{u}_{j,i}(\bar{x})\right)$ between strain-rate and velocity-gradient, and adding the incompressibility condition, we obtain:

$$\left|\begin{array}{ll} \bar{L}_{ijkl}\, \tilde{u}_{k,lj}(\bar{x}) + \tilde{\sigma}^m_{,i}(\bar{x}) + f_i\,(\bar{x}) = 0 & (5-9a) \\ \tilde{u}_{k,k}(\bar{x}) = 0 & (5-9b) \end{array}\right.$$

where the fictitious volume force associated with the heterogeneity is:

$$f_i\,(\bar{x}) = -\bar{L}_{ijkl}\varepsilon^*_{kl,j}(\bar{x}) = \sigma^*_{ij,j}(\bar{x}) \qquad (5\text{-}10)$$

The field $\sigma^*_{ij}(\bar{x}) = -\bar{L}_{ijkl}\varepsilon^*_{kl}(\bar{x})$ defined in (5-10) will be called in what follows eigen-stress field.

1-5-2 Green function method and Fourier transform solution

System (5-9) consists of four differential equations with four unknowns: three are the components of velocity deviation vector $\tilde{u}_i(\bar{x})$, and one is the mean stress deviation $\tilde{\sigma}^m(\bar{x})$. A system of N linear differential equations with N unknown functions and an inhomogeneity term, such as (5-9), can be solved using the Green function method, as explained in what follows. Let us call $G_{km}(\bar{x})$ and $H_m(\bar{x})$ the Green functions associated with $\tilde{u}_i(\bar{x})$ and $\tilde{\sigma}^m(\bar{x})$, which solve the auxiliary problem of a unit volume force, with a single non-vanishing m-component, and applied at $\bar{x} = 0$:

$$\left|\begin{array}{ll} \bar{L}_{ijkl}\, G_{km,lj}(\bar{x}) + H_{m,i}\,(\bar{x}) + \delta_{im}\,\delta(\bar{x}) = 0 & (5-11a) \\ G_{km,k}(\bar{x}) = 0 & (5-11b) \end{array}\right.$$

Here $\delta(\bar{x})$ is Dirac's delta function and δ_{im} is the Kronecker delta. Once the solution of (5-11) is obtained, the solution of (5-9) is given by the convolution integrals:

$$\tilde{u}_k(\bar{\mathbf{x}}) = \int_{R^3} G_{ki}(\bar{\mathbf{x}} - \bar{\mathbf{x}}')\, f_i\,(\bar{\mathbf{x}}')\, d\bar{x}' \qquad (5\text{-}12)$$

$$\tilde{\sigma}^{m}(\bar{x}) = \int_{R^3} H_i(\bar{x}-\bar{x}')\, f_i\,(\bar{x}')\, d\bar{x}' \tag{5-13}$$

System (5-11) can be solved using the Fourier transform method (Lebensohn et al., 2003). Expressing the Green functions in terms of their inverse Fourier transforms, the differential system (5-11) transforms into an algebraic system:

$$\left|\begin{array}{ll} \alpha_j\,\alpha_l\,\bar{L}_{ijkl}\,k^2\hat{G}_{km}(\bar{k}) + \alpha_i\, ik\hat{H}_m(\bar{k}) = \delta_{im} & (5-14a) \\ \alpha_k\,k^2\hat{G}_{km}(\bar{k}) = 0 & (5-14b) \end{array}\right.$$

where k and $\bar{\alpha}$ are the modulus and the unit vector associated with a point of Fourier space $\bar{k} = k\bar{\alpha}$, respectively. Calling $A^{d}_{ik} = \alpha_j\,\alpha_l\,\bar{L}_{ijkl}$, system (5-14) can be expressed as a matrix product $A \times B = C$ where A, B and C are matrices given by:

$$\begin{array}{cc|c} & & \begin{array}{ccc} k^2\hat{G}_{11} & k^2\hat{G}_{12} & k^2\hat{G}_{13} \\ k^2\hat{G}_{21} & k^2\hat{G}_{22} & k^2\hat{G}_{23} \\ k^2\hat{G}_{31} & k^2\hat{G}_{32} & k^2\hat{G}_{33} \\ ik\hat{H}_1 & ik\hat{H}_2 & ik\hat{H}_3 \end{array} = B \\ \hline \begin{array}{cccc} A^{d}_{11} & A^{d}_{12} & A^{d}_{13} & \alpha_1 \\ A^{d}_{21} & A^{d}_{22} & A^{d}_{23} & \alpha_2 \\ A^{d}_{31} & A^{d}_{32} & A^{d}_{33} & \alpha_3 \\ \alpha_1 & \alpha_2 & \alpha_3 & 0 \end{array} = A & \begin{array}{ccc} 1 & 0 & 0 \\ 0 & 1 & 0 \\ 0 & 0 & 1 \\ 0 & 0 & 0 \end{array} = C \end{array} \tag{5-15}$$

The 4x4 matrix A is real and symmetric. As a consequence, its inverse will also be real and symmetric. Using the explicit form of matrix C, we can write the solution of (5-15) as:

$$B = A^{-1} \times C = \begin{bmatrix} A^{-1}_{11} & A^{-1}_{12} & A^{-1}_{13} \\ A^{-1}_{21} & A^{-1}_{22} & A^{-1}_{23} \\ A^{-1}_{31} & A^{-1}_{32} & A^{-1}_{33} \\ A^{-1}_{41} & A^{-1}_{42} & A^{-1}_{43} \end{bmatrix} \tag{5-16}$$

Finally, comparing (5-15) and (5-16):

$$k^2\hat{G}_{ij} = A^{-1}_{ij} \tag{5-17}$$

$$ik\hat{H}_i = A_{4i}^{-1} \tag{5-18}$$

Since the components of A are real functions of α_i, so are the components of A^{-1}, and so are $k^2\hat{G}_{ij}$ and $ik\hat{H}_i$. This property leads to real integrals in the derivation that follows.

1-5-3 Viscoplastic inclusion and Eshelby tensors

Now that we have a solution for the Green tensors, we can write the solution of our eigen-strain-rate problem using the convolution integrals (5-12)-(5-13). Taking partial derivatives to Eq. (5-14) we obtain:

$$\tilde{u}_{k,l}(\bar{\mathbf{x}}) = \int_{R^3} G_{ki,l}(\bar{\mathbf{x}} - \bar{\mathbf{x}}')\, f_i\,(\bar{\mathbf{x}}')\, d\bar{x}' \tag{5-19}$$

Replacing (5-10) in (5-19), recalling that $\partial G_{ij}(\bar{x} - \bar{x}')/\partial\bar{x} = -\partial G_{ij}(\bar{x} - \bar{x}')/\partial\bar{x}'$, integrating by parts, and using the divergence theorem, we obtain:

$$\tilde{u}_{k,l}(\bar{\mathbf{x}}) = \int_{R^3} G_{ki,jl}(\bar{\mathbf{x}} - \bar{\mathbf{x}}')\, \sigma_{ij}^{*}(\bar{x}')\, d\bar{x}' \tag{5-20}$$

Equation (5-20) provides an exact implicit solution to the problem. Such solution requires knowing the local dependence of the eigen-stress tensor. However, we know from the elastic Eshelby inclusion formalism that if the eigen-strain is uniform over an ellipsoidal domain where the stiffness tensor is uniform, then the stress and the strain are constant over the domain of the inclusion (r). The latter suggests us to assume an eigen-stress of constant value (a priori unknown) within the volume Ω of the inclusion, and zero outside. This allows us to average the local field (5-20) over the domain Ω and obtain an average strain-rate inside the inclusion of the form:

$$\tilde{u}_{k,l}^{(r)} = \left(-\frac{1}{\Omega} \int_{\Omega}\int_{\Omega} G_{ki,jl}(\bar{\mathbf{x}} - \bar{\mathbf{x}}')\, d\bar{x}\, d\bar{x}' \right) \bar{L}_{ijmn} \varepsilon_{mn}^{*(r)} \tag{5-21}$$

where $\tilde{u}^{(r)}_{k,l}$ and $\varepsilon^{*(r)}_{mn}$ have to be interpreted as average quantities inside the inclusion (r). Expressing the Green tensor in terms of the inverse Fourier transform and taking derivatives we obtain:

$$\tilde{u}^{(r)}_{k,l} = \left(\frac{1}{8\pi^3 \Omega} \int_{\Omega} \int_{\Omega} \int_{R^3} \alpha_j \alpha_l \left(k^2 \hat{G}_{ki}(\bar{k}) \right) \exp\left[-i\bar{k}(\bar{x} - \bar{x}') \right] d\bar{k} d\bar{x} d\bar{x}' \right) \bar{L}_{ijmn} \varepsilon^{*(r)}_{mn} \qquad (5\text{-}22)$$
$$= T_{klij} \bar{L}_{ijmn} \varepsilon^{*(r)}_{mn}$$

Writing $d\bar{k}$ in spherical coordinates: $d\bar{k} = k^2 \sin\theta \, dk \, d\theta \, d\varphi$ and using relation (5-17), the Green interaction tensor T_{klij} can be expressed as:

$$T_{klij} = \frac{1}{8\pi^3 \Omega} \int_0^{2\pi} \int_0^{\pi} \alpha_j \alpha_l A^{-1}_{ki}(\bar{\alpha}) \Lambda(\bar{\alpha}) \sin\theta \, d\theta \, d\varphi \qquad (5\text{-}23)$$

where θ and φ are the spherical coordinates of the Fourier unit vector $\bar{\alpha}$ and:

$$\Lambda(\bar{\alpha}) = \int_0^{\infty} \left(\int_{\Omega} \int_{\Omega} \exp\left[-i\bar{k}(\bar{x} - \bar{x}') \right] d\bar{x} \, d\bar{x}' \right) k^2 dk \qquad (5\text{-}24)$$

Integration of (5-24) inside an ellipsoidal grain with main axes (a, b, c) gives (Bervellier et al. 1987):

$$\Lambda(\bar{\alpha}) = \frac{8\pi^3}{3} \frac{(abc)^2}{[\rho(\bar{\alpha})]^3} \qquad (5\text{-}25)$$

Where $\rho(\bar{\alpha}) = \left[(a\alpha_1)^2 + (b\alpha_2)^2 + (c\alpha_3)^2 \right]^{1/2}$. Replacing (5-25) in (5-23), the expression of T_{klij} for an ellipsoidal grain results in:

$$T_{klij} = \frac{abc}{4\pi} \int_0^{2\pi} \int_0^{\pi} \frac{\alpha_j \alpha_l A^{-1}_{ki}(\bar{\alpha})}{[\rho(\bar{\alpha})]^3} \sin\theta \, d\theta \, d\varphi \qquad (5\text{-}26)$$

The convolution integral over the Green tensor $\hat{H}(\bar{x})$ allows us to obtain an expression for the mean stress deviation $\tilde{\sigma}^{m}(\bar{x})$, which is the fourth unknown function in differential system (5-9). This way of computing the hydrostatic pressure field has been used by Lebensohn et al. (1998) in a particular application of VPSC, to make a transition from viscoplastic incompressible loading to elastic unloading.

Expression (5-26) has to be integrated numerically using, for instance, a Gauss-Legendre technique. The evaluation of the integrand requires us to invert the 4x4 linear system (5-17) for each integration point. The symmetric and skew-symmetric Eshelby tensors are defined as:

$$S_{ijkl} = \frac{1}{4}\left(T_{ijmn} + T_{jimn} + T_{ijnm} + T_{jinm}\right)\bar{L}_{mnkl} \tag{5-27}$$

$$\Pi_{ijkl} = \frac{1}{4}\left(T_{ijmn} - T_{jimn} + T_{ijnm} - T_{jinm}\right)\bar{L}_{mnkl} \tag{5-28}$$

(see SUBROUTINE_ESHELBY for the numerical implementation of Eqs. 5-26 to 5-28)

Taking symmetric and skew-symmetric components to (5-22) and using (5-27)-(5-28), we obtain the strain-rate and rotation-rate deviations in the ellipsoidal domain:

$$\tilde{\varepsilon}_{ij}^{(r)} = S_{ijkl}\varepsilon_{kl}^{*(r)} \tag{5-29}$$

$$\tilde{\omega}_{ij}^{(r)} = \Pi_{ijkl}\varepsilon_{kl}^{*(r)} = \Pi_{ijkl}S_{klmn}^{-1}\tilde{\varepsilon}_{mn}^{(r)} \tag{5-30}$$

1-5-4 Interaction and localization equations

Expressions similar to Eq. (5-7), relating deviations with respect to overall quantities, also holds for the average stress, strain-rate, and eigen-strain-rates in the grains:

$$\tilde{\sigma}_{ij}^{(r)} = \bar{L}_{ijkl}\left(\tilde{\varepsilon}_{kl}^{(r)} - \varepsilon_{kl}^{*(r)}\right) \tag{5-31}$$

Replacing the eigen-strain-rate given by (5-29) into the deviation equation (5-31), we obtain the following interaction equation:

$$\tilde{\varepsilon}_{ij}^{(r)} = -\tilde{M}_{ijkl}\,\tilde{\sigma}_{kl}^{(r)} \tag{5-32}$$

where the interaction tensor is given by:

$$\tilde{M}_{ijkl} = \left(I - S\right)^{-1}_{ijmn} S_{mnpq}\,\overline{M}_{pqkl} \tag{5-33}$$

Replacing the local and overall deviatoric constitutive relations (5-4) and (5-5) into the interaction equation (5-32) we can write, after some manipulation, the following localization equation:

$$\sigma_{ij}^{(r)} = B_{ijkl}^{(r)}\,\Sigma_{kl} + b_{ij}^{(r)}$$

(5-34)

where the localization tensors are defined as:

$$B_{ijkl}^{(r)} = \left(M^{(r)} + \tilde{M}\right)^{-1}_{ijmn}\left(\overline{M} + \tilde{M}\right)_{mnkl} \tag{5-35}$$

$$b_{ij}^{(r)} = \left(M^{(r)} + \tilde{M}\right)^{-1}_{ijkl}\left(E_{kl}^{o} - \varepsilon_{kl}^{o(r)}\right) \tag{5-36}$$

1-5-5 Selfconsistent equations

The derivation presented in the previous sections solves the problem of a viscoplastic incompressible inclusion embedded in a viscoplastic incompressible effective medium being subject to external loading conditions. In this section we are going to use the previous result to construct a polycrystal model, consisting in regarding each grain as an ellipsoidal inclusion embedded in an effective medium which represents the polycrystal. The properties of such medium are not known a priori but have to be found thorough an iterative self-consistent procedure. Replacing the stress localization equation (5-34) in the local constitutive equation (5-4) we obtain:

$$\varepsilon_{ij}^{(r)} = M_{ijkl}^{(r)}\,\sigma_{kl}^{(r)} + \varepsilon_{ij}^{o(r)} = M_{ijkl}^{(r)}\,B_{klmn}^{(r)}\,\Sigma_{mn} + M_{ijkl}^{(r)}\,b_{kl}^{(r)} + \varepsilon_{ij}^{o(r)} \tag{5-37}$$

Enforcing the condition that the weighted average of the strain-rate over the aggregate has to coincide with the macroscopic quantities, i.e.:

$$E_{ij} = \left\langle \varepsilon_{ij}^{(r)} \right\rangle \tag{5-38}$$

In what follows the brackets "$\langle\ \rangle$" denote average over the grains, weighted by the associated volume fraction. Using (5-37) and the macroscopic constitutive equation (5-5) we obtain:

$$\overline{M}_{ijmn}\,\Sigma_{mn} + E_{ij}^{o} = \left\langle M_{ijkl}^{(r)}\, B_{klmn}^{(r)} \right\rangle \Sigma_{mn} + \left\langle M_{ijkl}^{(r)}\, b_{kl}^{(r)} + \varepsilon_{ij}^{o(r)} \right\rangle \tag{5-39}$$

Equating the linear and independent terms leads to the following self-consistent equations for the homogeneous compliances and back-extrapolated term:

$$\overline{M}_{ijkl} = \left\langle M^{(r)} : B^{(r)} \right\rangle \tag{5-40a}$$

$$E_{ij}^{o} = \left\langle M^{(r)} : b^{(r)} + \varepsilon^{o(r)} \right\rangle \tag{5-40b}$$

The self-consistent equations (5-40), are derived imposing the average of the local strain-rates to coincide with the applied macroscopic strain-rate (Eq. 5-38). If the grain ellipsoids have the same shape and orientation, it can be shown that the same equations are obtained from the condition that the average of the local stresses coincides with the macroscopic stress. If the grains have each a different shape, they have associated different Eshelby tensors, and the interaction tensors cannot be factored from the averages. In this case, the following general self-consistent expressions should be used (Walpole 1969; Lebensohn et al. 1996; Lebensohn et al 2003, 2004):

$$\overline{M}_{ijkl} = \left\langle M^{(r)} : B^{(r)} \right\rangle : \left\langle B^{(r)} \right\rangle^{-1} \tag{5-41a}$$

$$E_{ij}^{o} = \left\langle M^{(r)} : b^{(r)} + \varepsilon^{o(r)} \right\rangle - \left\langle M^{(r)} : B^{(r)} \right\rangle : \left\langle B^{(r)} \right\rangle^{-1} : \left\langle b^{(r)} \right\rangle \tag{5-41b}$$

The self-consistent equations (5-40) are a particular case of (5-41). Both sets constitute fix-point equations that provide improved estimates of $\overline{M}_{ijkl}$ and E_{ij}^{o}, when they are

solved iteratively starting from an initial guess. From a numerical point of view, Eqs. (5-41) are more robust and improve the speed and stability of the convergence procedure, even when solving a problem where all the inclusions have the same shape.

1-5-6 Algorithm

To illustrate the use of this formulation, we describe here the steps required to predict the local and overall viscoplastic response of a polycrystal, for an applied macroscopic velocity gradient $U_{i,j} = E_{ij} + W_{ij}$ (decomposed here into the symmetric strain-rate E_{ij} and the skew-symmetric rotation-rate W_{ij}). In order to start an iterative search of the local states, one should assume initial values for the local deviatoric stresses and moduli. Starting with an initial Taylor guess, i.e.: $\varepsilon_{ij}^{(r)} = E_{ij}$ for all grains, we solve the non-linear Eq. (5-1) and use an appropriate linearization scheme (see next subsection) to calculate initial values of $\sigma_{ij}^{(r)}$, $M_{ijkl}^{(r)}$ and $\varepsilon_{ij}^{o(r)}$, respectively, for each grain (r) (Eq. 5-4). Next, initial guesses for the macroscopic moduli $\overline{M}_{ijkl}$ and E_{ij}^{o} (usually simple averages of the corresponding grain moduli) are obtained (Eq. 5-5). With them, and the applied strain-rate E_{ij}, the initial guess for the macroscopic stress follows from the inversion of the macroscopic constitutive law (Eq. 5-5), while the Eshelby tensors S_{ijmn} and Π_{ijmn} can be calculated using the macroscopic moduli and the grain shape by means of the procedure described above (Eqs. 5-27, 5-28). Subsequently, the interaction tensor $\tilde{M}_{ijkl}$ (Eq. 5-33), and the localization tensors $B_{ijkl}^{(r)}$ and $b_{ij}^{(r)}$ (Eqs. 5-35 and 5-36), can be obtained as well. With these tensors, new estimates of $\overline{M}_{ijkl}$ and E_{ij}^{o} are obtained by solving iteratively the selfconsistent equations (5-40) (for unique grain shape) or (5-41) (for a distribution of grain shapes). After achieving convergence on the macroscopic moduli (and, consequently, also on the macroscopic stress Σ_{ij} and the interaction tensor

$\tilde{M}_{ijkl}$), a new estimate of the grain stress can be obtained combining the local constitutive equation and the interaction equation (5-32) as follows:

$$\gamma_o \sum_s m_{ij}^s \left(\frac{m_{pq}^s \ \sigma_{pq}^{(r)}}{\tau^s} \right)^n - E_{ij} = -\tilde{M}_{ijkl} \left(\sigma_{kl}^{(r)} - \Sigma_{kl} \right) \qquad (5\text{-}42)$$

Equation (5-42) constitutes a 5x5 non-linear system of algebraic equations, where the unknowns are the five independent components of the deviatoric stress tensor $\sigma_{kl}^{(r)}$ of the grain. If the recalculated local stresses are different from the input values for any of the grains that constitute the polycrystal, a new iteration should be started. Otherwise, the iterative scheme is completed and the shear-rates on the slip (or twinning) of each system (s) in each grain (r) are calculated as (c.f. Eq.5-2):

$$\gamma^{s(r)} = \gamma_o \left(\frac{m_{pq}^s \ \sigma_{pq}^{(r)}}{\tau_o^s} \right)^n \qquad (5\text{-}43)$$

The rotation-rates of the inclusion and the lattice associated with each grain are obtained respectively as:

$$\omega_{ij}^{inc(r)} = W_{ij} + \tilde{\omega}_{ij}^{(r)} \qquad (5\text{-}44a)$$

$$\omega_{ij}^{lat(r)} = W_{ij} + \tilde{\omega}_{ij}^{(r)} - W_{0ij}^{(r)} \qquad (5\text{-}44b)$$

where $\tilde{\omega}_{ij}^{(r)}$ is given by Eq. (5-30) and:

$$W_{0ij}^{(r)} = \sum_s q_{ij}^s \ \gamma^{s(r)} \qquad (5\text{-}45)$$

where:

$$q_{ij}^s = \frac{1}{2} \left(n_i^s \, b_j^s - n_j^s \, b_i^s \right) \qquad (5\text{-}46)$$

The above numerical scheme can be used either to obtain the anisotropic response of the polycrystal, probing it along different strain-paths (i.e.: applying different strain-rates E_{ij}

and obtaining the corresponding stress response Σ_{ij}), or to predict texture development, by applying incremental deformation steps. The latter case requires the incremental updating of the shape and the orientation of the grains (due to both to slip and twinning reorientation) and updating the critical stress of the deformation systems, due to strain hardening, as well. Details of these updating schemes are given in the next section.

1-5-7 Secant, affine, tangent and intermediate linearizations

As stated earlier, different choices are possible for the linearized behavior at grain level (Eq. 5-4). Evidently, the results of the self-consistent scheme depend on this choice. The following are the linearization schemes implemented in the VPSC code:

a) Secant (Hutchinson, 1976):

$$M_{ijkl}^{(r),sec} = \gamma_o \sum_s \frac{m_{ij}^s \, m_{kl}^s}{\tau_o^s} \left(\frac{m_{pq}^s \, \sigma_{pq}^{(r)}}{\tau_o^s} \right)^{n-1} \tag{5-47a}$$

$$\varepsilon_{ij}^{o(r),sec} = 0 \tag{5-47b}$$

b) Affine (Masson et al., 2000, Lebensohn et al., 2003, 2004):

$$M_{ijkl}^{(r),aff} = n\gamma_o \sum_s \frac{m_{ij}^s \, m_{kl}^s}{\tau_o^s} \left(\frac{m_{pq}^s \, \sigma_{pq}^{(r)}}{\tau_o^s} \right)^{n-1} \tag{5-48a}$$

$$\varepsilon_{ij}^{o(r),aff} = \left(M_{ijkl}^{(r),sec} - M_{ijkl}^{(r),aff} \right) \sigma_{kl}^{(r)} = (1-n)\, \varepsilon^{(r)} \tag{5-48b}$$

c) Tangent (Lebensohn and Tomé, 1993):

In this case $M_{ijkl}^{(r),tg} = M_{ijkl}^{(r),aff}$ and, formally, $\varepsilon_{ij}^{o(r),tg} = \varepsilon_{ij}^{o(r),aff}$. However, instead of Eqs. (5-48), use is made of the tangent-secant relation: $\overline{M}^{tg} = n\overline{M}^{sec}$ derived by (Hutchinson, 1976), and the interaction is expressed in terms of $\overline{M}^{sec}$ (Eq. 5-47). The interaction tensor (Eq. 5-33) is given by:

$$\tilde{\mathbf{M}} = (\mathbf{I}-\mathbf{S})^{-1} : \mathbf{S} : \overline{\mathbf{M}}^{tg} = n(\mathbf{I}-\mathbf{S})^{-1} : \mathbf{S} : \overline{\mathbf{M}}^{sec} \qquad (5\text{-}49)$$

An inspection of the interaction equation (5-32) indicates that the smaller the compliance, the smaller is going to be the local deviation of the strain-rate with respect to the average. As a consequence, for $n \to \infty$ the tangent approximation tends to a uniform stress state (Sachs or lower-bound approximation). On the other hand, it has been proved that the secant interaction is stiff and tends to a uniform strain-rate state (Taylor or upper-bound approximation) in the rate-insensitive limit. On the contrary, the affine model remains between bounds for $n \to \infty$. Another intermediate approximation that gives polycrystal's responses in-between the stiff secant and the compliant tangent approaches, can be obtained introducing an adjustable parameter n^{eff}, such that $1 < n^{eff} < n$. The interaction tensor is therefore given by:

$$\tilde{\mathbf{M}} = n^{eff} (\mathbf{I}-\mathbf{S})^{-1} : \mathbf{S} : \overline{\mathbf{M}}^{sec} = (n^{eff}/n)(\mathbf{I}-\mathbf{S})^{-1} : \mathbf{S} : \overline{\mathbf{M}}^{tg} \qquad (5\text{-}50)$$

On top of the above first-order approximations (i.e. the linearized moduli assigned to grain (r) depend only on the average stress in the grain $\sigma^{(r)}$), VPSC7 allows using a more sophisticated and accurate approach based on second-order moments (see section 1-8).

(See SUBROUTINE VPSC for implementation of the self-consistent formalism discussed in this Section).

1-6 HARDENING OF SLIP AND TWINNING SYSTEMS

The threshold stress τ^s which appears in Eq. 5-1 describes (in an average way) the resistance for activation that the deformation modes experience and it usually increases with deformation. The code has the capability of using a reference hardening function for each system, described by an extended Voce law (Tomé et al. 1984), or using a threshold stress given by the Mechanical Threshold Stress (MTS) model (Kok et al. 2002).

1-6-1 Voce hardening

It is characterized by an evolution of the threshold stress with accumulated shear strain in each grain of the form

$$\hat{\tau}^s = \tau_0^s + (\tau_1^s + \theta_1^s \Gamma)(1 - \exp(-\Gamma \left| \frac{\theta_0^s}{\tau_1^s} \right|)) \qquad (6\text{-}1)$$

where $\Gamma = \sum_s \Delta\gamma^s$ is the accumulated shear in the grain; τ_0, θ_0, θ_1, $(\tau_0+\tau_1)$ are the initial CRSS, the initial hardening rate, the asymptotic hardening rate and the back-extrapolated CRSS. While θ_0 and τ_1 are usually positive, their absolute values are used in (6-1) in order to accommodate some special cases. In addition, we allow for the possibility of 'self' and 'latent' hardening by defining coupling coefficients $h^{ss'}$ which empirically account for the obstacles that new dislocations associated with *s'* activity represent for the propagation of system *s*. Eventually, the increase in the threshold stress of a system due to shear activity $\Delta\gamma^{s'}$ in the grain systems is calculated as:

$$\Delta\tau^s = \frac{d\hat{\tau}^s}{d\Gamma} \sum_{s'} h^{ss'} \Delta\gamma^{s'} \qquad (6\text{-}2)$$

where

$$\frac{d\hat{\tau}^s}{d\Gamma} = \left[\theta_1 + (\left| \frac{\theta_0}{\tau_1} \right| \tau_1 - \theta_1) \exp(-\Gamma \left| \frac{\theta_0}{\tau_1} \right|) + \left| \frac{\theta_0}{\tau_1} \right| \theta_1 \Gamma \exp(-\Gamma \left| \frac{\theta_0}{\tau_1} \right|) \right] \qquad (6\text{-}3)$$

We use self-hardening as a reference and set $h^{ss}=1$. It is evident that when 'self' and 'latent' hardening are indistinguishable then $h^{ss'}=1$ and the evolution of the threshold

stress is given by only the Voce hardening function:

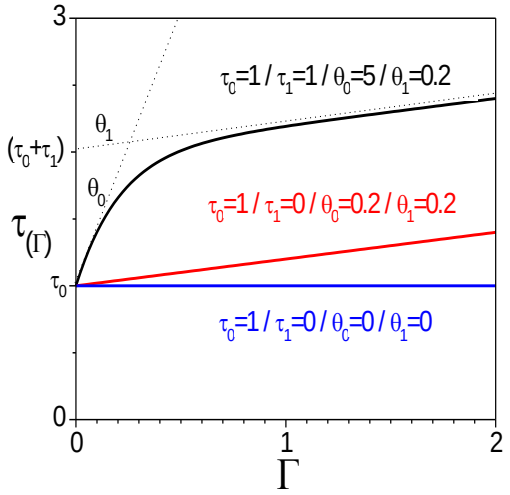

$$\Delta\tau^s = \frac{d\hat{\tau}^s}{d\Gamma}\Delta\Gamma \qquad (6\text{-}4)$$

The hardening law described by Eqs. 6-1 to 6-3 permits us to describe the high hardening rate observed at the onset of plasticity, and its decrease towards a constant hardening rate at large strains. The condition $\theta_0 \geq \theta_1 \geq 0, \tau_1 \geq 0$ corresponds to increasing yield stress and decreasing hardening rate tending to linear saturation. Linear hardening is a limit case of this law corresponding to $\tau_1^s = 0$ and the case of rigid-perfectly-plastic hardening corresponds to $\theta_0 = \theta_1 = \tau_1 = 0$ (see Figure). The hardening parameters in Eqs. (6-1) and (6-2) for each slip mode are read at the end of file FILECRYS.

The threshold associated with each system in each grain is updated inside SUBROUTINE UPDATE_CRSS_VOCE. However, the incremental expression (6-2) represents a forward extrapolation which tends to overestimate the hardening and make it dependent on the step size, more so when the derivative is large. As a consequence, we have implemented an analytic integration of Eq. (6-2) inside SUBROUTINE UPDATE_CRSS_VOCE. **The**

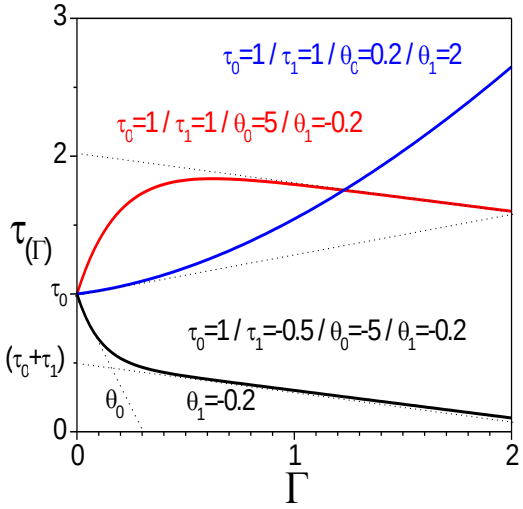

procedure is described in Appendix C.

Non-kosher Voce hardening: Normally, the evolution of the threshold stress represented by Eq. 6-1 is monotonically increasing and the hardening rate (Eq. 6-2) is monotonically decreasing. This is achieved using a 'kosher' set of parameters $\tau_0>0$, $\tau_1>0$, $\theta_0>\theta_1>0$ However, for some empirical special cases, one may want to use parameters giving monotonic decrease ($\tau_0>0$, $\tau_1<0$, $\theta_0<\theta_1<0$), or increased hardening rate ($\theta_1>\theta_0>0$). The equations 6-1 and 6-2 are mathematically applicable for these cases, as is the incremental update derived in Appendix C. VPSC accepts parameters describing negative hardening. SUBROUTINE CHECK_VOCE will verify that hardening is not ill-posed upon reading the parameters and will warn the user if it detects non-kosher parameters. The adjacent figure shows some of the possible configurations of Voce parameters leading to non-classic hardening.

1-6-2 Mechanical Threshold Stress (MTS) hardening

The Mechanical Threshold Stress model is characterized by a dependence of the threshold stress with strain rate, accumulated strain and temperature in each grain of the form. The kinematic equation links strain rate in crystal to resolved shear stress in systems:

$$\dot{\varepsilon}_{ij} = \dot{\gamma}_0 \sum_s m^s_{ij} \left(\frac{m^s_{kl}\,\sigma_{kl}}{\tau^s} \right)^n \qquad (6\text{-}8)$$

We scale $\dot{\gamma}_0 \approx \|\dot{\varepsilon}\|$ in order to keep $\frac{m^s : \sigma}{\tau^s} \approx 1$ and so to avoid rate effects induced by the power *n*. Rate and temperature effects are accounted for by τ^s, given by the MTS model.

A SUBROUTINE UPDATE_CRSS_MTS is provided in VPSC. The parameters of the MTS model are read from the end of the file containing the single crystal slip systems to be used (FILECRYS). Parameters are available for Al, steel and Ta (Kok et al, 2002).

Example 6 in this manual describes an application of the MTS model for rolled Aluminum.

Crystallographic MTS Model → Associated equations and parameters for Ta

Main equation $\frac{\tau}{\mu} = \frac{\tau_a}{\mu} + S_i(\dot{\varepsilon}, T)\frac{\hat{\tau}_i}{\mu_0} + S_\varepsilon(\dot{\varepsilon}, T)\frac{\hat{\tau}_\varepsilon}{\mu_0}$	Where: τ_a = 16.46 MPa
Shear modulus vs T $\mu = \mu_0\left\{1 - \frac{D_0}{\exp(T_0/T) - 1}\right\}$	Where: μ_0 = 62250 MPa D_0 = 0.00582 MPa T_0 = 40 K
Forest independent structure factor $S_i(\dot{\varepsilon}, T) = \left\{1 - \left[\frac{kT}{\mu b^3 g_{0i}}\ln\left(\frac{\dot{\varepsilon}_{0i}}{\dot{\varepsilon}}\right)\right]^{1/q_i}\right\}^{1/p_i}$	Where: $\dot{\varepsilon}_{0i}$ = 1x10^7 s^{-1} q_i = 3/2 p_i = 1/2 g_{0i} = 0.1236 $\hat{\sigma}_i$ = 495 MPa
Forest related structure factor $S_\varepsilon(\dot{\varepsilon}, T) = \left\{1 - \left[\frac{kT}{\mu b^3 g_{0\varepsilon}}\ln\left(\frac{\dot{\varepsilon}_{0\varepsilon}}{\dot{\varepsilon}}\right)\right]^{1/q_\varepsilon}\right\}^{1/p_\varepsilon}$	Where: $\dot{\varepsilon}_{0\varepsilon}$ = 1x10^7 s^{-1} $g_{0\varepsilon}$ = 1.6 q_ε = 1 p_ε = 2/3
Forest related hardening $\frac{d\hat{\tau}_\varepsilon}{d\varepsilon} = \theta_0 \cdot \frac{\mu}{\mu_0}\left[1 - \frac{\hat{\tau}_\varepsilon}{\hat{\tau}_{\varepsilon v}}\right]^\kappa$	Where: κ = 2.0 θ_0 =1.479 MPa
Saturation stress vs rate and temperature $\ln\left(\frac{\hat{\tau}_{\varepsilon s}}{\hat{\tau}_{\varepsilon s0}}\right) = \frac{kT}{\mu b^3 g_{0\varepsilon s}}\ln\left(\frac{\dot{\varepsilon}}{\dot{\varepsilon}_{0\varepsilon s}}\right)$	Where: $g_{0\varepsilon s}$ = 0.2625 $\hat{\tau}_{\varepsilon s0}$ =144 MPa $\dot{\varepsilon}_{0\varepsilon s}$ = 1x10^7 s^{-1}

1-6-3 Dislocation density model of Beyerlein et al *placeholder*

SUBROUTINE UPDATE_CRSS_DD --> VERSION 29/JUNE/2011

Updates the CRSS taking into account dislocation activities. Based on Beyerlein and Tomé, IJP (2008). Capolungo replaced 'mode densities' by 'system densities', but retained the form of the equations (May 2011)

Sanitized version of SUBROUTINE UPDATE_CRSS_CG_DISL in VPSC7c, where algorithms associated with twin barriers, dislocation transfer, and with Composite Grain were eliminated (CT - June 2011)

1-6-4 Dislocation density model of Rauch et al *placeholder*

SUBROUTINE UPDATE_CRSS_DD_CE2 --> VERSION 30/Nov/2011

Model based on Rauch et al (MSE 2011) continuum model of dislocation evolution, modified to follow forward and reversible dislocations in individual systems (Kitayama et al, 2012)

1-7 PTR TWINNING MODEL

While here we assume that twinning has associated, as slip, a critical resolved shear of activation in the twinning plane and along the twinning direction, it differs from slip in its directionality, which we model by allowing activation only if the resolved shear stress is positive (along the Burgers vector of the twin).

Another aspect of twinning that needs to be incorporated into the models is the fact that the twinned fractions are regions (usually of lamellar morphology) with a different orientation than the surrounding matrix. These twinned regions not only contribute to the texture of the aggregate but, most important, act as effective barriers for the propagation of dislocations or of other twin lamellae. The hardening induced by the twins is empirically enforced here by assigning high values to the latent hardening coefficients $h^{ss'}$ describing slip-twin and twin-twin interactions.

As for the effect on texture of the twinned fractions, here we use the Predominant Twin Reorientation Scheme (PTR) proposed by Tomé et al [1991], which works as follows:

within each grain *g* we keep track of the shear strain $\gamma^{t,g}$ contributed by each twin system *t*, and of the associated volume fraction $V^{t,g} = \gamma^{t,g} / S^t$ as well (S^t is the characteristic twin shear). The sum over all twin systems associated with a given twin mode, and over all grains, represents the 'accumulated twin fraction' $V^{acc,\ mode}$ in the aggregate for the particular twin mode (the one that one would measure by SEM).

$$V^{acc,mode} = \sum_g \sum_t \gamma^{t,g} / S^t \qquad (7\text{-}1)$$

Since it is not numerically feasible to consider each twinned fraction as a new orientation, the PTR scheme adopts a statistical approach. At each incremental step we fully reorient some grains by twinning provided certain conditions are fulfilled. We call 'effective twinned fraction' $V^{eff,\ mode}$ the volume associated with the fully reoriented grains for that mode, and define a threshold volume fraction as

$$V^{th,mode} = A^{th1} + A^{th2} \frac{V^{eff,mode}}{V^{acc,mode}} \qquad (7\text{-}2)$$

After each deformation increment we pick a grain at random and identify the twin system with the highest accumulated volume fraction. If the latter is larger than the threshold $V^{th,\ mode}$ then the grain is allowed to reorient and $V^{eff,\ mode}$ and $V^{th,\ mode}$ are updated. The process is repeated until either all grains are randomly checked or until the effective twin volume exceeds the accumulated twin volume. In the latter case we stop reorientation by twinning and proceed to the next deformation step. Two things are achieved in this process: a) only the historically most active twin system in each grain is considered for reorienting the whole grain by twinning; b) the twinned fraction is consistent with the shear activity that the twins contribute to deformation. The algorithm given by Eq. 7-2 prevents grain reorientation by twinning until a threshold value A^{th1} is accumulated in any given system (typically 10-25% of grain volume) and rapidly raises the threshold to a value around $A^{th1}+A^{th2}$ (typically 50-60% of grain volume).

The PTR scheme is implemented inside SUBROUTINE UPDATE_TWINNING, and the user can define different values of A^{th1} and A^{th2} for each twin mode. These parameters are read from file FILECRYS and are stored in arrays THRES1 & THRES2. The user has the option to allow or prevent twin reoriented grains from undergoing a second reorientation by twinning. Secondary twinning is controlled by ISECTW (=1 → allow

retwinning, =0 → no retwinning) which is read from FILECRYS for each twin mode. This feature is also handled inside SUBROUTINE UPDATE_TWINNING.

1-8 SECOND-ORDER FORMULATION

1-8-1 Second-order moments

The effective stress potential $\overline{U}_T$ of a linear 'thermoelastic' polycrystal described by Eq. (5-5) may be written in the form (Liu and Ponte Castañeda, 2004):

$$\overline{U}_T = \frac{1}{2}\overline{M} :: (\Sigma \otimes \Sigma) + E^o : \Sigma + \frac{1}{2}\overline{G} \tag{8-1}$$

where $\overline{M}$ and E^o are calculated by means of Eqs. 5-40 and $\overline{G}$ is the energy under zero applied stress a stress potential. Let us rewrite the expressions for $\overline{M}$ and E^o and add the expression for $\overline{G}$ as:

$$\overline{M} = \left\langle M^{(r)} : B^{(r)} \right\rangle = \sum_r c^{(r)}\, M^{(r)} : B^{(r)} \tag{8-2}$$

$$E^o = \left\langle M^{(r)} : b^{(r)} + \varepsilon^{o(r)} \right\rangle = \sum_r c^{(r)}\, \varepsilon^{o(r)} : B^{(r)} \tag{8-3}$$

$$\overline{G} = \sum_r c^{(r)}\, \varepsilon^{o(r)} : b^{(r)} \tag{8-4}$$

where $c^{(r)}$ is the volume fraction associated with grain (r).

The average second-order moment of the stress over grain (r) is given by (Liu and Ponte Castañeda, 2004):

$$\langle \sigma \otimes \sigma \rangle^{(r)} = \frac{2}{c^{(r)}} \frac{\partial \overline{U}_T}{\partial M^{(r)}} = \frac{1}{c^{(r)}} \frac{\partial \overline{M}}{\partial M^{(r)}} :: (\Sigma \otimes \Sigma) + \frac{1}{c^{(r)}} \frac{\partial E^o}{\partial M^{(r)}} : \Sigma + \frac{1}{c^{(r)}} \frac{\partial \overline{G}}{\partial M^{(r)}} \tag{8-5}$$

The first derivative in the right term can be obtained solving the following equation [9]:

$$\Omega_{ijkl} \frac{\partial \overline{M}_{kl}}{\partial M^{(r)}_{uv}} = \pi^{(r,uv)}_{ij} \tag{8-6}$$

where Ω_{ijkl} and $\pi_{ij}^{(r,uv)}$ are given elsewhere (Lebensohn et al, 2005). Expression (8-6) is a linear system of 25 equations with 25 unknowns (i.e. the components of $\partial\overline{M}_{kl}/\partial M_{uv}^{(r)}$). In turn, the other two derivatives appearing in Eq. (8-5) can be calculated as:

$$\frac{\partial E_i^o}{\partial M_{uv}^{(r)}} = \theta_i^{(r,uv)} + \zeta_{ikl}\frac{\partial \overline{M}_{kl}}{\partial M_{uv}^{(r)}} \ , \quad \frac{\partial \overline{G}}{\partial M_{uv}^{(r)}} = \eta^{(r,uv)} + \vartheta_i \frac{\partial E_i^o}{\partial M_{uv}^{(r)}} \tag{8-7}$$

where ζ_{ikl}, ϑ_i, $\theta_i^{(r,uv)}$ and $\eta^{(r,uv)}$ are given in Lebensohn et al (2005).

Once the average second moments of the stress are obtained, the corresponding second moments of the strain-rate can be calculated as follows:

$$\langle \varepsilon \otimes \varepsilon \rangle^{(r)} = \left(M^{(r)} \otimes M^{(r)} \right) :: \langle \sigma \otimes \sigma \rangle^{(r)} + \varepsilon^{(r)} \otimes \varepsilon^{o(r)} + \varepsilon^{o(r)} \otimes \varepsilon^{(r)} - \varepsilon^{o(r)} \otimes \varepsilon^{o(r)} \tag{8-8}$$

(See SUBROUTINE FLUCTUATIONS for details of the implementation of the calculation of second-order moments).

The above average second moments over grain (r) (Eqs. 8-5 and 8-8) can be used to generate the average second moment of the equivalent stress and strain-rate in grain (r) as:

$$\overline{\overline{\sigma}}_{eq}^{(r)} = \left(\frac{3}{2} I :: \langle \sigma \otimes \sigma \rangle^{(r)} \right)^{1/2} \tag{8-9a}$$

$$\overline{\overline{\varepsilon}}_{eq}^{(r)} = \left(\frac{2}{3} I :: \langle \varepsilon \otimes \varepsilon \rangle^{(r)} \right)^{1/2} \tag{8-9b}$$

The standard deviations of the equivalent magnitudes in grain (r) are defined as:

$$SD^{(r)}\left(\sigma_{eq}\right) = \sqrt{\left(\overline{\overline{\sigma}}_{eq}^{(r)}\right)^2 - \left(\sigma_{eq}^{(r)}\right)^2} \tag{8-10a}$$

$$SD^{(r)}\left(\varepsilon_{eq}\right) = \sqrt{\left(\overline{\overline{\varepsilon}}_{eq}^{(r)}\right)^2 - \left(\varepsilon_{eq}^{(r)}\right)^2} \tag{8-10b}$$

The standard deviations of the equivalent magnitudes over the whole polycrystal are defined as:

$$SD\left(\sigma_{eq}\right) = \sqrt{\overline{\overline{\Sigma}}_{eq}^2 - \Sigma_{eq}^2} \tag{8-11a}$$

$$SD\left(\varepsilon_{eq}\right)=\sqrt{\bar{\bar{E}}_{eq}^{2}-E_{eq}^{2}} \tag{8-11b}$$

where:

$$\bar{\bar{\Sigma}}_{eq}^{2}=\left\langle\left(\bar{\bar{\sigma}}_{eq}^{(r)}\right)^{2}\right\rangle=\sum_{r} c^{(r)}\left(\bar{\bar{\sigma}}_{eq}^{(r)}\right)^{2} \tag{8-12a}$$

$$\bar{\bar{E}}_{eq}^{2}=\left\langle\left(\bar{\bar{\varepsilon}}_{eq}^{(r)}\right)^{2}\right\rangle=\sum_{r} c^{(r)}\left(\bar{\bar{\varepsilon}}_{eq}^{(r)}\right)^{2} \tag{8-13b}$$

It is worth noting that the overall SD's defined by Eqs. (8-11) are a global scalar indicators that contain information about both intergranular and intragranular stress and strain-rate heterogeneity.

(See SUBROUTINE SDPX and output file FLUCT.OUT).

1-8-2 Second-order procedure

Once the average second-order moments of the stress field over each grain are obtained by means of the calculation of the derivatives appearing in Eq. (8-5), the implementation of the SO procedure follows the work of Liu and Ponte Castañeda (2004). The covariance tensor of stress fluctuations is given by:

$$C_{\sigma}^{(r)}=\left\langle\sigma\otimes\sigma\right\rangle^{(r)}-\sigma^{(r)}\otimes\sigma^{(r)} \tag{8-14}$$

The average and the average fluctuation of resolved shear stress on slip system (k) of grain (r) is given by:

$$\bar{\tau}_{(k)}^{(r)}=m^{k}:\sigma^{(r)}\ ,\ \hat{\tau}_{(k)}^{(r)}=\bar{\tau}_{(k)}^{(r)}\pm\left(m^{k}:C_{\sigma}^{(r)}:m^{k}\right)^{1/2} \tag{8-15}$$

where the positive (negative) branch should be selected if $\bar{\tau}_{(k)}^{(r)}$ is positive (negative). The slip potential of slip system (k) in every grain is defined as:

$$\phi_{(k)}(\tau)=\frac{\tau_o^k}{n+1}\left(\frac{|\tau|}{\tau_o^k}\right)^{n+1} \tag{8-16}$$

Two scalar magnitudes associated with each slip system (k) of each grain (r) are defined by (see SUBROUTINE SOP and arrays ASO and ESO):

$$\alpha_{(k)}^{(r)}=\frac{\phi'^{(r)}_{(k)}\left(\hat{\tau}^{(r)}_{(k)}\right)-\phi'^{(r)}_{(k)}\left(\bar{\tau}^{(r)}_{(k)}\right)}{\hat{\tau}^{(r)}_{(k)}-\bar{\tau}^{(r)}_{(k)}}\ ,\ e_{(k)}^{(r)}=\phi'^{(r)}_{(k)}\left(\bar{\tau}^{(r)}_{(k)}\right)-\alpha^{(r)}_{(k)}\bar{\tau}^{(r)}_{(k)} \tag{8-17}$$

where $\phi'_{(k)}(\tau)=d\phi_{(k)}/d\tau\,(\tau)$. The linearized local behavior associated with grain (r) is then given by $\varepsilon^{(r)}=M^{(r),SO}:\sigma^{(r)}+\varepsilon^{o(r),SO}$, where (See SUBROUTINE SOMOD):

$$M^{(r),SO}=\sum_k \alpha^{(r)}_{(k)}\left(m^k\otimes m^k\right),\ \varepsilon^{o(r),SO}=\sum_k e^{(r)}_{(k)}\ m^k \tag{8-18}$$

The SO procedure requires iterating over $M^{(r),SO}$ and $\varepsilon^{o(r),SO}$ to derive improved estimations of a linear comparison polycrystal. Each of these polycrystals has associated different first- and second-order moments of the stress field in the grains. These statistical moments can be used to obtain new values of $\alpha^{(r)}_{(k)}$ and $e^{(r)}_{(k)}$, which in turn define a new linear comparison polycrystal, etc. This convergence procedure is terminated when the input and output values of $\alpha^{(r)}_{(k)}$ and $e^{(r)}_{(k)}$ coincide within a certain tolerance.

1-8-3 Numerical implementation of the SO

Initial guess for $\alpha^{(r)}_{(k)}$ and $e^{(r)}_{(k)}$*:*

The above scheme to adjust the values of $\alpha^{(r)}_{(k)}$ and $e^{(r)}_{(k)}$ requires the adoption of initial guesses for these magnitudes. In the present implementation we adopted the "affine" guess. From Eq. (43), the "affine" local compliance and back-extrapolated term of grain (r) are given by:

$$M^{(r),aff} = n\gamma_o \sum_k \frac{\left(m^k : \sigma^{(r)}\right)^{n-1}}{\left(\tau_o^k\right)^n} \left(m^k \otimes m^k\right) \tag{8-19}$$

$$\varepsilon^{o(r),aff} = (1-n)\gamma_o \sum_k \left(\frac{m^k : \sigma^{(r)}}{\tau_o^k} \right)^n m^k \tag{8-20}$$

The "affine" initial guesses for $\alpha_{(k)}^{(r)}$ and $e_{(k)}^{(r)}$ are given by (see SUBROUTINE GRAIN_RATE_AND_MODULI called by INITIAL_STATE_GUESS)

$$\alpha_{(k)}^{(r)[o]} = n\gamma_o \frac{\left(m^k : \sigma^{(r)}\right)^{n-1}}{\left(\tau_o^k\right)^n} \tag{8-21}$$

$$e_{(k)}^{(r)[o]} = (1-n)\gamma_o \left(\frac{m^k : \sigma^{(r)}}{\tau_o^k} \right)^n \tag{8-22}$$

'Incremental' procedure for low rate-sensitive materials:

If a SO calculation should be performed for a low rate sensitive material, the procedure described above for the adjustment $\alpha_{(k)}^{(r)}$ and $e_{(k)}^{(r)}$ of could fail to converge. In that case, the convergence could be achieved by using incremental steps in the exponent n. Typically, it is necessary to: a) obtain converged values of $\alpha_{(k)}^{(r)}$ and $e_{(k)}^{(r)}$ for the first three values in a sequence of increasing exponents n, b) use those three initial values of $\alpha_{(k)}^{(r)}$ and $e_{(k)}^{(r)}$ to perform a quadratic interpolation for each of these magnitudes, c) obtain extrapolated estimations of $\alpha_{(k)}^{(r)}$ and $e_{(k)}^{(r)}$ to be used as initial guesses for the subsequent exponent in the incremental sequence (see Increasing rate exponent loop: DO JXRS=JXRSINI, JXRSFIN, JXRSTEP in SUBROUTINE VPSC, and SUBROUTINE EXTRAPOLSO).

'Partial' update of $\alpha_{(k)}^{(r)}$ and $e_{(k)}^{(r)}$

Since the values of the second moments are strongly dependent on the 'linear comparison polycrystal' (determined by the set of $\alpha_{(k)}^{(r)}$ and $e_{(k)}^{(r)}$) and this set of values is obtained precisely from second moments, it is sometimes necessary to adopt a 'partial' update criterion for iterative adjustment of $\alpha_{(k)}^{(r)}$ and $e_{(k)}^{(r)}$. For example, if $\alpha_{(k)}^{(r)[i]}$ and $\alpha_{(k)}^{(r)[new]}$ are, respectively, the current value and the corresponding new estimation of $\alpha_{(k)}^{(r)}$ obtained by means of Eq. (62), a smooth convergence requires the actual updated value of $\alpha_{(k)}^{(r)}$ be calculated as: $\alpha_{(k)}^{(r)[i+1]} = 2/3\,\alpha_{(k)}^{(r)[i]} + 1/3\,\alpha_{(k)}^{(r)[new]}$ (see SUBROUTINE FLUCTUATIONS).

1-8 REFERENCES

M. Berveiller, O. Fassi-Fehri and A. Hihi, 1987. “The problem of two plastic and heterogeneous inclusions in an anisotropic medium”. Int. J. Eng. Sci. **25,** 691-709.

I.J. Beyerlein, R.A. Lebensohn and C.N. Tomé, "Modeling of texture and microstructural evolution in the equal channel angular process", Mats. Sc. and Engineering **A345** (2003) 122-138

I.J. Beyerlein and C.N. Tomé, “A dislocation based constitutive law for pure Zr including temperature effects”, Int. J. of Plasticity **24** (2008) 867-895

O. Engler, M.Y. Huh and C.N. Tomé, 2000. "A study of through-thickness texture gradients in rolled sheets". Metall. Mater. Trans. **31A**, 2299-2315

M.E. Gurtin, 1981. "An Introduction to Continuum Mechanics", Academic Press (San Diego).

J.W. Hutchinson, 1976. “Bounds and self-consistent estimates for creep of polycrystalline materials”. Proc. R. Soc. London A **348**, 101-121.

G.C. Kaschner, C.N. Tomé, I.J. Beyerlein, S.C. Vogel, D.W. Brown, R.J. McCabe, 2006. “Role of twinning in the hardening response of Zr during temperature reloads”, Acta Materialia **54**, 2887-96

U.F. Kocks, C.N. Tomé and H.-R. Wenk, 2000. “Texture and Anisotropy”, Cambridge University Press (2nd edition).

S. Kok, A.J. Beaudoin and D.A. Tortorelli, 2002. "A polycrystal plasticity model based on the mechanical threshold", Int. J. Plasticity **18**, 715-741.

R.A. Lebensohn and C.N. Tomé, 1993. "A self-consistent anisotropic approach for the simulation of plastic deformation and texture development of polycrystals - Application to zirconium alloys", Acta Metall Mater **41** (1993) 2611-2624.

R.A. Lebensohn, D. Solas, G.R. Canova and Y. Brechet, 1996. "Modelling damage of Al-Zn-Mg alloys". Acta Mater. **44**, 315-325.

R.A. Lebensohn, P.A. Turner, J.W. Signorelli, G.R. Canova and C.N. Tomé, 1998a. "Calculation of intergranular stresses based on a large strain visco-plastic self-consistent model", Mod. Sim. Mats. Sc. Eng. **6**, 447-465.

R.A. Lebensohn, H.-R. Wenk and C.N. Tomé, 1998b. "Modeling deformation and recrystallization textures in calcite", Acta mater. **46**, 2683-2693.

R.A. Lebensohn, C.N. Tomé and P.J. Maudlin, 2003. “An extended self-consistent visco-plastic formulation: application to polycrystals with voids”. Int. Report of Los Alamos Natl. Lab. LA-UR-03-1193. (available at http://www.lanl.gov/mst/voids.shtml).

R.A. Lebensohn, C.N. Tomé and P.J. Maudlin, 2004. “A selfconsistent formulation for the prediction of the anisotropic behavior of viscoplastic polycrystals with voids”. J. Mech. Phys. Solids **52**, 249-278.

R.A. Lebensohn, C.N. Tomé and P. Ponte Castañeda, 2005. "Improving the self-

consistent predictions of texture development of polycyrystals incorporating intragranular field fluctuations" Materials Science Forum **495-497**, 955-964.

Y. Liu and P. Ponte Castañeda. 2004 "Second-order theory for the effective behavior and field fluctuations in viscoplastic polycrystals. J. Mech. Phys. Solids **52**, 467–495.

R. Masson., M. Bornert, P. Suquet and A. Zaoui, 2000. "An affine formulation for the prediction of the effective properties of nonlinear composites and polycrystals". J. Mech. Phys. Solids **48**, 1203-1227.

A. Molinari., G.R. Canova and S. Ahzi, 1987. "A self-consistent approach of the large deformation polycrystal viscoplasticity". Acta metall. **35**, 2983-2994.

Mura T., 1987. Micromechanics of defects in solids (2^{nd} edition). Martinus Nijhoff Publishers, Dordrecht, The Netherlands.

E.F. Rauch, J.J. Gracio, F. Barlat, G. Vincze, "Modelling the plastic behavior of metals under complex loading conditions", Modell. Sim. Mats. Sc. and Engng. **19** (2011) 035009 1-18

C.N. Tomé, 1999. "Self-consistent polycrystal models: a directional compliance criterion to describe grain interactions ", Mod. Sim. Mats. Sc. Eng. **7**, 723-738.

C.N. Tomé, G.R. Canova, U.F. Kocks, N. Christodoulou and J.J. Jonas, 1984."The relation between macroscopic and microscopic strain hardening in FCC polycrystals", Acta metall. **32**, 1637-1653.

C.N. Tomé and R.A. Lebensohn, 2004. "Self consistent homogeneization methods for texture and anisotropy", in "Continuum Scale Simulation of Engineering Materials: Fundamentals, Microstructures, Process Applications", edited by D. Raabe, F. Roters, F. Barlat and L.Q. Chen, Wiley-VCH Verlag GmbH & Co, KGaA, Weinheim, pp 473-499.

C.N. Tomé, R. A. Lebensohn and U.F. Kocks, 1991. "A model for texture development dominated by deformation twinning: application to zirconium alloys", Acta Metall. Mater. **39**, 2667.

C.N. Tomé, R.A. Lebensohn and C.T. Necker, "Anisotropy and orientation correlations of recrystallized aluminum", Metall. and Materials Transactions **33A** (2002) 2635-48

C.N. Tomé, P.J. Maudlin, R.A. Lebensohn and G.C. Kaschner, 2001. "Mechanical response of zirconium. Part I: Derivation of a polycrystal constitutive law and Finite Element analysis", Acta Materialia **49**, 3085-96

L.J. Walpole, 1969. On the overall elastic moduli of composite materials, J. Mech. Phys. Solids **17,** 235-251.

SECTION 2: DESCRIPTION OF THE VPSC CODE

2-1 NUMERICAL ALGORITHM

The self-consistent algorithm is solved inside SUBROUTINE VPSC. It consists of two nested iterations. The outer iteration varies the stress (and so the grain compliance) in each grain. The inner iteration varies the overall viscoplastic moduli of the aggregate. The previous loops are nested inside two more external loops, which are usually not activated: the outermost allows for an incremental variation of the rate sensitivity exponent 'n' (used to achieve numerical convergence); the innermost corresponds to the Second Order (SO) procedure (is only required when running this approximation). When comparing tensors inside VPSC we calculate the norm of their difference divided by the norm of their average. This criterion permits to define relative discrepancies and to use always the same relative tolerance (typically 0.001).

Increasing rate exponent loop: *DO N=NRSINI, NRSFIN, NRSTEP*

Second order loop: DO ITSO=1, ITMAXSO (or tolerance<ERRSO)

Grain stresses loop: DO IT1=1,ITMAX1 (or tolerance<ERRS & ERRD)

For the first iteration define initial stress guess $\sigma^{(r)}$ in each grain enforcing an upper-bound (Taylor) interaction (impose same $\varepsilon^{(r)} = E$ in every grain), and define an initial guess for the overall compliance $\overline{M}$ as the inverse of the average of the inverse grain compliances. Define also an initial guess for E^o compatible with the latter (Eq 5-5). For every step calculate in each grain $\sigma^{(r)}$ (using the interaction equation), and the plastic compliance $M^{(r)}$ and the back-extrapolated term $\varepsilon^{o(r)}$ as a function of $\sigma^{(r)}$ (Sect 1-5-7).

Overall moduli loop: DO IT2=1,ITMAX2 (or tolerance<ERRM)

1) Calculate Eshelby tensor as a function of $\overline{M}$ and the ellipsoid axes; 2) Calculate $\tilde{M}$ and $B^{(r)}$ and $b^{(r)}$ using Eqs.(5-33 to 5-36); 3) Calculate $\overline{M}$ using Eq.(5-41) and if this tensor coincides with the $\overline{M}$ used as initial input (within a typical tolerance of

ERRM=0.001) go past the end of the inner loop. If not, redefine this as the new overall compliance and iterate again within the inner loop.

End of overall moduli loop

End of grain stresses loop

End of second order procedure loop

End of rate exponent loop

Once convergence has been achieved VPSC provides the shear rate in every system of every grain, the strain rate and the stress in every grain, the overall strain rate and stress in the aggregate. Rates are assumed to be constant through a certain time increment, and hardening, grain orientation, and grain shape are updated incrementally as described in Sections 1-3 and 1-6.

2-2 SIMULATION OF DEFORMATION: INPUT / OUTPUT OPTIONS

Deformation is simulated imposing successive deformation increments. At each deformation step we impose the boundary conditions (velocity gradient components (strain rate + spin), or stress components or a combination of strain-rate and stress components) to the aggregate, and calculate the stress and strain-rate in each grain. The shear rates are used to make a forward extrapolation for reorienting the grains (crystallographic texture development), updating the yield stresses in the grains (hardening), and updating the grain shapes (morphologic texture development). The overall (macroscopic) stress and strain tensor components are given by volume averages over the corresponding grain components. Anisotropy of response and properties follows from such averaging procedure over the distribution of orientations.

Version 7 of VPSC (VPSC7) has the following options and models implemented:

- Simulate a sequence of mechanical processes. For example: tension followed by torsion; or, shear followed by a calculation of the Yield Locus; or rolling followed by a calculation of the Lankford coefficients. Yet another ‘process’ can be a rigid

rotation of the crystallographic texture and the grain morphology, as found in sequential ECAE routes.

- Mixed boundary conditions (complementary components of stress and velocity gradient) can be imposed. In particular, creep conditions.
- Twinning modes can be used to accommodate shear, and twinning reorientation is treated according to the Predominant Twin Reorientation (PTR) scheme described above.
- Non-reversible slip modes can be used. In this case slip takes place in the sense of the Burgers vector read from FILECRYS but not in the opposite sense. This feature is useful for representing non-centro-symmetric slip observed in geologic materials. Twin shear is treated using this feature.
- Grain reorientation can be 'coupled' to the reorientation of one or more neighbors.
- Evolution of fcc rolling components (Brass, Goss, copper, cube, S, rotated cube) can be followed during deformation.
- Evolution of individual grain ellipsoid shape and orientation (morphologic texture) can be followed. Evolution of the average (macroscopic) ellipsoid is always followed.
- Mixed exponents: slip and twinning systems may have different rate sensitivities (exponent *n*).
- Simulate a non-uniform deformation path (parameter IVGVAR=1) by entering a history of deformation. See description of SUBROUTINE VAR_VEL_GRAD in following page.
- It is possible to calculate a 2-dim projection of the Polycrystal Yield Surface (PCYS) declaring IVGVAR=2 in VPSC.IN (requires to enter components of the 2-d subspace), or to calculate Lankford coefficients between 0 and 90 deg with respect to. the RD by declaring IVGVAR=3 (requires to provide angular increment for 'probing').
- It is possible to calculate a full 5-dim Polycrystal Yield Surface (PCYS) by sampling either the strain rate or the stress space at regular intervals. Use option IVGVAR=-2 in VPSC.IN. The type of probe and the angular increment for probing are prompted through the screen.

- It is possible to save the state of grains and polycrystal corresponding to deformation step *n* in a file POSTMORT.OUT by setting ISAVE=*n* in VPSC.IN, and start a simulation from POSTMORT.IN by setting IRECOVER=1. By default ISAVE=0 and no postmortem file is written.
- It is possible to simulate deformation of a multiphase aggregate. Initial texture and hardening parameters of each phase are entered through VPSC.IN.
- The code has been adapted for future interfacing with Finite Element codes, to be used as a material subroutine of the latter. As a consequence, it contains a 'multi-element' option. *Note: an FE material subroutine based on VPSC7 has yet to be developed. The last one available (VPSC5FE) was based on VPSC5.*
- The code solves the self-consistent algorithm defined by Eqs. 5-40 or 5-41. It also allows one to impose the Taylor condition of equal strain increment to every grain. *Note: Relaxed Constraint conditions are not provided in VPSC7. However, RC is a limit case of the Self Consistent model, when the grain shape becomes highly distorted.*

The input to the code consists in:

- Initial crystallographic texture (grain orientations and weights).
- Single crystal properties (active slip and twinning systems, their critical resolved shear stresses, and the associated hardening parameters).
- Initial morphological texture (initial grain shapes and shape orientations).
- Boundary conditions (overall velocity gradient components, or overall stress components. Also temperature if running the MTS model (IHARDLAW=1).
- Parameters controlling convergence, precision and type of run.
- Optional input: strain history, rolling components (CUBCOMP.IN), previous state of grains (POSTMORT.IN).

The output of the code is:

- Final (optionally intermediate) crystallographic and morphologic textures of each phase after deformation.
- Evolution of the stress and strain components during deformation.

- Statistics of slip and twinning systems activity during deformation.
- Statistic over grain stress and strain-rate components and their standard deviations.
- Optional output: morphologic texture of each phase, rolling components, PCYS scan, Lankford scan, directional Young modulus, state of grains and polycrystal (POSTMORT.OUT)

2-3-1 GRAIN SHAPE EVOLUTION OPTIONS

The VPSC model treats each grain as an ellipsoidal inclusion, and explicitly accounts for individual grain shape and its evolution with strain. As a consequence, VPSC provides a tool to analyze how grain shape affects slip activity, hardening and texture evolution. Refer to Section 1.3, describing the connection between grain shape and the deformation gradient, and to Section 1.5.3, describing the Eshelby tensor. See Beyerlein et al (2003) for 'grain fragmentation model'. (Inside the code see implementation in SUBROUTINE UPDATE_SHAPE)

Under severe plastic deformation grains adopt distorted shapes and extreme aspect ratios, and tend to rotate with the flow field at a faster rate than equiaxed grains. However, there are physical and numerical limits to how distorted a grain can become. From a numerical point of view the evaluation of the integrals associated with the Eshelby tensor (5-27) becomes less accurate. From a physical point of view, severely distorted grains are likely to split into sub-grains. VPSC has two options for dealing with grain shape evolution (see description of ISHAPE in Section 2-6-1):

Option 1 (IFRAG=0): when the ratio between the longest and shortest axes of the ellipsoid ($d_l/d_{s)}$ reaches a critical value CRIT_SHP (typically, CRIT_SHP=25), the code 'freezes' the shape and stops updating the axes. The ellipsoid is still allowed to rotate rigidly.

Option 2 (IFRAG=1): (Beyerlein et al, 2003) When the ratio between the longest and shortest axes of the ellipsoid reaches a critical value CRIT_SHP (typically, CRIT_SHP=5), a *grain splitting scheme* is applied: subdivision of grains is determined according to the length ratios of the long (d_l), medium (d_m) and short (d_s) axes of the ellipsoidal grain in comparison with a critical value R= CRIT_SHP. As illustrated in Fig.

2.3.1, a grain is divided into two grains when $d_l/d_s \geq R$ and $d_m/d_s < R/2$ are satisfied, or into four grains when $d_l/d_s \geq R$ and $d_m/d_s \geq R/2$. The crystallographic orientation of the split grain remains the same and, since the two or four split-grains are identical, only one grain with redefined aspect ratios is retained in the simulation (the total number of grains remains constant).

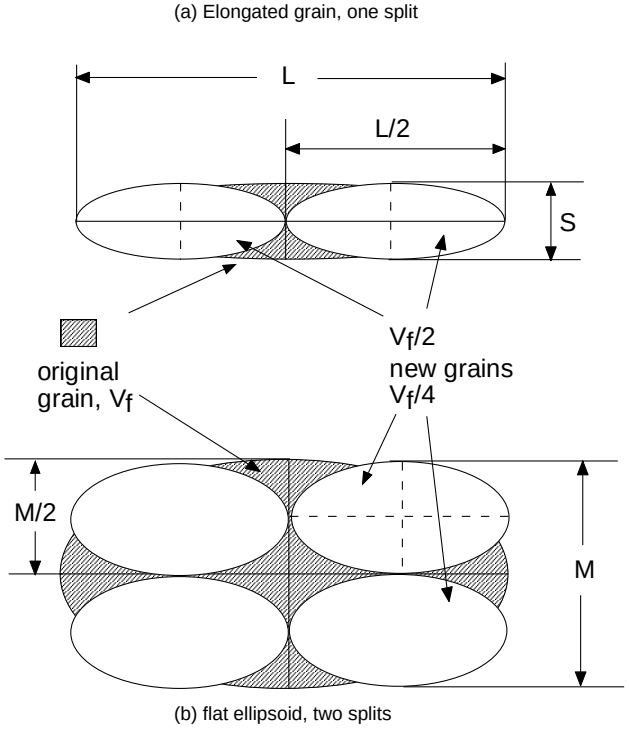

2-3-2 VARIABLE VELOCITY GRADIENT OPTION

It is possible to run a non-uniform deformation path by setting IVGVAR=1 in input file VPSC7.IN, and providing the path & name of the strain history file. The history file may correspond to the output for a given element from a Finite Element run, or may be a file created previously by the user. Under this option the code will call the SUBROUTINE VAR_VEL_GRAD (VARiable VELocity GRADient) and set the boundary conditions to 'fully imposed velocity gradient' (this setting is hardwired but may be changed if needed). VAR_VEL_GRAD is called at each incremental step and the following information is read: the 9 components of the velocity gradient UDOT(i,j) and the time increment TINCR for the step (see file LIJ_HIST.DAT in Example 2, corresponding to rolling with a superimposed variable shear). Inside VAR_VEL_GRAD the following

magnitudes are calculated and passed to the calling module: the strain rate tensor DSIM(I,J) (symmetric component of the velocity gradient), and its 5-dimensional vector representation DBAR(I).

2-4 CODE ARCHITECTURE

The modules of the code are: 1) a driver VPSC7.FOR; 2) an array declaration file VPSC7.DIM; 3) a library of specific plasticity routines VPSC7.SUB; 4) a library of general numerical routines LIBRARY7.SUB.

1) VPSC7.FOR: Controls the simulation run and the output. Ideally the user should not need to modify subroutines for performing a specific calculation (such as calculating Lankford coefficients, or yield surfaces). The opening of I/O units and the unit numbers are also controlled from this module. At the end of VPSC7.FOR the following two statements:

INCLUDE VPSC7.SUB

INCLUDE LIBRARY7.SUB

include the subroutines into the main file when compiling the code.

2) VPSC7.DIM: Dimensions arrays to be shared by MAIN and SUBROUTINES in COMMON declarations. This file is included through a statement:

INCLUDE VPSC7.DIM

which appears in VPSC7.FOR and in most subroutines of VPSC7.SUB. The user controls dimensions by modifying only this file. Access to meaningful variables and arrays (in COMMON areas) is made available through this module for manipulation and output to be done from VPSC7.FOR.

The following parameters are used for dimensioning arrays and have to be defined by the user. When launched, the code checks the input data against the maximum dimensions declared and issues a warning if they are exceeded. The actual number of systems, modes, phases or grains in a particular may be smaller than the dimension declared by the parameters:

NPHPEL (number of phases per element): maximum number of (crystallographic) phases in the aggregate. When running the Finite Element material subroutine only one crystallographic phase can be considered per element.

NPHMX (number of phases maximum): maximum number of (crystallographic) phases in the aggregate or (alternatively) maximum number of elements. The latter applies to a multi-element run or a finite element application.

NMODMX: maximum number of active slip plus twinning modes in any of the crystallographic phases.

NSYSMX: maximum number of slip & twinning systems in any of the crystallographic phases.
NTWMMX: maximum number of twinning modes in any of the crystallographic phases.

NGRMX: maximum number of grains over all the phases in the aggregate (when NELEM=1) or maximum number of grains over all the elements considered (when NELEM>1).

NGRPEL: maximum number of grains per element. It represents the grains in the aggregate independently of whether NELEM=1 or NELEM>1).

NNEIMX: maximum number of neighbors considered in the grain-neighbor interaction (usually 1).

3) VPSC7.SUB: Library of specific subroutines. A list of them with a brief description will eventually be included in an Appendix.

4) LIBRARY7.SUB: Algebraic and mathematical subroutines (matrix inversion, linear systems, eigenvalues and eigenvectors, random number generator, etc) from the NUMERICAL RECIPES library.

2-5 UNITS, REFERENCE SYSTEM AND CONVENTIONS

Internally, the code works with a 5x1 and 5x5 matrix representation of second and fourth order tensors, respectively (see Kocks, Tomé and Wenk, Ch. 7, 2000). The convention used for the matrix representation is controlled by the basis of symmetric tensors defined

inside SUBROUTINE CHG_BASIS. In the current version stress and strain-rate components are represented using the following 'vector' convention:

$$(\sigma_1,\sigma_2,\sigma_3,\sigma_4,\sigma_5)=\left[(\sigma_{22}-\sigma_{11})/\sqrt{2},(2\sigma_{33}-\sigma_{22}-\sigma_{11})/\sqrt{6},\sqrt{2}\sigma_{23},\sqrt{2}\sigma_{13},\sqrt{2}\sigma_{12}\right]$$

The output file STR_STR.OUT gives cartesian components of stress (deviatoric or Cauchy) and strain rate using the Voigt convention:

$$(\sigma_1,\sigma_2,\sigma_3,\sigma_4,\sigma_5)=\left[\sigma_{11},\sigma_{22},\sigma_{33},\sigma_{23},\sigma_{13},\sigma_{12}\right]$$

As in any numerical code, units are implicit and the numerical values of all the parameters and magnitudes have to be consistent. Equation (5-1) indicates that the crystal strain-rate is in the same units as $\dot{\gamma}_0$ (i.e. 1/sec). As a consequence, the values of the imposed overall velocity gradient components UDOT(i) are implicitly assumed to be in the same units. Equation (5-1) also indicates that the grain stress tensor has to be in the same units as the threshold stress τ^s (i.e. MPa). As a consequence, the calculated macroscopic stress values will be in the same units. The time increment for each step (TINCR) has to be in inverse of the strain-rate units (i.e.: sec).

A frequent subject of confusion has to do with the set of axes in which texture and deformation are expressed. The texture is read from an input file containing sets of Euler angles and their respective volume fractions. These Euler angles represent three successive rotations required to bring the crystal axes (originally coincident with the sample axes) to their actual position in the aggregate. As a consequence, the sample axes to which the texture is referred (i.e.: RD=1, TD=2, ND=3) are the same axes in which the imposed deformation tensor (UDOT(i,j)) has to be expressed. For example, tension along the transverse direction of the rolled sheet requires to enforce the component UDOT(2,2).

2-6 DESCRIPTION OF INPUT FILES

The information about the run conditions and the paths and names of the various input files that the code may require are all declared in VPSC7.IN, which may be regarded as the 'master' input file.

2-6-1 File VPSC7.IN

Contains information about input files, deformation path to be simulated and test conditions.

Line by Line:

Line 1: number of elements 'NELEM' (nelem=1 unless running VPSC7FE).

Line 2: number of crystallographic phases in the aggregate 'NPH'.

Line 3: relative volume fractions of the phases 'WPH(1:nph)'.

Follows one block per phase with the information about each phase:

Line 4: reminder.

Line 5: grain morphology control (ISHAPE=0 to 3), grain fragmentation control (IFRAG), critical grain shape (CRIT_SHP).

a- If ISHAPE=0 : average grain shape (ellipsoid orientation and axes) is assumed for each grain when calculating the Eshelby tensor. This is the usual setting for ISHAPE.
If ISHAPE=1 : same as before, but keeps track of individual grain ellipsoid evolution, although they are not used in the simulation.
If ISHAPE=2 : uses individual grain ellipsoids to calculate Eshelby tensors and the grain-matrix interaction. The initial ellipsoid orientation and axes for each grain are the same (this option slows the code considerably).
If ISHAPE=3 : same as ISHAPE=2 but reads different initial ellipsoid orientation and axes for each grain from FILEAXES. The initial values usually follow from file MOR_PH1.OUT generated in a previous run.

b- IFRAG=0 : when the ratio between the longest and shortest axes of the ellipsoid reaches a critical value CRIT_SHP (typically, CRIT_SHP=25), the code 'freezes' the shape and stops updating the axes. The ellipsoid is still allowed to rotate rigidly.

IFRAG=1: when the ratio between the longest and shortest axes of the ellipsoid reaches a critical value CRIT_SHP (typically, CRIT_SHP=5) a *grain splitting scheme* is applied (see description in Section 2.3.1)

c- CRIT_SHP : the ratio between the longest and shortest axes of the ellipsoid defining the threshold for applying either the 'grain freeze' or the 'grain fragmentation' criterion.

Line 6: initial length of ellipsoid axes (length1, length2, length3) describing average grain shape for the corresponding phase (dummy if ISHAPE=3). Only the ratios matter, and not the absolute values.

Line 7: Euler angles describing the initial position of the average ellipsoid with respect to the sample axes (dummy if ISHAPE=3). Axis1 is assumed to have length1, axis2 to have length2, axis3 to have length3.

Line 8: reminder.

Line 9: name and path of crystallographic texture file FILETEXT.

Line 10: reminder.

Line 11: name and path of single crystal properties file FILECRYS.

Line 12: reminder.

Line 13: name and path of grain morphology file FILEAXES (dummy if ISHAPE=0,1,2).

Tolerance settings for convergence procedures (unless expert, use default):

Line 14: reminder.

Line 15: relative tolerances ERRS, ERRD, ERRM, ERRSO allowed in the convergence procedures inside SUBROUTINE VPSC7 (see Section 2-1). Typically 0.001 is used.

Line 16: maximum number of iterations ITMAXEXT and ITMAXINT allowed in the convergence procedure of the loop over grain stress states, and the loop over the overall modulus. Typically ITMAXEXT=100 and ITMAXINT=25. Also number of iterations associated with the Second Order loop (typically 25).

Line 17: parameter IRSVAR and related parameters. Controls the outermost loop in SUBROUTINE VPSC. If IRSVAR=0 (default) the other parameters are ignored.

Line 18: convergence parameter IBCINV. Inside SUBR VPSC solves either Eqs. 5-40 (IBCINV=0) or Eqs. 5-41 (IBCINV=1 → this is the default).

INPUT/OUTPUT settings for the run (unless expert, use 0 as default parameter):

Line 19: reminder

Line 20: parameter IRECOVER.

If IRECOVER=0 uses Taylor stresses as the initial guess in the first step. If IRECOVER=1 reads grain and polycrystal states from POSTMORT.IN.

Line 21 parameter ISAVE.

If ISAVE=0 does not write initial state of grains and polycrystal. If ISAVE=*n* writes grain and polycrystal states into POSTMORT.OUT for deformation step *n*. See EXAMPLE 8 for usage.

Line 22: parameter ICUBCOM.

If ICUBCOM=1 calculates the volume fraction associated with each of the typical fcc rolling components (copper, cube, Goss, S) for each deformation step. VPSC7 will look for file CUBCOMP.IN to read orientation of all crystallographically equivalent components.

If ICUBCOMP=0 skips such calculation.

Line 23: parameter NWRITE controls frequency of texture writing in file TEX_PHn.OUT. Texture is written every NWRITE incremental steps. If NWRITE=0 (default) texture is written only for the last step in each process.

Parameters controlling modeling conditions for the run (user needs to modify):

Line 24: reminder

Line 25: parameter IHARDLAW.

If IHARDLAW=0 uses the hardening parameters associated with the Voce law. Parameters are read at the end of file FILECRYS.

If IHARDLAW=1 uses MTS hardening parameters. Parameters are read at the end of file FILECRYS.

If IHARDLAW=20 or 21 uses a hardening model based on evolution of dislocation density. Parameters are read at the end of file FILECRYS.

Line 26: parameter IRATESENS.

If IRATESENS=1 it accounts for the rate sensitivity induced by the power *n* in Eq. 5-1.

If IRATESENS=0 it scales in Eq. 5-1 to the norm of the macroscopic strain-rate, which has the effect of making the result rate-insensitive. This option does not affect system activity or texture evolution; only affects the stress.

Line 27: type of inclusion-matrix INTERACTION to be used. (0:Taylor, 1:affine, 2:secant, 3:n^{eff}=10, 4:tangent, 5: second order). → see Sections 1-5-7 and 1-8-3.

Line 28: parameters IUPDORI, IUPDSHP, IUPDHAR.

If the corresponding parameter is =1 (default) updates grain orientation, grain shape and grain hardening after every incremental step.

If the corresponding parameter =0 it keeps constant the initial orientation, shape or CRSS throughout the run.

Line 29: parameter NNEIGH.

If NNEIGH=0 it does not couple the reorientation of the grains when updating orientation. This should be the default.

If NNEIGH=n it couples the reorientation of every grain with the reorientation of 'n' neighbors chosen randomly from the discrete texture file (typically NNEIGH=1). The effect of this coupling is to slow down the evolution of texture during deformation.

The following parameters are best left alone unless user has expertise:

Line 30: parameter IFLU. If IFLU=1 calculates intragranular stress fluctuations inside grains. Slows down the run considerably. Default is IFLU=0, unless running the Second Order approximation (INTERACTION=5).

Information about tests to be run (user needs to enter information):

Line 31: reminder.

Line 32: number of sequential tests (i.e.: strain paths, yield surface probes, etc) to be run in the simulation.

Line 33: reminder.

Each process requires two lines in what follows. The first line declares IVGVAR, the second line contains information pertinent to the process, as follows:

Line 34-35+: IVGVAR.

* If IVGVAR=0 the code will enforce the same velocity gradient in every step. The load conditions are read from a PROCESS file: path\name are declared in this line

* If IVGVAR=1 the code will call SUBROUTINE VAR_VEL_GRAD at each deformation step (see description in Section 2-3-2) and read the components of the velocity gradient UDOT and time increment TINCR from a file (typically, the deformation history of a given element generated by a FE code) whose path and name is declared in VPSC7.IN.

* If IVGVAR=2 the code calculates a 2-dimensional projection of the Polycrystal Yield Surface, by probing the aggregate with strain-rate vectors contained in the projection subspace. Instead of a PROCESS file the user should provide in this line the two components (out of the 5 deviatoric components) defining the projection sub-space (see Section 2-5 and EXAMPLE2).

* If IVGVAR=-2 the code calculates a 5-dimensional Polycrystal Yield Surface, by probing the aggregate with regularly spaced strain-rate vectors or stress vectors. Codes prompt user to enter spacing and type of probe.

* If IVGVAR=3 the code calculates the Lankford coefficient by simulating tensile tests in the (x_1,x_2) plane of the texture (see EXAMPLE2). Instead of a PROCESS file the user should provide in this line the angular increment (in degrees) for the tensile 'probing', from the RD to the TD.

* If IVGVAR=4 the code rotates rigidly the crystallographic and the morphologic texture of the grains. An example (see EXAMPLE10) is the simulation of an ECAE route, where after each pass the sample is rotated and reinserted in the die. The second line gives the path and name of a file containing the 3x3 rotation matrix to be used for the rigid rotation (see Section 2-3-3 for description).

Example of file VPSC7.IN (unit=0) (corresponding to EXAMPLE2):

```
1                    number of elements (nelem)
1                    number of phases (nph)
1.0  0.0               relative vol. fract. of phases (wph(i))
*INFORMATION ABOUT PHASE #1
0   0   25              grain shape contrl, fragmentn, crit aspect ratio
1.0  1.0  1.0            initial ellipsoid ratios (dummy if ishape=4)
0.0  0.0  0.0            init Eul ang ellips axes (dummy if ishape=3,4)
* name and path of texture file (filetext)
```

example2\rand500.tex
** name and path of single crystal file (filecrys)*
example2\fcc.sx2
** name and path of grain shape file (dummy if ishape=0) (fileaxes)*
shape1.100
**PRECISION SETTINGS FOR CONVERGENCE PROCEDURES (default values)*
0.001 0.001 0.001 0.001 errs,errd,errm,errso
100 100 25 itmax: max # of iter, external, internal and SO loops
0 2 10 2 irsvar & jrsini,jrsfin,jrstep (dummy if irsvar=0)
*1 ibcinv (0: don't use <Bc>**-1, 1: use <Bc>**-1 in SC eq)*
**INPUT/OUTPUT SETTINGS FOR THE RUN (default is zero)*
0 irecover:read grain states from POSTMORT.IN (1) or not (0)?
0 isave: write grain states in POSTMORT.OUT at step 'isave'?
1 icubcomp:calculate fcc rolling components?
0 nwrite (frequency of texture downloads)
**MODELING CONDITIONS FOR THE RUN*
0 ihardlaw (0:Voce, 1:MTS, 2:composite grain)
1 iratesens (0:rate insensitive, 1:rate sensitive)
1 interaction (0:FC,1:affine,2:secant,3:neff=10,4:tangent,5:SO)
1 1 1 iupdate: update orient, grain shape, hardening
0 nneigh (0 for no neighbors, 1 for pairs, etc.)
0 iflu (0: don't calc, 1: calc fluctuations)
**NUMBER OF PROCESSES (Lij const; Lij variable; PCYS ;LANKFORD; rigid rotatn)*
3
**IVGVAR AND PATH\NAME OF FILE OR STRESS SUBSPACE OR ANGULAR INCREMENT*
1
example2\lij_hist.dat
2 ivgvar=2 will calculate PCYS at the end
1 2 --> section of stress space
3 ivgvar=3 will calculate Lankford coefficients at the end
10 --> angular increment for tensile probing

2-6-2-1 MONOTONIC PROCESS file (path & name read from VPSC7.IN)

Contains information about velocity gradient and mechanical test conditions.

Line by line:

Line 1: parameters NSTEPS, ICTRL, CTRLINCR, TEMP:

- NSTEPS: number of incremental deformation steps.
- ICTRL: Type of incremental step imposed to achieve final deformation. If ICTRL=0 a Von Mises equivalent strain increment is imposed. If 1<ICTRL<6 one of the strain or stress tensor components is imposed, which one, depends on the value of IUDOT or ISCAU read below. (Voigt convention used: 1,2,3,4,5,6 indicate 11,22,33,23,13,12 respectively).

If ICTRL=7 the time increment TINCR is imposed and multiplies the imposed strain rate tensor to give the strain increment.

- CTRLINCR: Magnitude of increment imposed to achieve final deformation.

  If ICTRL=0 the CTRLINCR is the Von Mises strain increment.

  If 1<ICTRL<6 the CTRLINCR is the increment of the strain tensor component when a strain component is enforced or the time increment when a stress component (creep) is enforced.

  If ICTRL=7 then CTRLINCR is the time increment. Case of strain rate imposed.

- TEMP: temperature (not used unless running MTS hardening: IHARDLAW=1).

Line 2: reminder.

Lines 3-5: flags IUDOT(3,3) associated with each of the nine components of the velocity gradient tensor $L_{i,j}$. The corresponding component is enforced or not when IUDOT(i,j) is 1 or 0 respectively. Three of the non-diagonal components have to be enforced because the rigid body rotation of the sample is part of the boundary conditions.

Lines 6-8: components of the macroscopic velocity gradient in arbitrary units. All nine are to be given in order to make an initial guess. Only those with IUDOT=1 are enforced.

Lines 9-11: flags ISCAU(6) associated with each of the six independent components of the Cauchy stress tensor. The corresponding component is enforced or not when ISCAU(i) is 1 or 0 respectively. ISCAU and IUDOT have to be complementary.

Lines 12-14: components of the macroscopic Cauchy stress in arbitrary units. Only those with IUDOT=1 are enforced and need to be given (usually equal to zero for free surfaces).

Example of process file (the sample below corresponds to EXAMPLE2\ROLLING):

```
50  3  0.02   298.          nsteps  ictrl  eqincr  temp
* boundary conditions
  1     1     1       iudot  |  flag for vel.grad.
  1     1     1              |  (0:unknown-1:known)
  1     1     1              |
                             |
  1.0   0.    0.      udot   |  vel.grad
  0.    0.    0.             |
  0.    0.   -1.0            |
                             |
  0     0     0       iscau  |  flag for Cauchy
```

0 *0* |
0 |
|
0. *0.* *0.* *scauchy* | *Cauchy stress*
0. *0.* |
0. |

2-6-2-2 VARIABLE PROCESS file (path & name read from VPSC7.IN)

Contains information about velocity gradient components and time increment to be enforced at each step. In its present version it enforces all the components. See meaning of parameters in description 2-6-2-1 above

Line 1: parameters NSTEPS, ICTRL, CTRLINCR, TEMP

(CTRLINCR & TEMP are dummy, ICTRL has to be equal to 7)

Line 2: remainder

Line 3+: dummy sequential number, Lij, time increment

51 7 0.02 298. nsteps ictrl eqincr temp

step	L11	L12	L13	L21	L22	L23	L31	L32	L33	tincr
1	0.1000E+01	0.0000E+00	0.0000E+00	0.0000E+00	0.0000E+00	0.0E+00	0.0000E+00	0.0E+00	-0.1000E+01	0.2E-01
2	0.1000E+01	0.0000E+00	0.1567E+00	0.0000E+00	0.0000E+00	0.0E+00	0.1567E+00	0.0E+00	-0.1000E+01	0.2E-01
3	0.1000E+01	0.0000E+00	0.3109E+00	0.0000E+00	0.0000E+00	0.0E+00	0.3109E+00	0.0E+00	-0.1000E+01	0.2E-01
4	0.1000E+01	0.0000E+00	0.4602E+00	0.0000E+00	0.0000E+00	0.0E+00	0.4602E+00	0.0E+00	-0.1000E+01	0.2E-01
5	0.1000E+01	0.0000E+00	0.6022E+00	0.0000E+00	0.0000E+00	0.0E+00	0.6022E+00	0.0E+00	-0.1000E+01	0.2E-01

……

2-6-3 File FILETEXT (path & name read from VPSC7.IN)

Contains information about initial crystallographic texture.

Line by Line:

Line 1: dummy.

Line 2: dummy.

Line 3: dummy.

Line 4: first letter of the texture convention being used (Roe, Bunge, Kocks) and the number of orientations to be read from the file.

Line 5 to end: the three Euler angles defining each orientation, and the associated volume fraction. They are read using free format.

Example of input texture file FILETEXT (unit=2):

AXES OF THE REPRESENTATIVE ELLIPSOID
5.0 1.0 0.2
DISCRETE TEXTURE FROM ODF FILE PT420.ODF (1=axis,2=hoop,3=radious)
B 1144
95.00 5.00 5.00 0.00014528
135.00 5.00 5.00 0.00016130
145.00 5.00 5.00 0.00084955
155.00 5.00 5.00 0.00014641
95.00 15.00 5.00 0.00033814
... ...

2-6-4 File FILECRYS (path & name read from VPSC7.IN)

Contains information about crystal deformation modes and hardening parameters.

Line by Line:

Line 1: reminder

Line 2: crystal symmetry 'ICRYST'. Could be CUBIC, HEXAGonal, TRIGOnal, TETRAgonal, ORTHOtropic, MONOClinic, TRICLinic. Only the first five letters of the word are read.

Line 3: crystal lattice parameters: relative length (a,b,c) of the unit cell axes, and angles (α, β, γ) between the axes.

Line 4: reminder.

Line 5-10: elastic constants of the crystal (Voigt notation). VPSC calculates the Voigt, Reuss and Self-Consistent elastic constants of the initial texture, and writes them in RUN_LOG.OUT. Elastic constants are a bonus and do not enter in the plastic simulation.

Line 11: reminder.

Line 12: thermal expansion coefficients of the crystal (Voigt notation). Read but ignored by VPSC.

Line 13: reminder.

Line 14: total number of deformation modes listed in the file.

Line 15: the number of modes to be used in the calculation 'NMODES'.

Line 16: the correlative numbers that identify the active modes.

Next follows the information about each mode:

Line 17: a label for the mode.

Line 18: sequential # for the mode; number of systems in each mode (only the direct systems are listed); an indicator of shear reversibility (ISENSE=1: bi-directional; ISENSE=0: unidirectional, usually associated with twinning but also works for directional slip systems); an indicator for twinning (ITWTYPE=0: for slip systems; ITWTYPE=1: for a mode I twin; ITWTYPE=2 for a mode II twin).

Line 18+: characteristic twin shear *S* (TWSH). Line is inserted only if ITWTYPE=1 or 2.

Line 19+: Miller indices of the normal (n) and slip (b) vectors of each system. For cubic, tetragonal, orthotropic, monoclinic & triclinic symmetry use 3-index Miller notation. For hexagonal and trigonal crystals use 4-index Miller-Bravais notation.

Line 20: reminder

Line 21: label identifying constitutive law (IHARDLAW) → *Voce=0, MTS=1, DD=2x*

Line 22: parameter for suppressing rate sensitivity induced by exponent *n* (IRATESENS) → 0:rate insensitive run, 1:rate sensitive run

Line 23: grain size (usually in microns) (GRSZE) → grain size only matters if Hall-Petch factor is non-zero

Up to this point the data is independent of the hardening model used. The following lines are specific of the hardening law.

In case of a Voce law + a Predominant Twin Reorientation (PTR) scheme, the data is the following:

Line 24: reminder for slip or twin mode parameters coming next.

Line 25: rate sensitivity *n* (NRS) for this mode

Line 26: parameters of the Voce law describing the hardening of the slip or twin systems that belong to this mode (see Section 1-6-1) → *tau0, tau1, thet0,thet1,hpfac*

Line 27: latent hardening parameters $h^{ss'}$ coupling the shear in each system with the other active systems. A total of 'NMODES' values are read from this line, and they couple only the modes being used in the simulation (see Section 1-6-1) → *hlatex(1,im), im=1,nmodes.*

Line 27+: if this is a twin mode, one extra line is required containing: a flag for allowing secondary twin reorientation (ISECTW=1) or not (ISECTW=0); threshold volume fractions THRES1, THRES2 associated with Predominant Twin Reorientation scheme described in Section 1-7.

Example of input file FILECRYS for an FCC crystal (examples 1 ,2, 5):

```
*Material: AUSTENITIC STEEL
cubic          crysym
  1.0   1.0   1.0   90.   90.   90.   unit cell axes and angles
Elastic stiffness (single crystal [GPa]; scaled=0.85xINTERPOLATED)
 205.0   138.0   138.0   000.0   000.0   000.0
 138.0   205.0   138.0   000.0   000.0   000.0
 138.0   138.0   205.0   000.0   000.0   000.0
 000.0   000.0   000.0   126.0   000.0   000.0
 000.0   000.0   000.0   000.0   126.0   000.0
 000.0   000.0   000.0   000.0   000.0   126.0
*Thermal expansion coefficients (single crystal in crystal axis):
 0.0e-6   0.0e-6  0.0e-6   0.0e0   0.0e0   0.0e0
*Info about slip & twinning modes in this file:
 2         nmodesx    (total # of modes listed in file)
 1         nmodes     (# of modes to be used in the calculation)
 1         mode(i)    (label of the modes to be used)
 <111>{110} SLIP
1  12  1   0                    modex,nsmx,iopsysx,itwtypex
  1  1  1       0  1 -1          slip (n & b)
  1  1  1       1  0 -1
  1  1  1       1 -1  0
 -1  1  1       0  1 -1
 -1  1  1       1  0  1
 -1  1  1       1  1  0
 -1 -1  1       0  1  1
 -1 -1  1       1  0  1
 -1 -1  1       1 -1  0
  1 -1  1       0  1  1
  1 -1  1       1  0 -1
  1 -1  1       1  1  0
 <111>{112} TWIN
2  12  0   2                    modex,nsmx,isensex,itwtypex
```

```
0.707                          twshx
  1  1  1       -2  1  1
  1  1  1        1 -2  1
  1  1  1        1  1 -2
 -1  1  1        2  1  1
 -1  1  1       -1 -2  1
 -1  1  1       -1  1 -2
 -1 -1  1        2 -1  1
 -1 -1  1       -1  2  1
 -1 -1  1       -1 -1 -2
  1 -1  1       -2 -1  1
  1 -1  1        1  2  1
  1 -1  1        1 -1 -2
*Constitutive law
  0      Voce=0, MTS=1
  1      iratesens (0:rate insensitive, 1:rate sensitive)
  50     grsze --> grain size only matters if HPfactor is non-zero
 <111>{110} SLIP ----------------------------------------
20                             nrsx
1.0   0.0   0.0   0.0  0.       tau0x,tau1x,thet0,thet1, hpfac
1.0   1.0                      hlatex(1,im),im=1,nmodes
 <111>{112} TWIN -----------------------------------
20                             nrsx
1.0   0.0    0.   0.   0.       tau0x,tau1x,thet0,thet1, hpfac
1.0   1.0                     hlatex(1,im),im=1,nmodes
0     0.05   0.50              isectw, thres1,thres2
```

Example of input file FILECRYS for MTS model and FCC crystal (example 1 ,2, 6):

```
*Constitutive law
  1      Voce=0, MTS=1
  0      iratesens (0:rate insensitive, 1:rate sensitive)
MTS PARAMETERS FOR Al5182 (from KOK et al.)
 0.5899  28815    0.1194   215        KOVB3 [MPa/K] / MU0 [MPa] / D0 / T0 [K]
 3.333   99.075   0.0      800   2.0  TAUa,TAUi,TAUeini,TH0 [MPa] / KAP
 1.196   1.e7     1.5      0.5        G0i / ED0i [1/s] / QQi / PPi
 1.6     1.e7     1.0      0.666666   G0e / ED0e [1/s] / QQe / PPe
 0.1058  1.e7     665.3              G0esat / EDesat0 [1/s] / TAUesat0 [MPa]
 0.00    16.6                    PSI    /RHO [Mg/m^3]        --> Ta!
 0.1455  9544.e-9 -68.9             Cp1,Cp2,Cp3 [MPa m^3/Mg/K]  --> Ta!
```

2-7 DESCRIPTION OF OUTPUT FILES

All output files have the extension *.OUT. Most output files are opened inside VPSC7.FOR for easier control by the user. All the input/output units are defined inside VPSC7.FOR.

2-7-1 Log file RUN_LOG.OUT (unit=10)

Contains input data read by the code. Provides the Voigt, Reuss and Self-Consistent elastic constants of the initial aggregate. If some WRITE statements are activated inside subroutines it also provides information about selected grains.

2-7-2 Optional output file PCYS.OUT (unit=14)

Gets written if IVGVAR=2. Contains the two cartesian coordinates of the 5-dim stress vector and the strain-rate states associated with a 2-dim projection of the Polycrystal Yield Surface. The user is prompted to choose two dimensions (i & j) of the 5 dimensional deviatoric space. Plot of S_i vs S_j gives the desired projection. The usual π-plane representation is obtained plotting S_2 vs S_1 (see EXAMPLE2 and EXAMPLE5).

The probing is done inside SUBROUTINE PCYS using normalized strain rate vectors $\hat{\dot{\varepsilon}}$ and calculating the associated stress $\hat{\sigma}$. Both tensors are renormalized to $\dot{\varepsilon}$ and σ, such as to give the same dissipation rate for every point of the yield surface, namely: $\dot{\varepsilon}_k \, \sigma_k = 1$

S1	*S2*	*D1*	*D2*
0.3712E+00	*0.8931E+01*	*-0.5489E-04*	*0.1000E+01*
0.9334E+00	*0.8784E+01*	*0.1760E+00*	*0.9984E+00*
0.1691E+01	*0.8484E+01*	*0.3572E+00*	*0.9820E+00*
0.3766E+01	*0.7483E+01*	*0.5341E+00*	*0.9253E+00*
0.7736E+01	*0.4803E+01*	*0.6634E+00*	*0.7918E+00*
0.8186E+01	*0.4257E+01*	*0.7595E+00*	*0.6384E+00*

. . .

2-7-3 Optional output file LANKFORD.OUT (unit=15)

Gets written if IVGVAR=3. For each ‘probe’ angle (with respect to the RD) gives the directional Young modulus, the Lankford coefficient (ratio between in-plane strain-rate D22 and through-thickness strain-rate D33), the diagonal strain rate components induced

by tensile deformation along axis 1. Also the tensile stress SCAU11 and the shear stress induced in the tensile sample SCAU12 are written in the output file.

ANGLE	*YOUNG*	*LANKF*	*D(1,1)*	*D(2,2)*	*D(3,3)*	*SCAU(1,1)*	*SCAU(1,2)*
0.0	*231.4*	*0.32*	*1.0000*	*-0.2419*	*-0.7581*	*11.353*	*0.114*
10.0	*225.1*	*0.39*	*1.0000*	*-0.2815*	*-0.7185*	*11.242*	*-0.576*
20.0	*208.8*	*0.60*	*1.0000*	*-0.3762*	*-0.6238*	*10.859*	*-1.087*
30.0	*192.4*	*1.07*	*1.0000*	*-0.5180*	*-0.4820*	*10.357*	*-1.102*

. . .

2-7-4 Convergence control file RERR.OUT (unit=12)

Output from convergence procedure associated with the outer, intermediate and inner loops in SUBROUTINE VPSC. Provides post-mortem analysis of the convergence procedure.

2-7-5 Mode Activity Statistic file ACT_PHn.OUT (units=51,52, …, one per phase)

Case 1: only slip systems

The first column displays the strain component being imposed at every deformation step. The second column displays the Average Active Systems per Grain. The third and subsequent columns display the relative amount of shear contributed by each mode used in the simulation, listed in the same order as they are read from file FILECRYS.

strain	*avacs*	*mode1*	*mode2*	*mode3....*
0.000	*3.607*	*1.000*		
0.025	*3.547*	*1.000*		
0.050	*3.443*	*1.000*		
0.075	*3.445*	*1.000*		
……				
……				
0.450	*3.417*	*1.000*		
0.475	*3.406*	*1.000*		

Case 2: when twinning systems are considered

The first column displays the strain component being imposed at every deformation step. The second column displays the Average Active Systems per Grain. The third and fourth columns display the volume fraction associated with primary twin reoriented grains and with secondary twin reoriented grains. The following columns display the relative amount of shear contributed by each mode used in the simulation for each step. The following columns display the Accumulated Twin Fraction and the Effective Twin Fraction for each of the twinning modes. When the aggregate is formed by more than one phase all the above information is displayed for each of the phases separately.

STRAIN	*AVACS*	*PRITW*	*SECTW*	*MODE1*	*MODE2*	*MODE3*	*MODE4*	*TWFR3*	*EFFR3*	*TWFR4*	*EFFR4*
0.000	*2.960*	*0.000*	*0.000*	*0.090*	*0.000*	*0.004*	*0.906*	*0.000*	*0.000*	*0.000*	*0.000*
0.002	*2.951*	*0.000*	*0.000*	*0.089*	*0.000*	*0.004*	*0.907*	*0.000*	*0.000*	*0.023*	*0.000*
…….											
0.220	*3.303*	*0.593*	*0.000*	*0.237*	*0.000*	*0.620*	*0.143*	*1.655*	*0.004*	*0.588*	*0.588*

2-7-6 Overall statistics file STATS.OUT (unit=11)

Displays general statistics at every incremental step. Most of it is commented out. What is presently displayed is: the standard deviation with respect to the average of the 5 components of strain rate and stress, expressed in the basis of symmetric tensors (matrix representation), (normalized with the norm of the strain-rate or the stress, respectively).

epsacu	*sdev1*	*sdev2*	*sdev3*	*sdev4*	*sdev5*	*ddev1*	*ddev2*	*ddev3*	*ddev4*	*ddev5*
0.000	*0.101*	*0.151*	*0.147*	*0.160*	*0.147*	*0.147*	*0.240*	*0.169*	*0.207*	*0.169*
0.020	*0.102*	*0.147*	*0.146*	*0.161*	*0.152*	*0.141*	*0.230*	*0.166*	*0.204*	*0.169*
0.040	*0.101*	*0.142*	*0.139*	*0.155*	*0.151*	*0.144*	*0.234*	*0.168*	*0.206*	*0.174*
…	…	…	…	…	…					
0.980	*0.159*	*0.090*	*0.075*	*0.062*	*0.231*	*0.054*	*0.077*	*0.101*	*0.373*	*0.192*
1.000	*0.161*	*0.090*	*0.075*	*0.061*	*0.235*	*0.053*	*0.074*	*0.100*	*0.376*	*0.192*

2-7-7 Stress-strain file STR_STR.OUT (unit=13)

Contains 14 columns with the following information for each deformation step: First two columns give the overall Von Mises strain and the Von Mises stress. Next six columns give the six component of the accumulated strain tensor (E11, E22, E33, E23, E13, E12).

Next six columns give the six components of the deviatoric stress tensor (S11, S22, S33, S23, S13, S12) or the six components of the Cauchy stress tensor when the boundary conditions imposed permit to infer the pressure (i.e.: axial compression test).

Evm Svm E11 E22 E33 E23 E31 E12 SDEV11 SDEV22 SDEV33 SDEV23 SDEV13 SDEV12
0.0000E+00 0.2706E+01 0.000E+00 0.000E+00 0.000E+00 0.000E+00 0.000E+00 0.000E+00 -0.180E+01 0.929E+00 0.875E+00 0.356E-02 -0.124E-02 -0.941E-02
0.2500E-01 0.4357E+01 -0.250E-01 0.125E-01 0.125E-01 0.000E+00 0.000E+00 0.000E+00 -0.290E+01 0.149E+01 0.141E+01 0.142E-01 -0.621E-02 -0.169E-01
……
……
0.4498E+00 0.3292E+02 -0.450E+00 0.225E+00 0.225E+00 0.000E+00 0.000E+00 0.000E+00 -0.219E+02 0.115E+02 0.104E+02 -0.251E+00 -0.286E+00 -0.105E+00
0.4748E+00 0.3482E+02 -0.475E+00 0.238E+00 0.238E+00 0.000E+00 0.000E+00 0.000E+00 -0.232E+02 0.122E+02 0.110E+02 -0.283E+00 -0.308E+00 -0.945E-01

2-7-8 Final state in grains and PX file POSTMORT.OUT (unit=19)

Contains the distortion, constitutive moduli, stress of the polycrystal for the particular step at which it was downloaded. Also contains the stress, the CRSS of every system, the Euler angles and the accumulated shear in every grain. If appropriate, also contains information about twinning fractions in each grain and in each phase. The POSTMORT.OUT file is used to continue a run along the same path or along a different deformation path, accounting for grain shape, hardening and orientation. For using it as initial state in a subsequent run it has to be renamed POSTMORT.IN. The option to open and read it is controlled by the parameter IRECOVER=1 defined inside VPSC7.IN. This file was originally intended for running sequential strain path changes. Since VPSC7 allows to do sequential deformation histories in one run, now this file is not so relevant.

2-7-9 Output texture files TEX_PHn.OUT or TEX_ELn.OUT (units=31, 32 ….)

One texture file for each of the phases in the aggregate, or for each aggregate (element). The format is the same as the input texture file FILETEXT. It describes the crystal orientations with respect to the sample axes, and also gives the volume fraction of each orientation. The first 3 lines represent a heading. The fourth line contains a ‘B’ for Bunge convention and the number of orientations in the file. The following lines list, for each

grain, the three Euler angles and the associated volume fraction. It is possible to write also: the accumulated Von Mises strain, the Von Mises stress, the accumulated plastic work and the Taylor factor of each orientation. In order to do so, one line has to be un-commented inside SUBROUTINE WRITE_TEXTURE. If IWRITE=0 is used for the run, only the final texture is written in TEX_PHn.OUT. If IWRITE=m is used for the run, also the intermediate textures after every 'm' steps are written in TEX_PHn.OUT.

TEXTURE AT STRAIN = 0.0600
1.032 1.029 0.942 <-- axes length of macro ellipsoid
90.00 0.00 0.00 <-- Euler angles of macro ellipsoid (deg)
B 2916
4.93 8.02 85.07 0.0002751 0.6620E-01 0.4094E+01 0.1982E+00 0.9576E+00
5.19 8.03 74.82 0.0001615 0.6627E-01 0.4091E+01 0.1982E+00 0.9568E+00
5.34 8.06 64.66 0.0000407 0.6641E-01 0.4083E+01 0.1983E+00 0.9552E+00
5.32 8.10 54.68 0.0000076 0.6655E-01 0.4074E+01 0.1983E+00 0.9537E+00
5.13 8.13 44.87 0.0000046 0.6662E-01 0.4068E+01 0.1983E+00 0.9529E+00
……
……

2-7-10 Final morphologic texture MOR_PHn.OUT or MOR_ELn.OUT (units=41, 42 ….)

One texture file for each of the phases in the aggregate or for each aggregate (element). The format is the same as the input texture file FILEAXES. It describes the orientations of each grain's ellipsoid with respect to the sample axes, and gives the length of the ellipsoid axes. The first 3 lines represent dummy headings. The fourth line contains a 'B' for Bunge convention, and the number of orientations. The following lines list the three Euler angles and the length of the three axes for each grain.

MORPHOLOGY AT STRAIN = 0.5000
1.282 1.282 0.603 <- axes of macro ellipsoid
90.00 90.00 90.00 <- Euler angles of macro ellipsoid (deg)
B 500
94.60 99.56 25.35 1.5636 1.0729 0.5890
96.89 88.30 134.84 1.5549 1.1176 0.5679
98.97 95.30 58.33 1.5550 1.0552 0.6026
84.37 97.70 156.30 1.3533 1.1363 0.6454
80.06 93.30 109.18 1.5498 1.0561 0.6042
……

……

2-7-11 Rolling components for each phase CUBCOMPn.OUT (units=61, 62 ….)

One file for each of the phases in the aggregate or for each aggregate (element). Each line gives the current accumulated deformation and the volume fraction of each cubic rolling component: Balance, COPPER, BRASS, S, GOSS, CUBE , ROTATED CUBE and the average misorientation.

EPS	*OTH*	*CU*	*BR*	*S*	*GOS*	*CUB*	*ROT*	*AVMISO*
0.0100	*53.8*	*6.6*	*6.5*	*14.1*		*2.7*	*6.9*	*9.3*	*16.1*
0.0200	*53.8*	*6.6*	*6.7*	*13.9*		*2.7*	*6.9*	*9.3*	*16.1*
0.0300	*53.7*	*6.6*	*6.7*	*14.0*		*2.8*	*6.9*	*9.3*	*16.1*
……									
……									
0.1500	*52.4*	*4.2*	*10.3*	*12.1*		*3.5*	*6.9*	*10.6*	*16.3*
0.1600	*52.8*	*3.8*	*10.6*	*11.7*		*3.6*	*6.9*	*10.6*	*16.3*

2-7-12 Convergence control file for the second-order procedure SO.OUT (unit=97)

Output from convergence procedure associated with the rate exponent and second-order loops in SUBROUTINE VPSC. The relative errors ERRASO and ERRESO are calculated as averages of the relative errors of the two scalar magnitudes defined per system and per grain (see Eq. 8-17). It is written only if INTERACTION=5.

2-7-13 Average fluctuations and SD per grain FLUCT.OUT (unit=83)

This file contains the equivalent stress and strain-rate first-order moments (average values), second-order moments (average field fluctuations, Eqs. 8-9) and Standard Deviations (SD) (Eqs. 8-10) in every grain, plus the values of the overall SDs (inter+intragranular) (Eq. 8-11), and intergranular only (inter), after every deformation step. It is written only when IFLUCT=1.

STEP = 1
NRS = 3

GR#	SEQ1	SEQ2	SDSEQ	DEQ1	DEQ2	SDDEQ
1	0.639E-01	0.104E+00	1.272	0.147E-07	0.224E-07	1.693
2	0.729E-01	0.114E+00	1.350	0.156E-07	0.225E-07	1.623
. . .						
499	0.665E-01	0.105E+00	1.253	0.141E-07	0.221E-07	1.706
500	0.971E-01	0.126E+00	1.229	0.622E-08	0.181E-07	1.706

S SDPX (inter+intra) = 1.511
S SDPX (inter) = 0.771
D SDPX (inter+intra) = 1.836
D SDPX (inter) = 0.766

SECTION 3: EXAMPLES AND APPLICATIONS

In this Section we describe several application examples for which we provide the INPUT and the OUTPUT files. These examples illustrate the capabilities of VPSC, and the characteristics of the interaction approaches implemented in the code. These examples should be useful both, for testing the installation of the code, and for becoming acquainted with INPUT files and procedures corresponding to different loading conditions and material properties. Input files VPSC7.IN, initial texture, single crystal parameters, and process files are given in all cases. Output files with final texture, stress-strain history, statistics and activity are also included.

Examples #1 to #6 correspond to cubic aggregates. Example #7 corresponds to an HCP aggregate deforming by slip and twinning. Example #8 corresponds to orthotropic olivine, a geological material with less than 5 independent slip systems. Example #9 applies to (hexagonal) ice, and shows how the Second Order formulation deals with a material with mostly one active deformation mode (basal).

The associated I/O files are stored in separate directories labeled EXAMPLEn. The files themselves have the same name as described in the manual, but the extension identifies the different cases considered in the example. For example VPSC7.INb and TEX_PH1.b are the input file VPSC7.IN and the output file TEX_PH1.OUT, corresponding to Case b.

EXAMPLE 1: Tension and compression of FCC

This simple example is meant to familiarize the user with a basic simulation of texture evolution, and to visualize the difference that the interaction assumption makes in the response of the material. For experimental textures and a more comprehensive analysis of the modeling results see T&A, Chapter 5, Section 1.1, and T&A, Chapter 11, Section 5.1.

Run conditions:

- Random texture file with 500 orientations (file RAND500.TEX).
- FCC crystal with slip on (111)<110> and no hardening: Voce parameters $\tau_0 = 1, \tau_1 = 0, \theta_0 = 0, \theta_1 = 0$ (file FCC.SX). The rate sensitivity parameter is n=20.

- Axial tension and compression along x_3 up to ε_{33}=100%. All velocity gradient components are imposed (files TENSION.3 & COMPRE.3).

The results are illustrated in terms of inverse pole figures, showing the tensile or compressive axis in the crystal reference frame (Figure 1-1) and the stress-strain response and the slip system activity as a function of the deformation strain (Figure 1-2).

The simulations were done using: the Full Constraints approach (INTERACTION=0), the affine formulation (INTERACTION=1), the secant formulation (n^{eff}=1, INTERACTION=2), an intermediate grain-medium interaction (n^{eff}=10, INTERACTION=3), the tangent formulation (n^{eff}=20, INTERACTION=4), and the Second Order formulation (INTERACTION=5).

The output files provided are: stress vs strain (STR_STR.*), activity of slip systems (ACT_PH1.*) and final texture (TEX_PH1.*). The extension identifies tension (t) or compression (c) plus the particular interaction approach used (0-6). For example TEX_PH1.c3 is the texture after 100% compression using INTERACTION=3.

It is evident that the different approximations predict differences in final texture, stress evolution and system activity. The secant case represents a stiff grain-matrix interaction, and is close to the upper bound represented by the full constraints case (infinitely stiff). The more compliant cases, tangent and second order, are more efficient in accommodating deformation and closer to a lower bound: they require less active systems per grain because grains tend to deform by plane (as opposed to axial) strain, and they also require lower yield stress. The affine case and n^{eff}=10 give results between the upper and lower bounds, and their predictions are probably more realistic. The more relevant consequence of the SC formalism is that for compression it correctly predicts that the compressive axis tends to align with the <110> crystal direction, a result that the full constraints formulation fails to predict: the maximum predicted by the FC model is shifted away from such direction (see Fig 1-1).

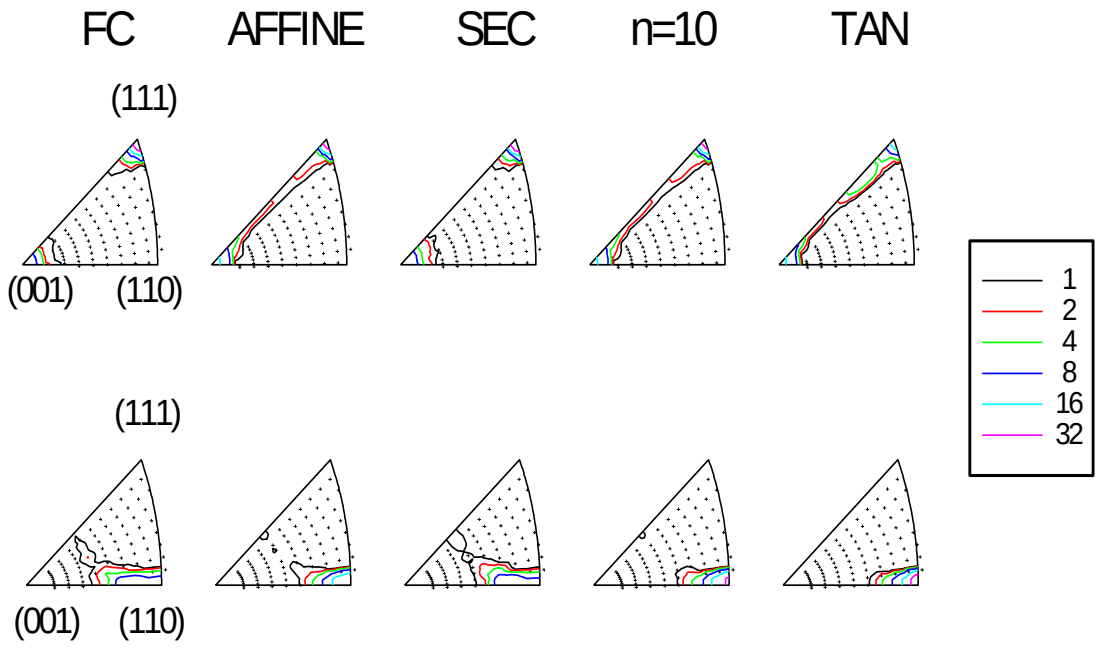

Figure 1-1: Inverse pole figure of the tensile (top) and the compressive axis (bottom) after 100% strain. Simulations were done using: Full Constraints (FC), affine, secant (SEC), n^{eff}=10, and tangent (TAN) in the interaction equation. In all cases n=20 was used.

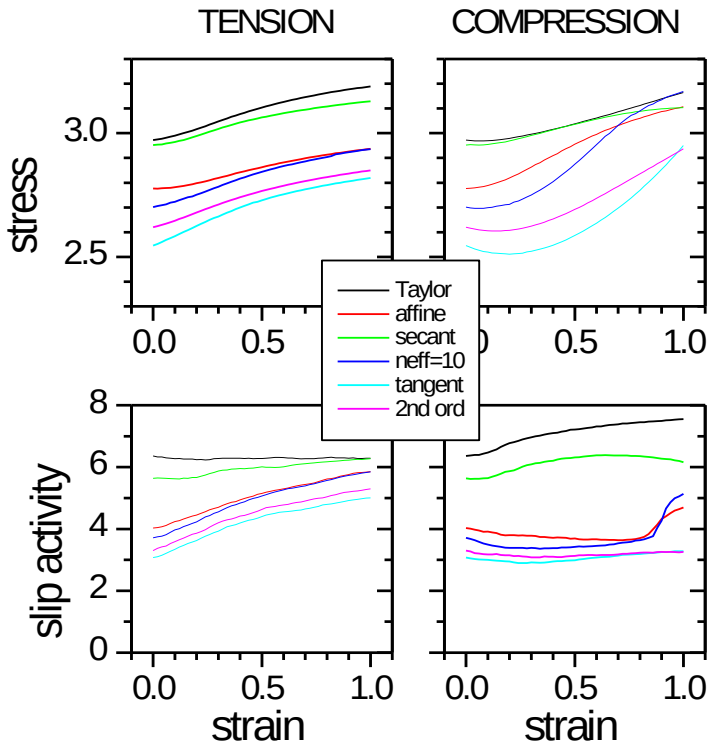

Figure 1-2: Evolution of stress and Average Active Systems per Grain during tensile and compressive deformation of FCC polycrystal up to 100% strain. See also caption to Figure 1-1.

EXAMPLE 2: Rolling of FCC

This example is meant to familiarize the user with the simulation of sequential processes and the rolling 'capabilities' of VPSC7. Rolling (plane strain) to 63% reduction is followed by a calculation of the Polycrystal Yield Surface, and a calculation of Lankford coefficients and directional Young modulus. The evolution of the characteristic rolling components is also provided.

In addition there is a simulation of non-uniform deformation path (variable shear superimposed to plane strain) using the SUBROUTINE VAR_VEL_GRAD.

For experimental textures and a more comprehensive discussion see Kocks et al (Chapter 5, Section 1.2) (2000), and Engler et al (2000).

Run conditions:

- Initial random texture file RAND500.TEX with 500 orientations.
- FCC crystals with slip on (111)<110> and linear hardening $\tau_0 = 1, \tau_1 = 0, \theta_0 = 1, \theta_1 = 1$ (file FCC.SX2).
- Rolling up to ε_{33}=100%. All velocity gradient components are imposed (file ROLLING).
- Linearization used: INTERACTION=3 (Neff=10)

Case A:

Plane strain deformation (rolling), followed by a calculation of a π-plane projection of the Polycrystal Yield Surface corresponding to ε_{33}=100%, followed by a calculation of the Lankford coefficients and the directional Young moduli in the plane of the sheet. Corresponding data is reported in files TEX_PH1.a, PCYS.a and LANKFORD.a. In addition, setting ICUBCOMP=1 allows us to calculate the evolution of several texture rolling components (Goss, cube, copper, etc) with deformation (see file CUBCOMP1.a). For calculating the π-plane projection of the PCYS set IVGVAR=2 and choose stress components #1 and #2 inside VPSC7.IN. The calculation of the Lankford coefficients

requires to declare IVGVAR=3 in VPSC7.IN. The tensile 'probing' is done at angular increments of 10° between the RD and the TD.

The linear hardening used in this example will not affect the final texture, or the Lankford coefficient, or the shape of the PCYS. Only the scale of the PCYS is affected.

Case B:

Same as Case A, but superimposing a shear/reverse shear component to the plane strain deformation ($udot_{13}$ = $udot_{31}$ = 1.25*sin($2\pi\varepsilon_{33}$)). The velocity gradient imposed at each step is read inside SUBROUTINE VAR_VEL_GRA from the input file LIJ_HIT.DAT, which contains the successive component of the velocity gradient and the time increments. See format below:

51 7 0.02 298. nsteps ictrl eqincr temp

step	L11	L12	L13	L21	L22	L23	L31	L32	L33	tincr
1	0.1000E+01	0.0000E+00	0.0000E+00	0.0000E+00	0.0000E+00	0.0E+00	0.0000E+00	0.0E+00	-0.1000E+01	0.2E-01
2	0.1000E+01	0.0000E+00	0.1567E+00	0.0000E+00	0.0000E+00	0.0E+00	0.1567E+00	0.0E+00	-0.1000E+01	0.2E-01
3	0.1000E+01	0.0000E+00	0.3109E+00	0.0000E+00	0.0000E+00	0.0E+00	0.3109E+00	0.0E+00	-0.1000E+01	0.2E-01
4	0.1000E+01	0.0000E+00	0.4602E+00	0.0000E+00	0.0000E+00	0.0E+00	0.4602E+00	0.0E+00	-0.1000E+01	0.2E-01
5	0.1000E+01	0.0000E+00	0.6022E+00	0.0000E+00	0.0000E+00	0.0E+00	0.6022E+00	0.0E+00	-0.1000E+01	0.2E-01

……

Texture, π-plane projection of the Yield Surface, and Lankford coefficients vs angle are calculated for the 100% rolled aggregate, and reported in files TEX_PH1.b, PCYS.b and LANKFORD.b. The evolution of the rolling components is also plotted and listed in file CUBCOMP1.b.

Observe in Fig 2-1 that the shear component breaks the orthotropic symmetry of the texture. Figure 2-2 shows that it also affects the formability properties of the rolled sheet, which now exhibits Lankford coefficients below one for every angle.

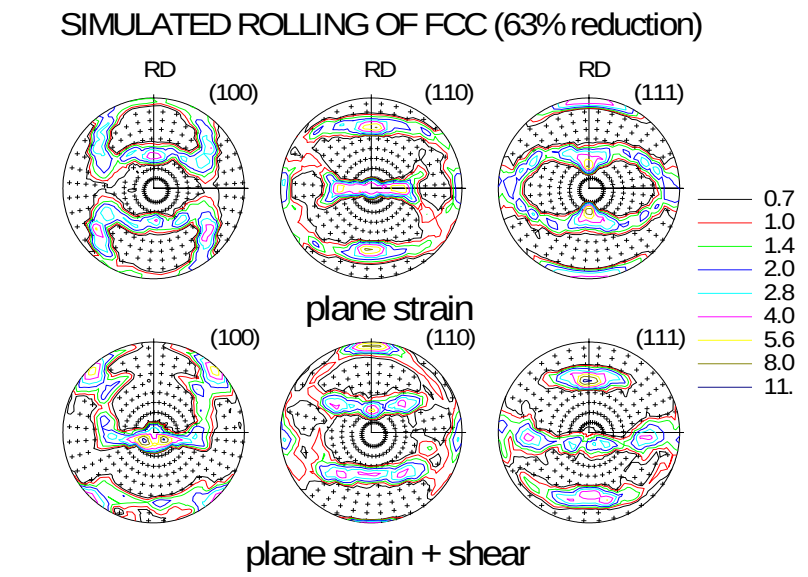

Figure 2-1: Simulated final textures after 63% rolling reduction. (a) enforcing plane strain; (b) superimposing a shear/reverse shear component to the plane strain component.

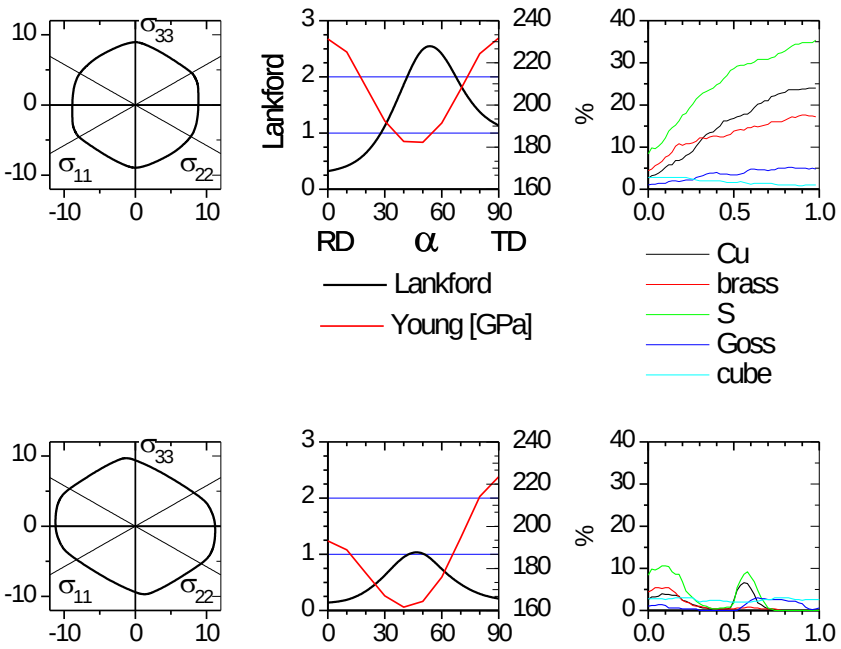

Figure 2-2: Polycrystal Yield Surface, Lankford coefficient, directional elastic Young modulus associated with plane strain (63% rolling reduction), and plain strain + shear. Also shown is the evolution of the FCC ideal rolling components of the texture.

EXAMPLE 3: Rolling of BCC

This example is meant to familiarize the user with the simulation of sequential processes, the calculation of Lankford coefficient, and with crystals that exhibit more than one deformation mode.

For experimental textures and a more comprehensive discussion see Kocks et al (2000) (Ch. 5, Section 2.3) and Engler et al (2000)

Run conditions:

- Initial random texture file RAND500.TEX with 500 orientations.
- BCC crystals with slip on {110}<111>, {112}<111>, {123}<111>. No hardening is assumed and all systems are assigned the same CRSS $\tau_0 = 2, \tau_1 = 0, \theta_0 = 1, \theta_1 = 0$ (file BCC_Fe.SXa and BCC_Fe.SXb).
- Plane strain up to ε_{33}=100% (63% reduction) using one or three deformation modes.
- The affine linearization (INTERACTION=1) was used for the calculations. Itgives similar results as the n^{eff}=10 linearization (INTERACTION=3).

Cases A and B:

These two cases differ in that deformation is accommodated using either {110}<111> slip, or {110}<111> + {112}<111> + {123}<111> slip, respectively. The latter case can be regarded as a good approximation to 'pencil glide'. Corresponding output files are identified with extensions *.a and *.b , respectively. Figure 3-1 depicts the texture and Figure 3-2 shows the mode activity and the Lankford coefficient of the rolled sheet.

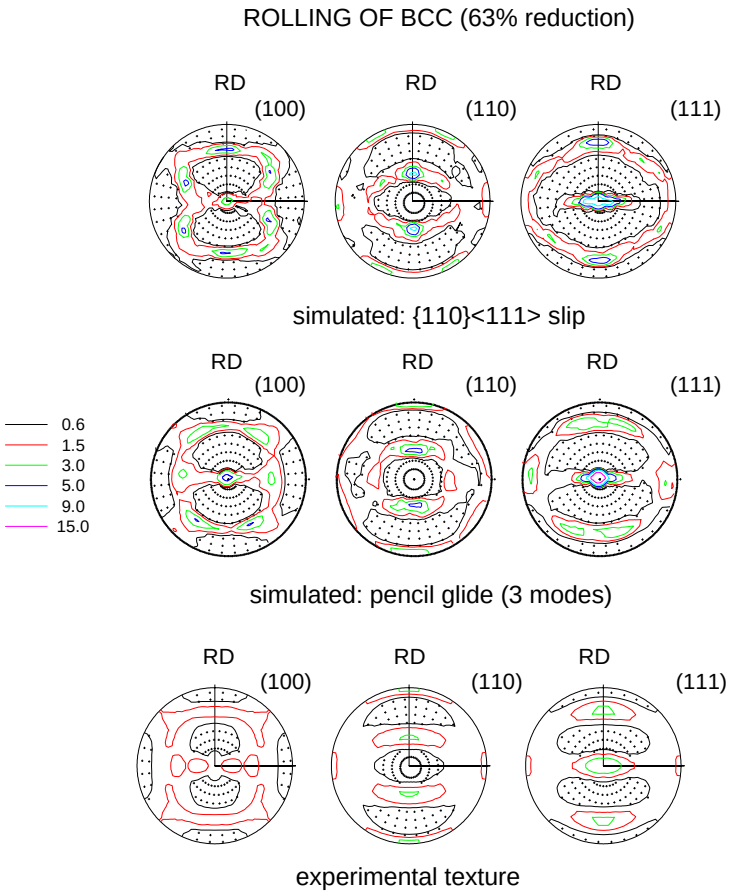

Figure 3-1: Texture of BCC after 63% rolling reduction. Simulations assume either {110}<111> slip, or {110}<111> + {112}<111> + {123}<111> slip (pencil glide).

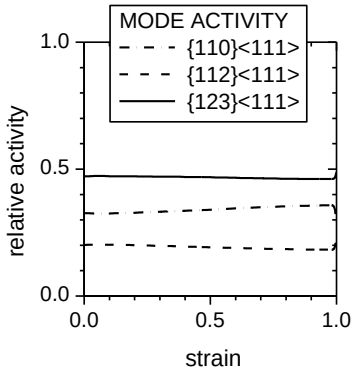

Figure 3-2: BCC after 63% rolling reduction. Relative contribution to deformation of the three modes associated with pencil glide.

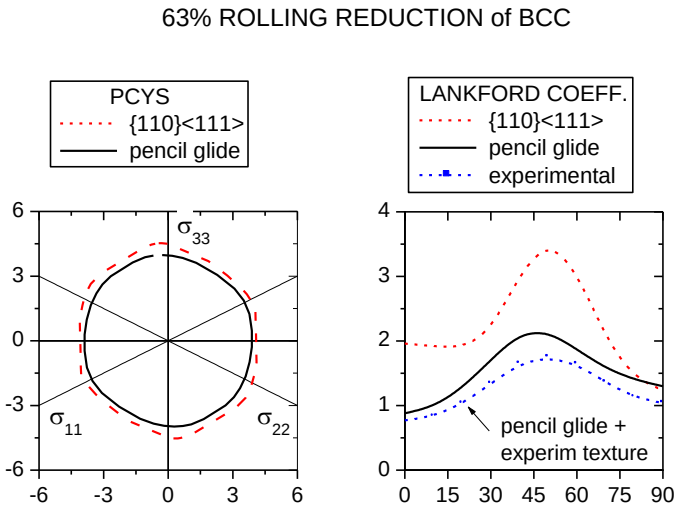

Figure 3-3: BCC after 63% rolling reduction. Effect of using single or pencil glide. (a) Polycrystal yield surface; (b) Lankford coefficient predicted following rolling. Comparison with Lankford coefficient calculated directly from the experimental texture of Fig. 3-1.

It is possible to see that using two or three slip modes gives very similar results for the final texture, the PCYS and the Lankford coefficient. This result suggests that two modes suffice to simulate pencil glide. In addition, pencil glide gives a texture that more closely resembles the experimental one (see Fig. 3-1). When three modes are used activity is dominated by {123}<111> slip, since it has 24 systems associated, as opposed to 12 for each of the other two modes (Fig. 3-2). In addition, in the case of pencil slip the Average Number of Active Systems per grain (AVACS) is about 9 and the PCYS is more rounded.

EXAMPLE 4: Rolling of a two-phase FCC+BCC aggregate

This example is meant to familiarize the user with the multi-phase feature in VPSC. An aggregate is defined containing 50% volume fraction of FCC grains and 50% of BCC grains. The former harden according to the linear law of EXAMPLE 2 (FCC.SX2). The latter correspond to the CASE A of EXAMPLE 3, and do not harden (Fe.SXa). There is only one deformation mode in each phase: {111}<110> in FCC, and {110}<111> in BCC.

Run conditions:

- Initial random texture file RAND500.TEX with 500 orientations, for each phase.
- FCC crystals with slip on {111}<110> and linear hardening $\tau_0 = 1, \tau_1 = 0, \theta_0 = 1, \theta_1 = 1$ (file FCC.SX2).
- BCC crystals with slip on {110}<111> and no hardening $\tau_0 = 1, \tau_1 = 0, \theta_0 = 1, \theta_1 = 0$ (file Fe.SXa).
- Plane strain up to ε_{33}=100%. All velocity gradient components are imposed. INTERACTION=1 corresponding to affine linearization.

The final texture of each phase is plot in Figure 4-1 and the relative contribution to deformation of each phase is reported in Figure 4-2. The corresponding texture output files are TEX_PH1.OUT and TEX_PH2.OUT, while the activity files are ACT_PH1.OUT and ACT_PH2.OUT. At the beginning the FCC phase contributes more to the total shear because the CRSS for slip is half the CRSS in the BCC phase. However, as the FCC phase hardens, the slip activity decreases in FCC and increases in the BCC phase, and eventually the latter accommodates more deformation than the FCC. As a consequence, the texture of the FCC phase is similar to the one of Example 2 (FCC rolling to 63% reduction) and the texture of the BCC phase is similar to the one of Example 3 because the contribution from each phase to the total strain is similar.

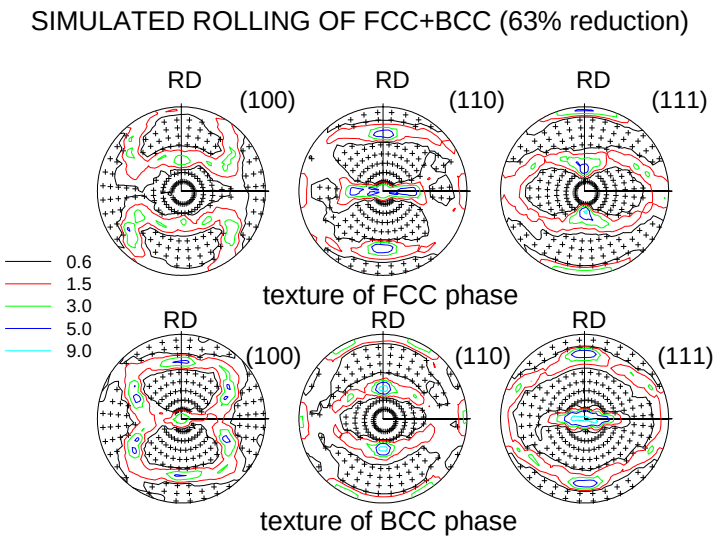

Figure 4-1: Texture of the FCC and BCC phases after 63% rolling reduction.

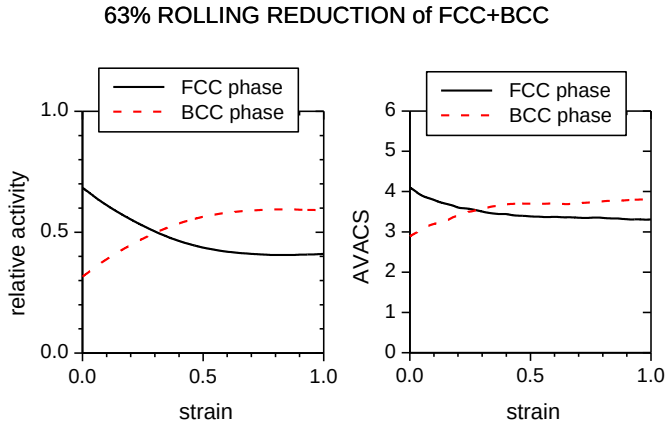

Figure 4-2: Relative slip activity (contribution to total shear) in the FCC and BCC phases during rolling. Average Number of Active Systems per grain (AVACS) in the FCC and BCC phases.

EXAMPLE 5: Torsion (shear) of FCC

This example is meant to familiarize the user with the simulation of sequential processes, the calculation of Polycrystal Yield Surfaces, and with imposing mixed conditions on velocity gradient and stress components.

For experimental textures and a more comprehensive discussion see Kocks et al (2000; Chapter 5, Section 1.3).

Run conditions:

- Initial random texture file RAND500.TEX with 500 orientations.
- FCC crystals with slip on (111)<110> and linear hardening $\tau_0 = 1, \tau_1 = 0, \theta_0 = 1, \theta_1 = 1$ (file FCC.SX2).
- Shear up to ε_{12}=200%. Some velocity gradient, and some stress components are imposed (files TORSION.a and TORSION.b).

Case A:

Fixed ends torsion up to ε_{12}=200%. 1 is the circumferential direction, 2 is the axial direction and 3 is the radial direction of the tube. σ_{11} and σ_{33} are enforced to be zero. During torsion σ_{22} increases up to -2.3 and then reverses trend and ends up being +0.7. The shear component σ_{12} increases monotonically to 8.1 (see Figure 5-2).

Case B:

Free ends torsion up to ε_{12}=200%. 1 is the circumferential direction, 2 is the axial direction and 3 is the radial direction of the tube. σ_{11} and σ_{33} are enforced to be zero. In addition, the axial stress σ_{22} is also imposed to be zero. During torsion ε_{22} increases monotonically to +34%. The shear component σ_{12} increases monotonically to 8.3 (see Figure 5-2). For the PCYS calculation, when prompted through the screen, choose stress components #1 and #5.

The final textures for Case A and Case B are depicted in Figure 5-1. They are very similar and typical FCC shear textures. However, the free ends texture is slightly rotated

clockwise with respect to the fixed end texture. Such difference is what leads to the development of an axial strain component. The situation is clearly illustrated by the PCYS in Figure 5-2. Observe that at ε_{12}=100% , the normal to the PCYS at the intersection with the σ_{22} axis has a marked positive component. Such component tends to disappear when ε_{12}=200%.

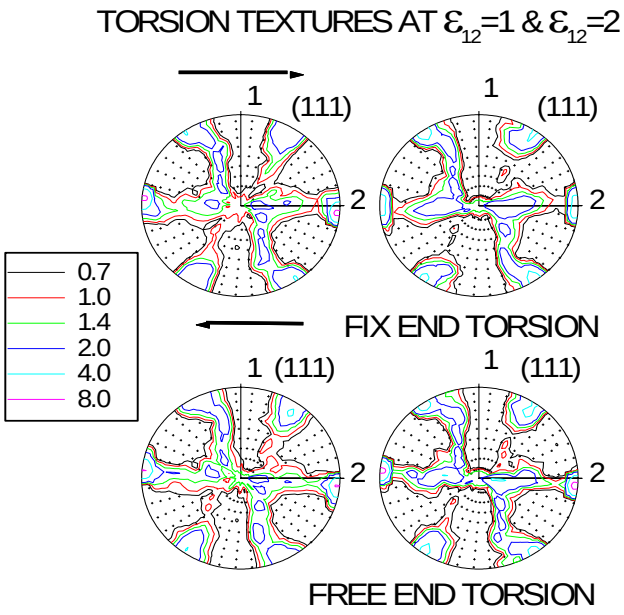

Figure 5-1: (111) pole figures associated with fix-end and free-end torsion testing.

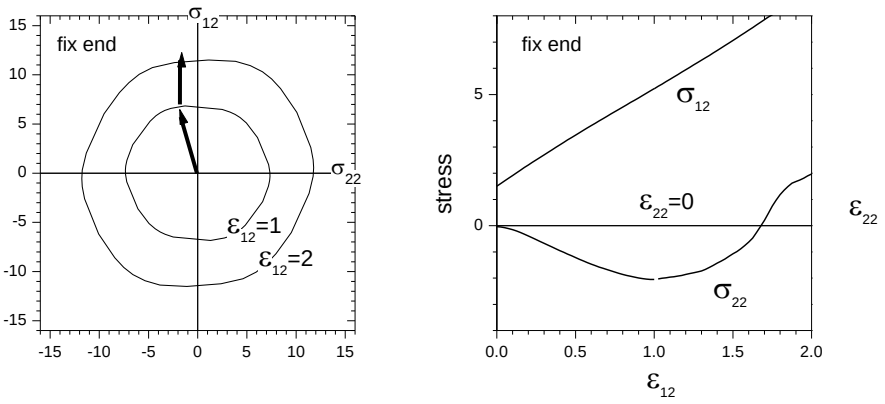

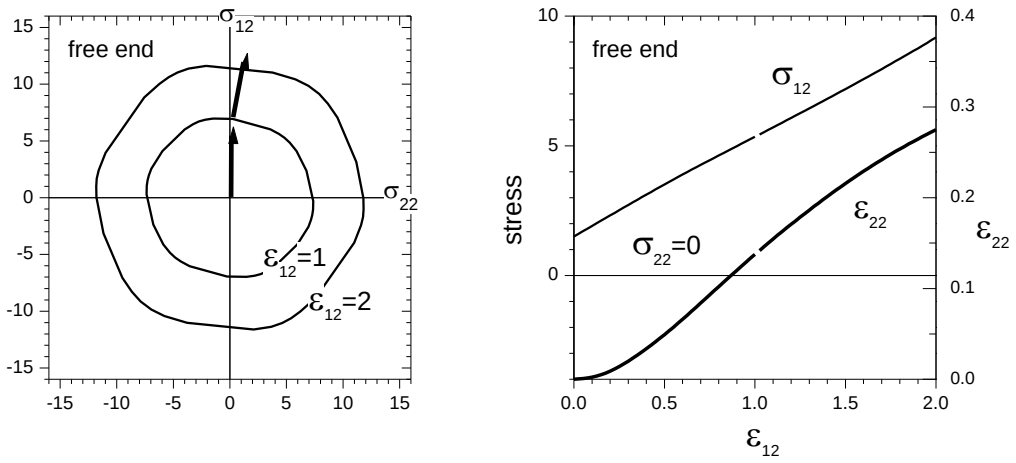

Figure 5-2: Fix-end case: PCYS at 100% and 200% shear, and variation of shear stress and axial stress components. Free-end case: PCYS at 100% and 200% shear, and variation of shear stress and axial strain components. Notice interpretation in terms of normality rule in both cases.

EXAMPLE 6: Application of MTS model to rolled aluminum

This example is the only one in the manual where we use the MTS hardening model described in Section 6-2. This application compares evolution of yield stress during compression, at different temperature and/or rates. It includes a simulation of strain-rate jump.

Run conditions:

- Mesured initial texture of a rolled cold-strip aluminum (file Al_ROLL.TEX → 956 orientations). Directions {1,2,3} correspond to {RD,TD,ND}.
- FCC crystals with slip on (111)<110> and MTS parameters adjusted to reproduce experimental compression results by Kok et al (2002) (file Al_5182.SX).
- Uniaxial compression up to ε_{11}=30% along the RD. σ_{11} and σ_{22} are enforced to be zero. The following conditions are simulated:

  Reference: T=298K at a rate of 10^{-3} s^{-1} . File COMP_RF1.30

  High temp: T=598K at a rate of 10^{-3} s^{-1} . File COMP_HT1.30

  High rate: T=298K at a rate of 10^{3} s^{-1} . File COMP_HR1.30

  Mix rates: T=298K, 15% at 10^{-3} s^{-1}, 15% at 10^{3} s^{-1} . Files COMP_RF1.15 and COMP_HR1.15

The texture of the initial and compressed material is depicted in Figure 6-1. The stress-strain response is given in Figure 6-2.

Case A:

A file VPSC7.INa is provided. The user has to replace the proper 'process' file at the end in order to reproduce the data. Those files are COMP_RF1.30, COMP_HT1.30, and COMP_HR1.30

The initial texture is depicted in Fig 6-1 (a) and the 30% compression texture in Fig. 6-1 (b). Rate or temperature conditions do not affect the texture development.

The stress is clearly much lower at 598K, and much higher at $10^{3}s^{-1}$ (see Fig. 6-2)

Case B:

A file VPSC7.INb is provided containing the sequence of 15% deformation processes: COMP_RF1.15 (low temp & low rate) followed by COMP_HR1.15 (low temp & high rate).

The final (30% compression) texture is shown in Fig. 6-1 (c). Observe that it is identical to Fig. 6-1 (b), indicating again that it is independent of the deformation rate.

The stress at the high rate transition evolves different than for the monotonic high rate case (see Fig. 6-2).

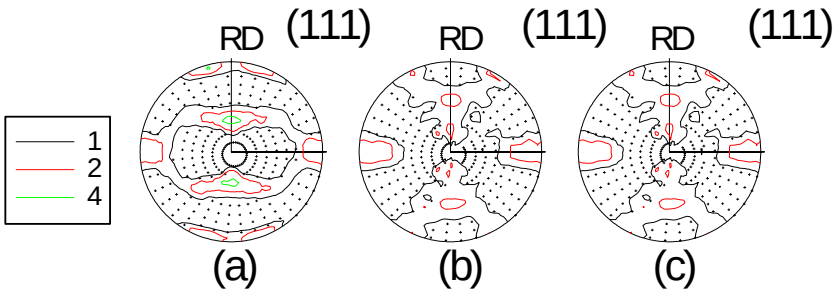

Figure 6-1: (111) pole figures of Aluminum 5182. (a) Initial rolling texture; (b) Texture after 30% compression along RD at reference temp and rate; (c) Texture after 15% deformation at low rate followed by 15% at high rate, all done at 298K. Observe that texture is independent of rate.

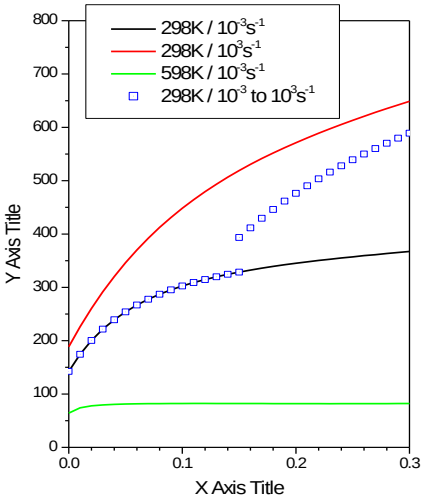

Figure 6-2: Macroscopic hardening of AA5182 in compression along RD, predicted by the MTS model, for different loading conditions discussed in the text.

EXAMPLE 7: Twinning and anisotropy of HCP Zr

Zirconium is an HCP metal below about 900 K. This example is meant to familiarize the user with a system which exhibits slip and twinning deformation modes, and which is highly anisotropic both, at the single crystal and polycrystal level. This is the only example in this manual where twinning is considered. Twinning is treated using the Predominant Twin Reorientation scheme described in Section 7.1. Hardening is treated with the extended Voce law and latent hardening parameters that empirically account for the barrier effect of twins upon dislocations or other twins.

In this example we use the constitutive law for Zr at room temperature reported by Kaschner et al (2006). The parameters are reported in Table 7.1 below. We also report the parameters for liquid nitrogen temperature (76K) but do not provide examples. These parameters are slightly different from the ones reported by Tomé et al (2000): the difference reflects a different Zr batch and modifications made in the treatment of hardening since 2000.

Run conditions:

- Initial texture (Zr_5678.TEX) is represented using 1944 orientations and corresponds to clock-rolled and annealed Zr plate with a strong basal component (hard) along the ND (direction 3) of the plate (see Fig. 7.1).
- HCP crystals deform by (10-10)<11-20> prismatic <a> slip, (10-11)<11-23> pyramidal <c+a> slip and (10-12)<11-23> tensile twinning at room temperature. We include (11-22)<11-2-3> compressive twins in the calculation, although their hardening parameters are such that they do not contribute to deformation at 293K. The single crystal hardening parameters (file Zr_293K.SX) were adjusted to experimental tensile and compression data. We also provide the 76K parameters in file Zr_76K.SX. See Table 7.1 below.

	τ_o [MPa]	τ_1 [MPa]	θ_o [MPa]	θ_1 [MPa]	$h^{*,PR}$	$h^{*,PY}$	$h^{*,TT}$	$h^{*,CT}$
T_1 = 76K								
Prismatic	45	42	1290	25	1	1	10	2
Pyramidal	495	100	1000	15	1	1	2	2
Tens Twin	102	17	100	30	1	1	10	16
Comp Twin	270	30	1000	178	1	1	10	5
T_2 = 293K								
Prismatic	19	16	1289	82	1	1	10	2
Pyramidal	145	192	1684	5	1	1	2	2
Tens Twin	102	17	100	30	1	1	10	16
Comp Twin	270	30	1000	178	1	1	10	5

Table 7-1. Voce and latent hardening parameters for VPSC/PTR constitutive model of Zr deformed at 76K and 300K. (Kaschner et al, 2006).

- We use the option INTERACTION=3 ($n^{eff}=10$) to represent the stiffness of the grain-matrix interaction in the Effective Medium formulation.
- Uniaxial Through Thickness Compression (TTC 300K) up to ε_{33}=30% at a rate of 10^{-3}. $\sigma_{11}$and σ_{22} are imposed to be zero in order to allow for ovalization of the sample.
- Uniaxial In-Plane Compression (IPC 300K) up to ε_{11}=30% at a rate of 10^{-3}. σ_{22} and σ_{33} are imposed to be zero in order to allow for ovalization of the sample
- Uniaxial In-Plane Tension (IPT 300K) up to ε_{11}=30% at a rate of 10^{-3}. σ_{22} and σ_{33} are imposed to be zero in order to allow for ovalization of the sample.
- Uniaxial In-Plane Compression (IPC 76K) up to ε_{11}=30% at a rate of 10^{-3}. σ_{22} and σ_{33} are imposed to be zero in order to allow for ovalization of the sample

- In the first three deformation simulations initial (0%), intermediate (15%) and final (30%) yield loci are calculated both, to provide an example to the user on how to use this VPSC code feature, and to show the effect of twinning upon the yield surface. Only π-plane projections, corresponding to the subspace $(\sigma_1, \sigma_2) = \left[(\sigma_{22} - \sigma_{11})/\sqrt{2}, (2\sigma_{33} - \sigma_{22} - \sigma_{11})/\sqrt{6}\right]$,are calculated (see Section 2.5)

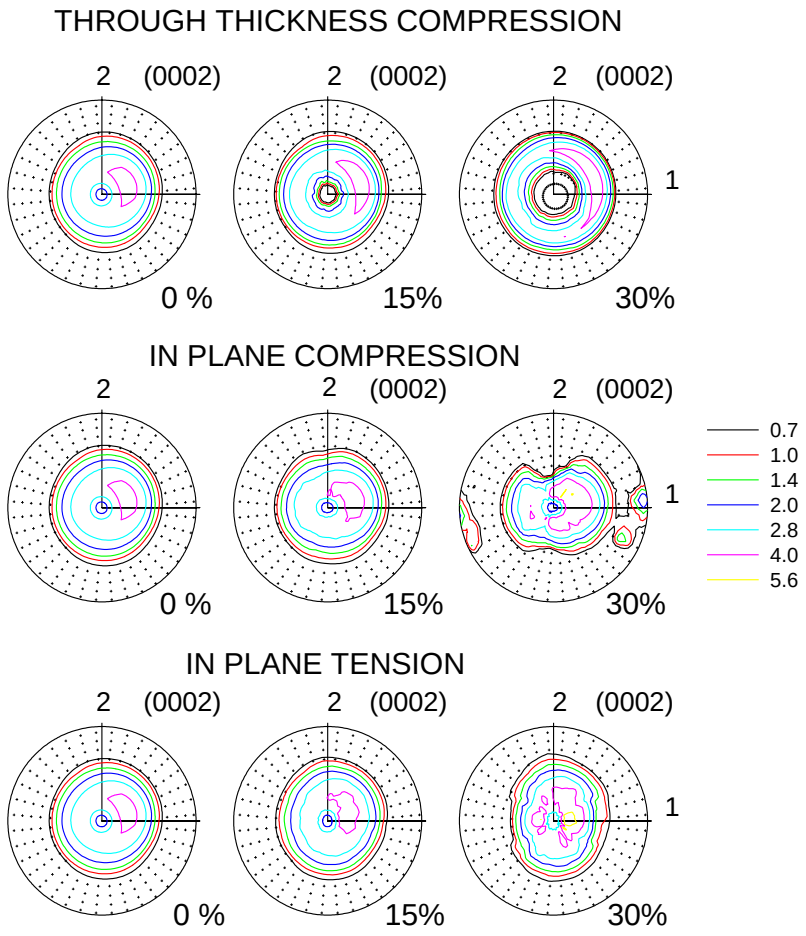

Figure 7-1: (0002) basal pole figures. Initial (0%) and predicted deformation textures of clock-rolled Zr after 15% and 30% deformation in Through Thickness Compression, In-Plane Compression and In-Plane Tension (referred to plate axes).

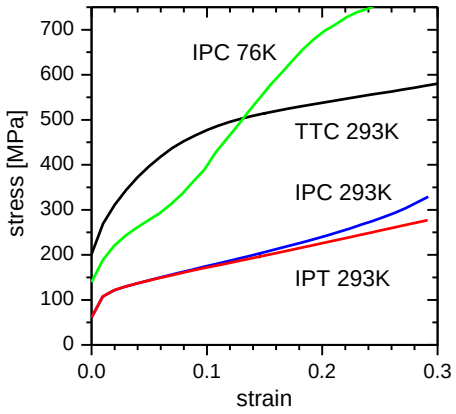

Figure 7-2: Predicted stress-strain curves of clock-rolled Zr deforming at room temperature in Through Thickness Compression, In-Plane Compression and In-Plane Tension (referred to plate axes).

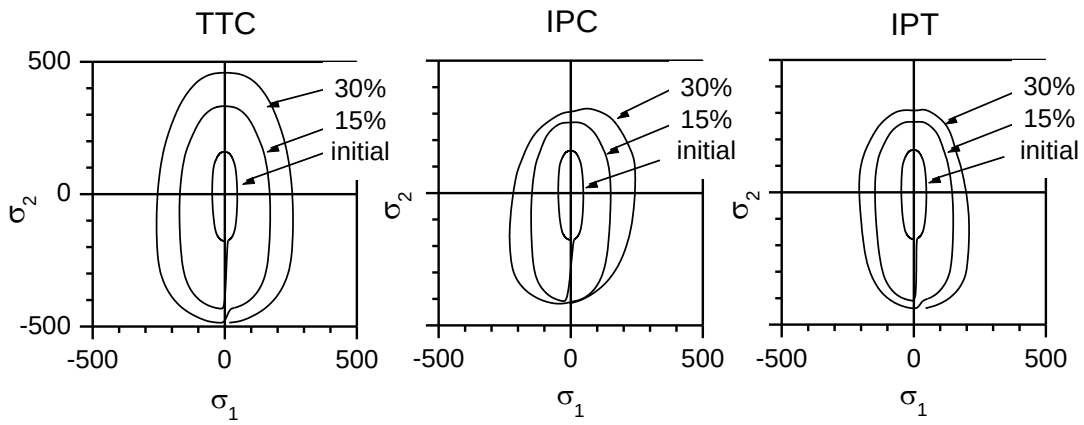

Figure 7-3: Polycrystal Yield Surface (π-plane projection) for Zr deforming in TTC, IPC and IPT at 300K. Intermediate projections calculated at 0%, 15% and 30% strain. Observe that the PCYS is not centro-symmetric due to the presence of tensile twinning. The increase in shape with deformation is associated with hardening. The shape distortion for the IPC case is associated with twinning reorientation.

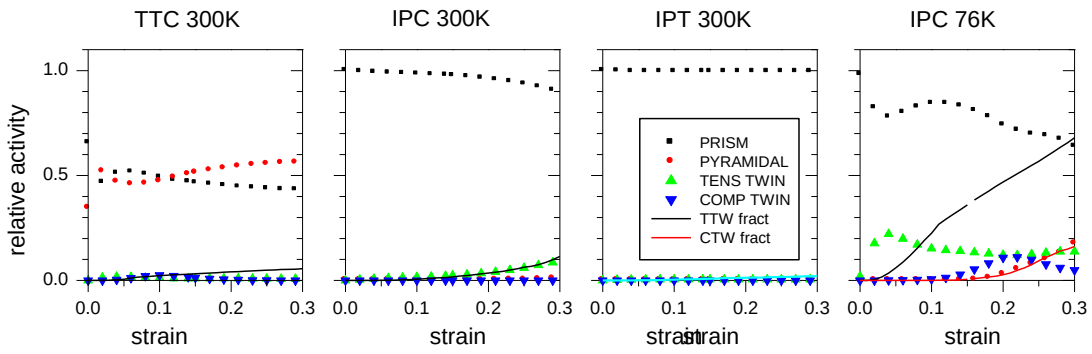

Figure 7-4: Relative contribution of prism slip, pyramidal slip and tensile twins to deformation for clock-rolled Zr, deforming at room temperature in TTC, IPC and IPT, plus IPC at 76K. Also shown is the volume fraction of twinned material as a function of strain. Compressive twinning does not contribute to deformation at room temperature but it does at liquid nitrogen.

Case A:

Through Thickness Compression ε_{33} =-30% (see file STR_STR.A and Fig. 7.2).The sample section remains approximately circular and the yield stress is much higher than the yield stress of Cases B & C because 'hard' <c+a> pyramidal slip has to be activated to accommodate TTC at room temperature. The reason is that deformation has to be accommodated using hard pyramidal slip in compression, together with easy prism slip. A small amount (5% volume fraction) of tensile twinning is predicted. See Figure 7-4 and file ACT_PH1.A.

Case B:

In Plane Compression ε_{11} =-30% (see file STR_STR.B and Fig. 7.2). The sample develops strong ovality, which practically amounts to plane strain deformation (ε_{22} =28.3% and ε_{33} =1.7%, see file STR_STR.B). About 12% of the aggregate twins but most deformation is accommodated with prism slip (see file ACT_PH1.B). The effect of twinning reorientation on the final texture is to develop a component along the compressive direction (see Figure 7-1).

Case C:

In Plane Tension ε_{11} =30% (see file STR_STR.C and Fig. 7.2). As in the case of IPC, the sample develops strong ovality (ε_{22} =-27.5% and ε_{33} =-2.5%, file STR_STR.C) because it deforms mostly by prism slip. Under this loading conditions the deviatoric stress along axis 3 is compressive: tensile twins cannot be activated, and pyramidal slip is too hard. As a consequence, all the deformation is accommodated with prism slip (see file ACT_PH1.C).

Case D:

In Plane Compression ε_{11} =-30% at 76K (see file STR_STR.D and Fig. 7.2). The sample develops strong ovality, which practically amounts to plane strain deformation (ε_{22} =25.5% and ε_{33} =4.5%, see file STR_STR.D). Most of the grains reorient: about 68% by tensile twinning and 16% by compressive twinning. Still, most deformation is accommodated with prism slip (see file ACT_PH1.D).

EXAMPLE 8: Compression of olivine ($MgSiO_4$)

Olivine (orthorhombic) enters in the composition of the Earth mantle. Olivine texture affects the characteristics of seismic wave propagation.

For a comprehensive discussion of simulation and experiments see Kocks et al (2000; Ch. 6, Sec. 1.4; Ch. 7, Sec. 3.5 and Ch. 11, Sec. 5.4).

This example is meant to familiarize the user with an application of VPSC to a material which lacks five independent slip systems, and show that the self-consistent formalism can still be used for describing plastic deformation to such systems. It also shows how to use the POSTMORTEM file, which is a feature of VPSC that allows to start from a previous deformation state, or to provide an initial guess for the first deformation step, in cases where the yield surface is open.

Run conditions:

- Initial random texture (RAND500.TEX → 500 orientations).
- Orthorhombic crystals with slip on:

  (010)<100> : $\tau_0 = 0.4$ and no hardening

  (001)<100> : $\tau_0 = 0.4$ and no hardening

  (010)<001> : $\tau_0 = 1.0$ and $\theta_1 = 4$ linear hardening.

In order to close the yield surface the following auxiliary slip systems with high CRSS are considered:

(110)<1-10>: $\tau_0 = 5.0$ and $\theta_1 = 4$ linear hardening.

(021)<1-12>: $\tau_0 = 5.0$ and $\theta_1 = 4$ linear hardening.

- Uniaxial compression. Strain increments of 2% up to ε_{33}=50% at a rate of 1^{-s}.

Case A:

Compression is simulated using the 5 slip modes described above. Texture and activity is recorded for comparison with Case B. Particularly relevant is the output file

POSTMORT.OUT, containing the initial stress tensor in every grain, and the initial polycrystal compliance. Observe that this file is written for the conditions following the first deformation step (ISAVE=1) but the simulation is run up for 25 deformation steps of 2%. POSTMORT.OUT can be written at any step in the deformation process (set ISAVE=istep), and used to restart the code from the associated polycrystal state.

Deformation is accommodated mostly by the three soft modes, which contribute from 90 to 80% of the shear (see ACT_PH1.a). Specifically, the mode (021)<1-12> exhibits a non-negligible activity in Case A, despite being much harder. The presence of the two hard modes has the effect of increasing the stress and the average number of active systems per grain by comparison with Case B (see Fig. 8.2). The final texture, though, is not affected by the extra slip modes (see Fig. 8.1).

Case B:

Compression is simulated using the 3 slip modes which are actually observed in olivine. The file POSTMORT.OUT of Case A is copied into POSTMORT.IN, and the variable IRECOVER is set to 1 in VPSC7.IN. The Single Crystal Yield Surface is open, but the run is started from the initial state contained in POSTMORT.IN in order to avoid the initial Taylor guess which is the default in VPSC. The code converges and simulates compression up to 50%. The final texture and the system activity are shown in Figure 8-1 and Figure 8-2. The final texture resembles the experimental one (Kocks et al, 2000) and deformation is accommodated using less than 3 active systems per grain (see Figure 8-2). See output files TEX_PH1.b and ACT_PH1.b. A comparison with Case A (files TEX_PH1.a and ACT_PH1.a) shows that the final texture is similar.

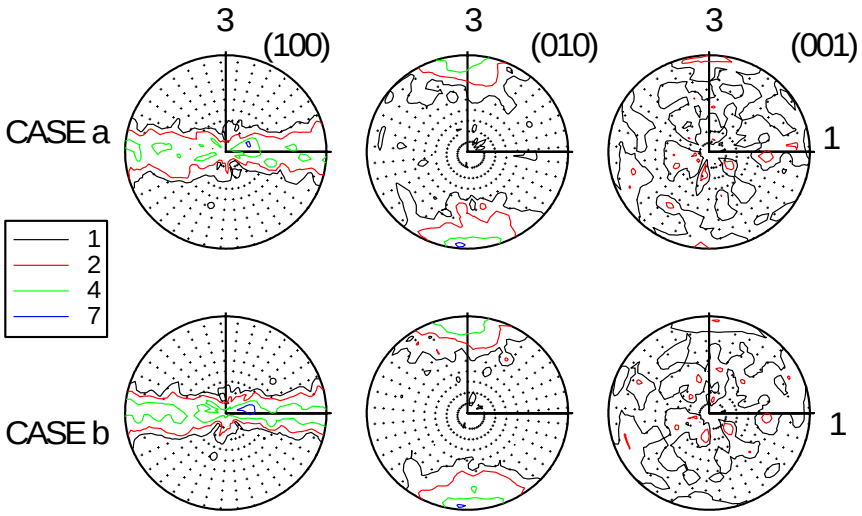

Figure 8-1: Pole figures after 50% compression along axis 3 of orthorhombic olivine. Observe that practically the same texture results from Cases A and B.

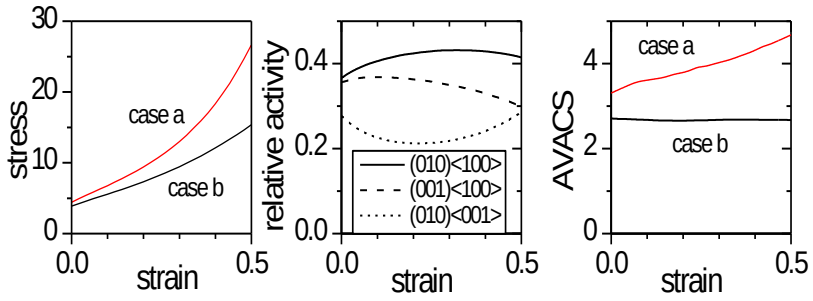

Figure 8-2: Comparison of compressive stress evolution for Cases A and B. Relative slip activity for case b. Average number of active systems per grain for Cases A and B.

EXAMPLE 9: Compression of polycrystaline ice (strain rate or stress imposed)

Due to the very large plastic anisotropy of hcp ice (i.e. while almost all the deformation in the single crystals is carried by basal dislocations, basal slip provides only two independent slip systems), the prediction of texture development of polycrystalline ice is a challenging problem serving to discriminate among the various SC approaches. Moreover, a better understanding of the deformation mechanisms and the microstructural evolution of ice deforming in compression is relevant in glaciology, since compression (together with shear) is one of the main deformation modes of glaciers. In what follows, we will use the basal texture factor along the axial direction (defined as the weighted average of the projections of the c-axis along that direction) to characterize the evolving texture of ice in compression.

Run conditions:

- Initial random texture (RAND500.TEX: 500 orientations).
- Hexagonal ice crystals deforming by easy (0001)<11-20> basal slip, hard (10-10)<11-20> prismatic <a> slip ($\tau_{pr}=20\times\tau_{bas}$), and harder (11-2-2)<11-23> pyramidal <c+a> slip ($\tau_{pyr}=200\times\tau_{bas}$). File ICE.SX.

Case A:

Uniaxial compression (strain fully imposed). 30 strain increments of 5%, up to ε=150% at a rate of $1x10^{-8}$ (order of magnitude compatible with glacier ice deformation) (file COMP150.3) using tangent (TG), affine (AF) and second-order linearization (SO). Files extensions are TGA, AFA and SOA. The auxiliary program TFACTOR.FOR uses the output texture file TEX_PH1 (renamed TFACTOR.IN) and gives the evolution on the basal texture factor along the axial direction.

On the one hand, the 'stiff' Taylor and SC secant models are not suitable to simulate plastic deformation of polycrystalline ice because the strong constraints that these models impose upon strain are incompatible with the shortage of independent slip systems in ice. On the other hand, the compression textures of ice typically exhibit a strong basal pole maximum along the axial direction. The formation of this maximum is related to the

crystallographic plastic rotations associated with basal slip. However, as the basal poles become aligned with the axial direction, the basal slip systems become unfavorably oriented to accommodate deformation. Therefore, at large strains even a 'soft' model like the tangent SC fails in reproducing the observed texture with only basal slip. Up to now, the oversimplified Sachs model (which completely disregards strain compatibility) has been the only approach able to give a reasonable effective behavior with predominant basal slip at large strains, when the basal texture along the compressive direction becomes very strong.

Fig. 9-1 shows the compression texture evolution (in terms of the basal texture factor along the axial direction), the effective stress, the relative basal activity, and the average number of active slip systems per grain, for the case of an initially random ice polycrystal. As expected, all models predict an increase of the basal texture factor along the axial direction, and a progressive geometric hardening. The tangent and the affine models predict the fastest and the slowest alignment of basal poles along the compression direction. This is consistent with the initial highest basal activity predicted by the tangent model, followed by the ones obtained with the SO and the affine formulations. However, at around 75% strain, the tangent results show a sudden drop in the basal activity, together with an increase in the effective stress (not attributable to geometric hardening only) and in the number of active deformation systems. All this indicates that, at large compressive deformation, the strain accommodation starts requiring the activation of the 200 times harder pyramidal systems. This is because within the tangent SC approach the basal slip is not enough to accommodate the compressive deformation once the basal poles become strongly aligned with the compression direction. The SO results are superior to the affine results, since the deformation takes place at higher basal activities, and also to the tangent results, since the SO model does not require the activation of the hard pyramidal mode, even after the texture factor reaches the value at which the tangent model predictions start to deteriorate.

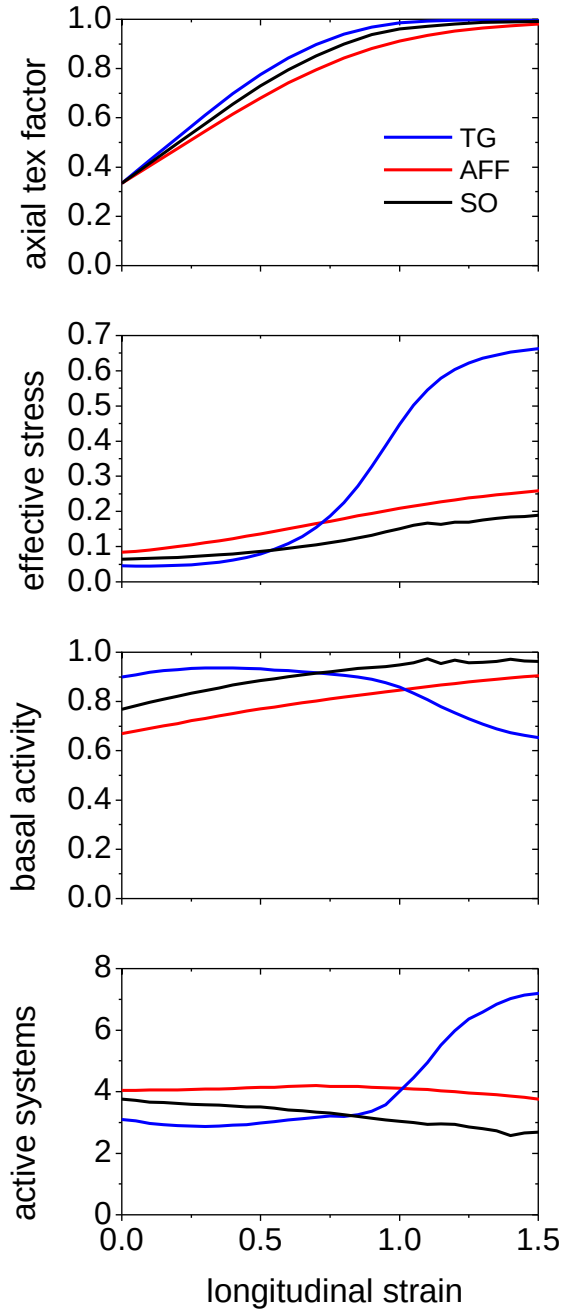

Figure 9-1: Basal texture factor along the compression direction, effective stress, relative basal activity, and the average number of active slip systems per grain. Case of compression of an initially random ice polycrystal, as predicted with the tangent, affine and second-order SC approaches.

Case B:

Axisymmetric creep (stress fully imposed, only non-vanishing component: Σ_{33}=-0.1). 500 (TG and AF) and 500 (SO) time increments of $1x10^6$s (files CREEP500.3 and CREEP250.3). Files extensions are TGB, AFB and SOB. Figure 9-2 shows the strain-rate vs strain curves predicted by the three models. This case shows the versatility of the code, which allows imposing stress states (creep). The results are consistent with the Case A. The TG case starts with the highest strain-rate for the same applied stress. However, at around 60% and 80% strain, TG rates cross over SO and AF, respectively (se Fig 9-2). Interestingly, a similar crossover at about the same strain is also observed in the stress-strain response of Fig. 9-1.

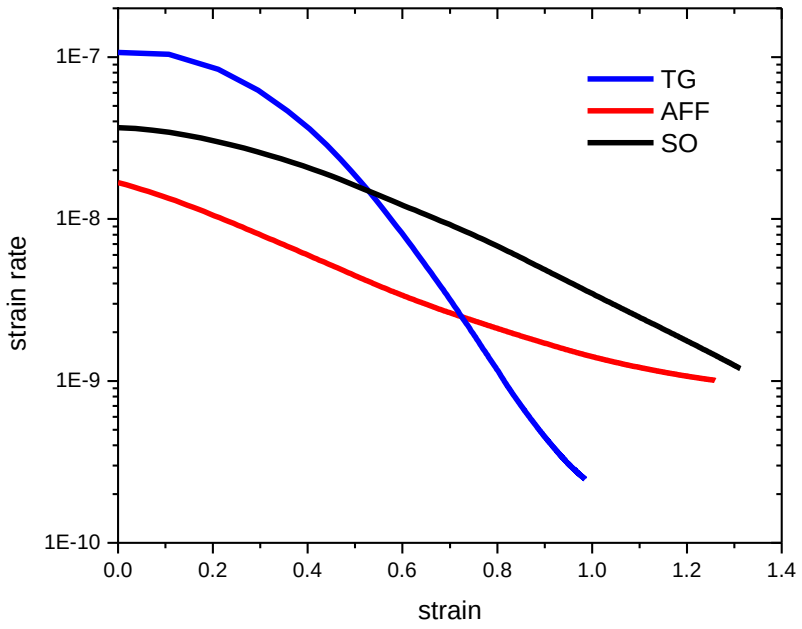

Figure 9-2: Strain-rate vs strain predicted by the TG, AF and SO models, for an axisymmetric compressive creep test, for the same ice polycrystal as in the previous case.

EXAMPLE 10: Equal Channel Angular Extrusion of FCC

This example is meant to familiarize the user with the simulation of sequential processes, consisting of plastic forming and rigid rotations of the sample (described in Section 1.3.1). It also uses the option of 'grain fragmentation' described in Section 2.3.1. ECAE consists in extruding the sample repeatedly through a 90° die. In each pass about 100% shear strain is enforced with the advantage that the section of the sample is kept constant. This process is meant to substantially reduce the grain size, while increasing yield stress and retaining ductility. In practice, four extrusion routes are used, and each one imposes a different deformation history to the sample. Here we describe two of them: Route B_A and Route C, and simulate two passes in each case. The extrusion process through the die is the same for all routes and passes (process file ECAE.50), and for all routes the sample is rotated 90°CW around die axis 3, in order to reinsert it in the die. What differentiates the routes is an extra rotation around axis 2 of the die, before reinserting it.

Route A: no rotations.

Route B_A: alternate rotations of 90°CW, 90°CCW, 90°CW, etc, around die axis 2.

Route B_C: same rotations of 90°CW, 90°CW, 90°CW, etc, around die axis 2.

Route C: same rotations of 180°CW, 180°CW, 180°CW,etc, around die axis 2. This route reverses the sense of shear at each pass.

For the simulations presented in Example 10 we use the following conditions:

- Initial random texture (file RAND500.TEX) with 500 orientations.
- FCC crystals with slip on (111)<110> and no hardening $\tau_0 = 1, \tau_1 = 0, \theta_0 = 0, \theta_1 = 0$ (file FCC.SX).
- Process file: 50 steps of shear at 45° with respect to the die axes (file ECAE.50), which represents a shear of ε_{12}=100%. The Exit:Entry:Flow axes of the die are axis 1:2:3 respectively

Case B_A:

The input file is VPSC7.inB; the output files have extension *.Ba. An input file POLE8.inB is provided for plotting the sequence of (111) poles for the initial, extruded, rotated and extruded sample. A plot of the poles is in file POLES_Ba.pdf

Case C:

The input file is VPSC7.in; the output files have extension *.C

See below the sequence of (111) poles that result from each process applied to the sample along both routes.

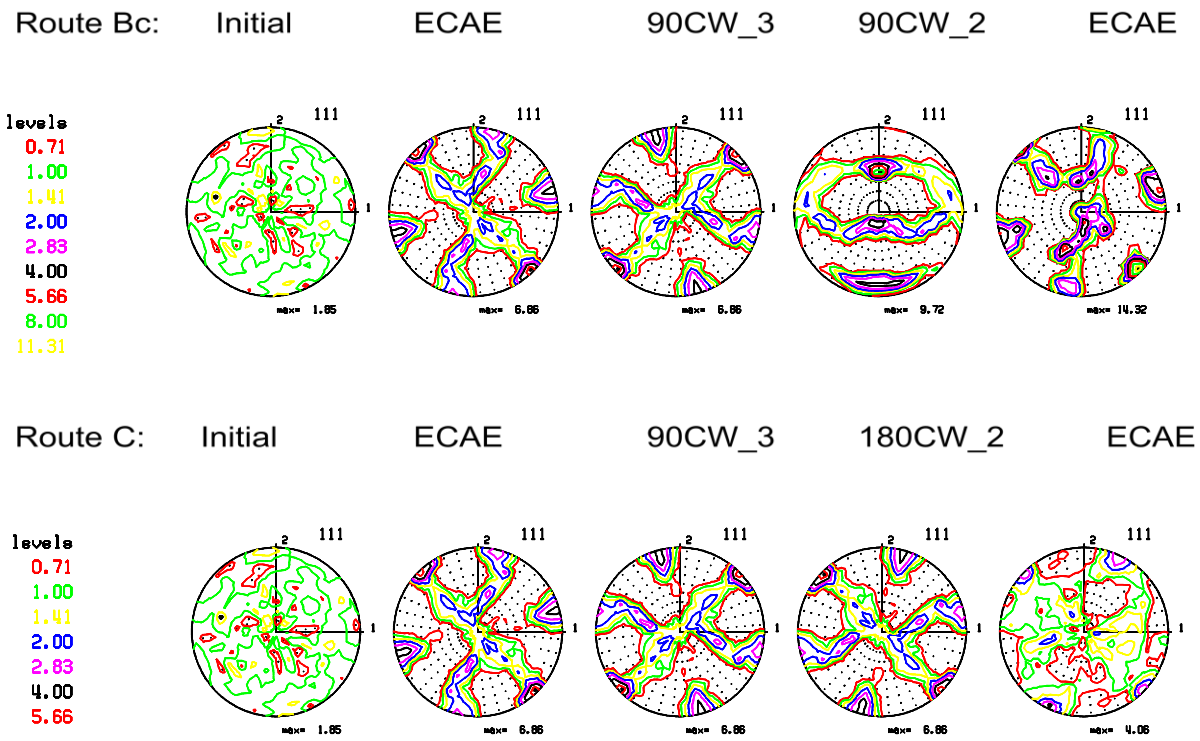

SECTION 4: Appendices

Appendix A: Taylor and Schmid factors. Generalized tensors.

The dissipation rate of a polycrystal, calculated with the macroscopic stress and strain rate, is the same as the volume average over the grains:

$$\bar{\sigma}_{ij}\bar{\dot{\varepsilon}}_{ij} = \sum_g \sigma_{ij}^g \dot{\varepsilon}_{ij}^g \omega^g = \sum_g \sum_s \tau^{s,g}\dot{\gamma}^{s,g}\omega^g \qquad \text{(A1)}$$

First assumption: if $\tau^{s,g} = \tau_{ref}$, the same for every system in every grain, the Eq. above can be written

$$\frac{\bar{\sigma}_{ij}\bar{\dot{\varepsilon}}_{ij}}{\tau_{ref}} = \sum_g \sum_s \dot{\gamma}^{s,g}\omega^g = \bar{\dot{\Gamma}} \qquad \text{(A2)}$$

Where $\bar{\dot{\Gamma}}$ is an average shear rate per grain. Define the norm of the strain rate as

$\left\| \bar{\dot{\varepsilon}} \right\| = \sqrt{\bar{\dot{\varepsilon}}_{ij}\bar{\dot{\varepsilon}}_{ij}}$ and rewrite (A2) above in terms of the normalized rate tensor:

$$\left\| \bar{\dot{\varepsilon}} \right\| \frac{\bar{\sigma}_{ij}\bar{\dot{\varepsilon}}_{ij}}{\tau_{ref}\left\| \bar{\dot{\varepsilon}} \right\|} = \left\| \bar{\dot{\varepsilon}} \right\| \hat{M} = \bar{\dot{\Gamma}} \qquad \text{(A3)}$$

Where $\hat{M} = \dfrac{\bar{\sigma}_{ij}\bar{\dot{\varepsilon}}_{ij}}{\tau_{ref}\left\| \bar{\dot{\varepsilon}} \right\|}$ is a general definition of **the Taylor factor** !

Second assumption: assume now that the stress state imposed is axial and that the symmetry is such that the strain-rate induced is diagonal

$$\bar{\sigma}_{ij} = \sigma_{33}\begin{bmatrix} 0 & 0 & 0 \\ 0 & 0 & 0 \\ 0 & 0 & 1 \end{bmatrix} \quad \text{and} \quad \bar{\dot{\varepsilon}}_{ij} = \dot{\varepsilon}_{33}\begin{bmatrix} -\nu & 0 & 0 \\ 0 & \nu - 1 & 0 \\ 0 & 0 & 1 \end{bmatrix}$$

and $\left\| \bar{\dot{\varepsilon}} \right\| = \dot{\varepsilon}_{33}\sqrt{2(1-\nu+\nu^2)}$. Only if the deformation is, in addition, transversely isotropic, it results that $\left\| \bar{\dot{\varepsilon}} \right\| = \dot{\varepsilon}_{33}\sqrt{3/2}$

For these particular conditions, the expression of the Taylor factor can be written:

$$\hat{M} = \frac{\bar{\sigma}_{ij}\dot{\bar{\varepsilon}}_{ij}}{\tau_{ref}\left\|\dot{\bar{\varepsilon}}\right\|} = \frac{\sigma_{33}\dot{\varepsilon}_{33}}{\tau_{ref}\,\dot{\varepsilon}_{33}\sqrt{3/2}} = \frac{\sigma_{33}}{\tau_{ref}\sqrt{3/2}}$$

Which can be written as: $\sigma_{33} = \sqrt{3/2}\hat{M}\tau_{ref} = M\tau_{ref}$

Where $M = \sqrt{3/2}\hat{M}$ is what is defined in the literature as the Taylor factor.

And the expression above for the rates can be rewritten as:

$$\left\|\dot{\bar{\varepsilon}}\right\|\hat{M} = \dot{\varepsilon}_{33}\sqrt{3/2}\hat{M} = \dot{\varepsilon}_{33}M = \dot{\bar{\Gamma}}$$

A generalized Schmid factor

The Schmid factor is a geometric factor defined for uniaxial stress states as the ratio between the resolved shear in a slip plane **n** and along the slip direction **b,** over the applied uniaxial stress. Two simple special cases, axial tension and simple shear, are sketched below.

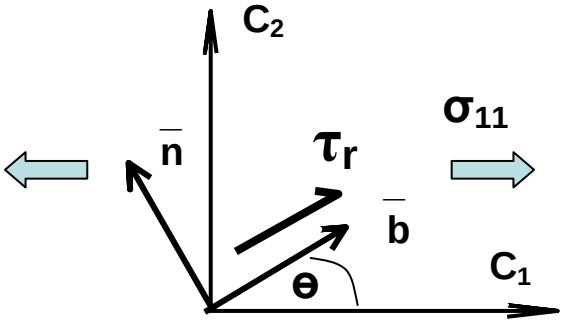

Axial tension

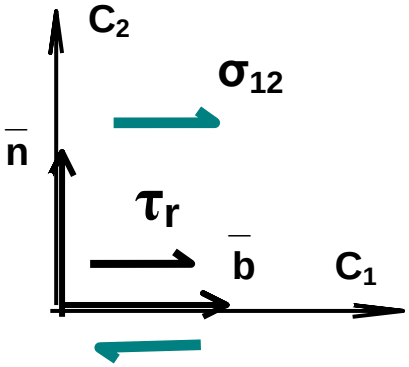

Simple shear

The corresponding stress tensors are

$$\sigma_{ij} = \begin{bmatrix} \sigma_{11} & 0 & 0 \\ 0 & 0 & 0 \\ 0 & 0 & 0 \end{bmatrix} \quad \text{and} \quad \sigma_{ij} = \begin{bmatrix} 0 & \sigma_{12} & 0 \\ \sigma_{12} & 0 & 0 \\ 0 & 0 & 0 \end{bmatrix}$$

The corresponding Schmid tensors are:

$$S = \frac{\tau_{res}}{\sigma_{11}} = \cos\theta \sin\theta \qquad \text{and} \qquad S = \frac{\tau_{res}}{\sigma_{12}} = 1$$

If we define a general Schmid tensor as

$$S = \frac{\tau_{res}}{\|\sigma\|} = \frac{m_{ij}\sigma_{ij}}{\|\sigma\|}$$

It reduces to the expressions above for the two simple cases, and can be applied to any arbitrary stress tensor.

Appendix B: Von Mises equivalent stress & strain

It is usual in materials science to define equivalent stress and strain rate measures, scalar magnitudes which are associated with stress and strain rate tensors. A widely used scalar measure is the Von Mises stress and strain, often used to produce scalar plots of tensorial results. Also used, but less common, is the ellipsoidal definition of Hill, containing parameters that account for anisotropy. Both, Von Mises and Hill, lead to the definition of a plastic potential, the gradient of which gives the strain rate tensor. As a consequence, for a general case, once the equivalent stress is defined, the form of the strain rate scalar follows from it.

Below we discuss some specific tensorial cases. Equivalent stress and strain rate $\sigma_{eq}, \dot{\varepsilon}_{eq}$ are scalar measures of stress and strain rate tensors. They have to be complementary, namely, they have to give the same dissipation rate as the tensor contraction:

$$\sigma_{ij}\dot{\varepsilon}_{ij} = \sigma'_{ij}\,\dot{\varepsilon}_{ij} = \sigma_{eq}\dot{\varepsilon}_{eq} \tag{B1}$$

A frequent mistake is to use *simultaneously* the following definition of Von Mises stress and strain rate:

$$\begin{aligned} \sigma_{eq}^{VM} &= \sqrt{\tfrac{3}{2}}\|\sigma'\| = \sqrt{\tfrac{3}{2}}\sqrt{\sigma'_{ij}\,\sigma'_{ij}} \\ \dot{\varepsilon}_{eq}^{VM} &= \sqrt{\tfrac{2}{3}}\|\dot{\varepsilon}\| = \sqrt{\tfrac{2}{3}}\sqrt{\dot{\varepsilon}_{ij}\dot{\varepsilon}_{ij}} \end{aligned} \tag{B2}$$

It is obvious that the product of these two scalars does not give $\sigma_{ij}\dot{\varepsilon}_{ij}$ in the case of tensors with arbitrary components. The valid way of doing this is to use the definition (B2) for only one scalar, say σ_{eq}^{VM}, and to define the other by enforcing the work conjugate condition:

$$\dot{\varepsilon}_{eq}^{VM} = \frac{\sigma_{ij}\dot{\varepsilon}_{ij}}{\sigma_{eq}^{VM}} \tag{B3}$$

Equation (B3) is how we define equivalent rate inside VPSC.FOR, and how it is listed in output file STR_STR.OUT. Follow some specific cases for illustration.

Axial tension or axial compression: the definition (C2) works for the simple case envisaged by Von Mises: the stress state is axial and the strain-rate is transversely isotropic

$$\sigma'_{ij} = \sigma_{33}\begin{bmatrix} -\frac{1}{3} & 0 & 0 \\ 0 & -\frac{1}{3} & 0 \\ 0 & 0 & \frac{2}{3} \end{bmatrix} \quad \textit{and} \quad \dot{\varepsilon}_{ij} = \dot{\varepsilon}_{33}\begin{bmatrix} -\frac{1}{2} & 0 & 0 \\ 0 & -\frac{1}{2} & 0 \\ 0 & 0 & 1 \end{bmatrix}$$

In this case $\sigma'_{ij}\dot{\varepsilon}_{ij} = \sigma_{33}\dot{\varepsilon}_{33}$, and since Von Mises defined the equivalent stress in (B2) such that it is equal to the measured tensile component (not the deviatoric component!)

$$\sigma_{eq}^{VM} = \sqrt{\tfrac{3}{2}}\|\sigma'\| = \sqrt{\tfrac{3}{2}}\sigma_{33}\sqrt{\tfrac{2}{3}} = \sigma_{33} \quad \text{and, from (B3)} \quad \dot{\varepsilon}_{eq}^{VM} = \frac{\sigma_{33}\dot{\varepsilon}_{33}}{\sigma_{33}} = \dot{\varepsilon}_{33} = \|\dot{\varepsilon}\|\sqrt{\tfrac{2}{3}} \ ,$$

which is the same scalar given by (B2). Observe that the previous definition of the Von Mises strain rate would not be valid if the tensor was not transversely isotropic. When:

$$\dot{\varepsilon}_{ij} = \dot{\varepsilon}_{33}\begin{bmatrix} -\nu & 0 & 0 \\ 0 & \nu - 1 & 0 \\ 0 & 0 & 1 \end{bmatrix}, \text{ the norm is } \|\dot{\varepsilon}\| = \dot{\varepsilon}_{33}\sqrt{2(1-\nu+\nu^2)}$$

Simple shear: in the case of simple shear we are dealing with tensors of the form

$$\sigma'_{ij} = \sigma_{12}\begin{bmatrix} 0 & 1 & 0 \\ 1 & 0 & 0 \\ 0 & 0 & 0 \end{bmatrix} \quad \textit{and} \quad \dot{\varepsilon}_{ij} = \dot{\gamma}\begin{bmatrix} 0 & \frac{1}{2} & 0 \\ \frac{1}{2} & 0 & 0 \\ 0 & 0 & 0 \end{bmatrix}$$

In which case, $\sigma'_{ij}\dot{\varepsilon}_{ij} = \sigma_{12}\dot{\gamma}$, and if we adopt the definition

$\sigma_{eq}^{VM} = \sqrt{\frac{3}{2}}\|\sigma'\| = \sqrt{\frac{3}{2}}\sigma_{12}\sqrt{2} = \sqrt{3}\sigma_{12}$, it turns from (B3) that for simple shear

$\dot{\varepsilon}_{eq}^{VM} = \dfrac{\sigma_{12}\dot{\gamma}}{\sqrt{3}\sigma_{12}} = \dfrac{\dot{\gamma}}{\sqrt{3}}$, which is the same as (B2) : $\sqrt{\frac{2}{3}}\|\dot{\varepsilon}\| = \dfrac{\dot{\gamma}}{\sqrt{3}}$.

Plane strain: need to add…….

Appendix C: Voce hardening and VPSC algorithm

Express Kocks-Mecking equation for evolution of density in terms of total shear rate in grain and Taylor law for the threshold stress τ^s (see Karaman et al, 2000):

$$\dot{\rho} = \left(k_1\sqrt{\rho} - k_2\rho\right)\dot{\Gamma} \qquad \text{(C1)}$$

$$\tau = \tau_0 + \alpha\mu b\sqrt{\rho} \qquad \text{(C2)}$$

Here $\dot{\Gamma} = \sum_s \dot{\gamma}^s$ is the sum of the shear rates over all systems. From (C2):

$$\sqrt{\rho} = (\tau - \tau_0)/\alpha\mu b \qquad \text{(C3)}$$

and $$\dot{\tau} = \frac{\alpha\mu b}{2\sqrt{\rho}}\dot{\rho} \qquad \text{(C4)}$$

Replace (C3) in (C1), and replace (C1) in (C4):

$$\dot{\tau} = \left(k_1\frac{\alpha\mu b}{2} - k_2(\tau - \tau_0)\right)\dot{\Gamma} = \left(\frac{\theta_0}{\tau_1}(\tau_0 + \tau_1) - \frac{\theta_0}{\tau_1}\tau\right)\dot{\Gamma} = (a - b\tau)\dot{\Gamma} \qquad \text{(C5)}$$

Where we define: $\theta_0 = k_1\frac{\alpha\mu b}{2}$, $\frac{\theta_0}{\tau_1} = \frac{k_2}{2}$, $a = \frac{\theta_0}{\tau_1}(\tau_0 + \tau_1)$, $b = \frac{\theta_0}{\tau_1}$ (C6)

Integrating (C5) gives:

$$\frac{-1}{b}\ln(a - b\tau)\Big|_{\tau_0}^{\tau} = \Gamma\Big|_0^{\Gamma}$$

From where: $(a - b\tau) = (a - b\tau_0)e^{-b\Gamma}$

Replacing the parameters defined in (C6) leads to a saturating Voce law describing the evolution of the threshold with shear:

$$\tau = \tau_0 + \tau_1(1 - \exp(-\Gamma\frac{\theta_0}{\tau_1})) \qquad \text{(C7)}$$

The increase in the threshold stress of a system due to shear activity $\Delta\gamma^{s'}$ in the grain systems is calculated as:

$$\Delta\tau^s = \frac{d\hat{\tau}^s}{d\Gamma}\sum_{s'} h^{ss'}\Delta\gamma^{s'} \qquad \text{(C8)}$$

where

$$\frac{d\hat{\tau}^s}{d\Gamma} = \left[\theta_1 + \left(\left|\frac{\theta_0}{\tau_1}\right|\tau_1 - \theta_1\right)\exp\left(-\Gamma\left|\frac{\theta_0}{\tau_1}\right|\right) + \left|\frac{\theta_0}{\tau_1}\right|\theta_1\Gamma\exp\left(-\Gamma\left|\frac{\theta_0}{\tau_1}\right|\right) \right] \tag{C9}$$

The threshold associated with each system in each grain is updated inside SUBROUTINE UPDATE_CRSS_VOCE. However, the incremental expression (C8) represents a forward extrapolation which tends to overestimate the hardening and make it dependent on the step size, more so when the derivative is large. As a consequence, we have implemented an analytic integration of Eq. (C9) inside SUBROUTINE UPDATE_CRSS_VOCE. The procedure is as follows.

$$\Delta\tau^s = \int_{\Gamma_0}^{\Gamma_0+\Delta\Gamma} \frac{d\hat{\tau}^s}{d\Gamma} \sum_{s'} h^{ss'} d\gamma^{s'} \tag{C10}$$

If we express: $\gamma^s = \gamma_0^s + \alpha\Delta\gamma^s$ and $\Gamma = \Gamma_0 + \alpha\Delta\Gamma \qquad (0 < \alpha < 1)$

Then: $d\Gamma = \Delta\Gamma d\alpha$ and $d\gamma^s = \Delta\gamma^s d\alpha = \frac{\Delta\gamma^s}{\Delta\Gamma} d\Gamma$

Replacing in (C10):

$$\Delta\tau^s = \int_{\alpha=0}^{\alpha=1} \frac{d\hat{\tau}^s}{d\Gamma} \sum_{s'} h^{ss'} \frac{\Delta\gamma^s}{\Delta\Gamma} d\Gamma = \int_{\Gamma_0}^{\Gamma_0+\Delta\Gamma} \frac{d\hat{\tau}^s}{d\Gamma} d\Gamma \left(\sum_{s'} h^{ss'} \frac{\Delta\gamma^s}{\Delta\Gamma} \right) \tag{C11}$$

Replacing in (C11) the derivative given by (C9), recalling the primitive integrals

$$\int e^{-ax} dx = -\frac{1}{a} e^{-ax} \quad \text{and} \quad \int x e^{-ax} dx = -\frac{e^{-ax}}{a^2}(1+ax) \quad \text{where} \quad a = \left|\frac{\theta_0}{\tau_1}\right|$$

and accounting for the integration extremes, gives the incremental change of the threshold stress as:

$$\Delta\tau^s = \left(\sum_{s'} h^{ss'} \frac{\Delta\gamma^s}{\Delta\Gamma} \right) \left(\begin{array}{l} \theta_1\Delta\Gamma - \frac{a\tau_1 - \theta_1}{a} e^{-a\Gamma_0} (e^{-a\Delta\Gamma} - 1) \\ \qquad - \frac{\theta_1}{a} e^{-a\Gamma_0} \left\{ e^{-a\Delta\Gamma} [1 + a(\Gamma_0 + \Delta\Gamma)] - [1 + a\Gamma_0] \right\} \end{array} \right) \tag{C12}$$

Appendix D: Crystal rotation and misorientation

An excellent paper discussing ways of representing crystal rotations and transformation matrices is: "A historical note on finite rotations", H. Cheng & K.C. Gupta, J. Appl. Mechanics, vol. 56 (1989) pp. 139-145.

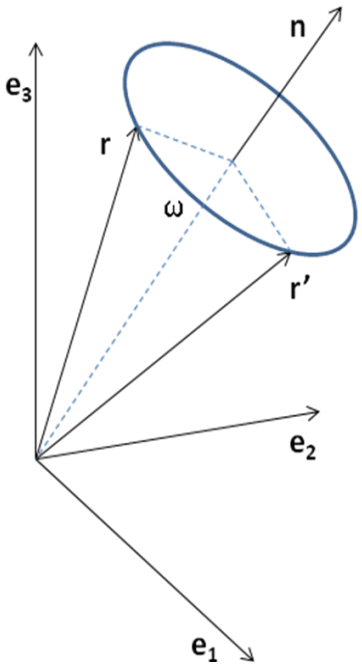

The authors show that the finite rotation of a vector **r** around an axis **n** by a finite angle ω is given by:

$$r' = r\cos\omega + (n \wedge r)\sin\omega + n(n.r)(1-\cos\omega)$$

Which can be written as a linear transformation:

$$r_i' = R_{ij} r_j$$

$$\text{with} \quad R = I + N\sin\omega + N^2(1-\cos\omega)$$

$$\text{and} \quad N = \begin{bmatrix} 0 & -n_3 & n_2 \\ n_3 & 0 & -n_1 \\ -n_2 & n_1 & 0 \end{bmatrix} \qquad \text{(D0)}$$

The previous is relevant for building the finite rotation associated with equation (3-1), which describes the rate of change of the crystal orientation matrix as

$$\dot{R}^c = \dot{\Omega} R^c \quad \text{where} \quad \dot{\Omega} = (W^c - W_o^{c,R}) \qquad \text{(D1)}$$

If the tensor $\dot{\Omega}$ is assumed to be constant within a time increment, the solution to (D1) is

$$R^c(t+\Delta t) = R^c(t)\exp(\dot{\Omega}\Delta t) = R^c(t)\exp(\Omega) \qquad \text{(D2)}$$

Where $\Omega = \dot{\Omega}\Delta t$ is a skew symmetric tensor and can be written in a form that will give a straightforward meaning to its components, namely, the form (D0) associated with a rotation around an axis **n** by a finite angle ω. We will identify the components of Ω with the components of the rotation axis:

$$\Omega = \begin{pmatrix} 0 & -\omega_3 & \omega_2 \\ \omega_3 & 0 & -\omega_1 \\ -\omega_2 & \omega_1 & 0 \end{pmatrix} = \omega\hat{\Omega} \qquad \text{(D3a)}$$

Here $\hat{\Omega} = \begin{pmatrix} 0 & -\hat{\omega}_3 & \hat{\omega}_2 \\ \hat{\omega}_3 & 0 & -\hat{\omega}_1 \\ -\hat{\omega}_2 & \hat{\omega}_1 & 0 \end{pmatrix}$, $\hat{\omega}_i = \frac{\omega_i}{\omega}$, $\omega = \sqrt{\omega_1^2 + \omega_2^2 + \omega_3^2}$ (D3b)

According to (D2), updating the crystal orientation matrix requires to evaluate the exponential of a tensor, which is done using the Taylor expansion

$$\exp(\Omega) = \sum_{n=0}^{\infty} \frac{\Omega^n}{n!} \quad \text{(D4)}$$

But because of the special form (D3) of Ω, the powers have the property:

$$\begin{aligned} \Omega^0 &= I \\ \Omega^1 &= \omega\hat{\Omega} \\ \Omega^2 &= \omega^2\hat{\Omega}^2 = \omega^2(-I + \hat{\omega}\otimes\hat{\omega}) \\ \Omega^3 &= -\omega^3\hat{\Omega} \\ \Omega^4 &= -\omega^4\hat{\Omega}^2 \\ \Omega^5 &= \omega^5\hat{\Omega} \\ &\text{.....} \end{aligned} \quad \text{(D5)}$$

Replacing in (D4) and regrouping alternate terms, one obtains a series expansion for sinω and cosω

$$\begin{aligned} \exp(\Omega) &= I + \omega\frac{\hat{\Omega}}{1!} + \omega^2\frac{\hat{\Omega}^2}{2!} - \omega^3\frac{\hat{\Omega}}{3!} - \omega^4\frac{\hat{\Omega}^2}{4!}... \\ \exp(\Omega) &= I + \hat{\Omega}\left[\frac{\omega}{1!} - \frac{\omega^3}{3!} + \frac{\omega^5}{5!} - ...\right] + \hat{\Omega}^2\left[\frac{\omega^2}{2!} - \frac{\omega^4}{4!} + \frac{\omega^6}{6!} - ...\right] \\ \exp(\Omega) &= I + \hat{\Omega}\sin\omega + \hat{\Omega}^2(1-\cos\omega) \end{aligned} \quad \text{(D6)}$$

This form of the transformation matrix based on a spin ω around a normalized axis $\hat{\omega}$ is often referred to as the Rodrigues equation. Sometimes it is cast in an alternative form, as follows:

Define $\Omega^R = \mathrm{tg}(\frac{\omega}{2})\hat{\Omega}$ (D7)

and replace in (D6) using trigonometric identities:

$$\exp(\Omega) = \mathrm{I} + \frac{\Omega^{\mathrm{R}}}{\mathrm{tg}\,\frac{\omega}{2}} 2\sin\frac{\omega}{2}\cos\frac{\omega}{2} + \frac{(\Omega^{\mathrm{R}})^2}{(\mathrm{tg}\,\frac{\omega}{2})^2} 2(\sin\frac{\omega}{2})^2$$

$$\exp(\Omega) = \mathrm{I} + \frac{2(\sin\frac{\omega}{2})^2}{(\mathrm{tg}\,\frac{\omega}{2})^2}\left[\Omega^{\mathrm{R}} + (\Omega^{\mathrm{R}})^2\right] = \mathrm{I} + \frac{2}{1+(\mathrm{tg}\,\frac{\omega}{2})^2}\left[\Omega^{\mathrm{R}} + (\Omega^{\mathrm{R}})^2\right] \qquad \text{(D8)}$$

Crystal misorientation

The transformation given by (D6) is also relevant to the definition of misorientation between two crystal systems. If one assumes that R_A and R_B transform from crystals A and B to sample axes, respectively, then $R_B{}^T R_A$ transforms from crystal A to crystal B. If one expresses such transformation using Rodrigues it will be of the form

$$\mathrm{R}_{\mathrm{B}}^{\mathrm{T}}\mathrm{R}_{\mathrm{A}} = \mathrm{I} + \hat{\Omega}\sin\omega + \hat{\Omega}^2(1-\cos\omega) \qquad \text{(D9)}$$

Taking the trace of the tensors and using the form of $\hat{\Omega}$ and $\hat{\Omega}^2$ given by (D3) and (D5) one obtains the rotation angle (misorientation angle) that makes A and B coincide

$$\omega = \cos^{-1}\left[\frac{\mathrm{tr}(\mathrm{R}_{\mathrm{B}}^{\mathrm{T}}\mathrm{R}_{\mathrm{A}})-1}{2}\right] \qquad \text{(D10)}$$